EFFECT OF TIM23 KNOCKDOWN *IN VIVO* ON PROTEIN IMPORT INTO MITOCHONDRIA AND RETROGRADE SIGNALING TO THE UPR^{MT} IN MUSCLE

ASHLEY N. OLIVEIRA

A THESIS SUBMITTED TO THE FACULTY OF GRADUATE STUDIES IN PARTIAL FULFILLMENT OF THE REQUIREMENTS FOR THE DEGREE OF

MASTER OF SCIENCE

GRADUATE PROGRAM IN KINESIOLOGY AND HEALTH SCIENCE

YORK UNIVERSITY
TORONTO, ONTARIO

SEPTEMBER 2017

ABSTRACT

The mitochondrial unfolded protein response (UPR^{mt}) is a protein quality control mechanism that strives to eliminate toxic effects exerted by misfolded and misassembled proteins. We sought to understand this mechanism by perturbing the coordination between the nuclear and mitochondrial genomes by reducing the expression of a major channel of the inner mitochondrial membrane. This established a relationship between protein import, and the maintenance of mitochondrial proteostasis. Next, we sought to explore the communication between the nucleus and the mitochondrion that mediates the activation of the UPR^{mt}. We investigated the role for proteolytically-derived peptides in this retrograde signaling. Here we highlight the relationship between the protein import pathway and its role in facilitating peptide-mediated communication in maintaining proteostasis. The UPR^{mt} has been implicated in aging, cancer, and neurodegenerative diseases. Thus, my work has contributed to improving our understanding of this quality control mechanism, thereby providing potential future therapeutic targets.

ACKNOWLEDGEMENTS

First and foremost, I would like to thank my mother, who probably still doesn't really understand what I've been doing these last two years, and still thinks I am going to be a medical doctor. I want to thank you for always blindly supporting me and for teaching me a valuable lesson, "whatever you do or accomplish in life is for yourself and no one else". Thank you for allowing me to be me, and I hope I make you proud.

Second, I would like to thank my supervisor, Dr. David Hood. I have no clue what you saw in me three years ago in your class on mitochondria, but I'm forever thankful for introducing me to the world of research and the powerhouse of the cell. Thank you for your support, your guidance, and your belief in me.

I would also like to thank Ryan, without whom I probably would have starved about a year ago and gone clinically insane. Straight-jacket and all! Thank you for being my support and for being the best damn partner a girl could ask for. RASH forever! And forever one hundred times!

Finally, I would like to thank my friends and my lab mates. Mika, for being the best pal a pal could ever hope for and so much more. Jon, for teaching me everything I know. Avi, for always being there for me in life and in science. Kait, for giving a shining example of work ethic to strive for, I don't know how you do it. And to the Hood lab, past and present, I am thankful for calling each and every one of you colleagues and above all, friends.

I would like to dedicate this body of work to my Tio Luis. With grandparents an ocean away, you and Tia raised me as your own and I am forever grateful. I love you and I miss you. *Juízo e vergonha.*

TABLE OF CONTENTS

LIST OF TABLES

CHAPTER 2: MANUSCRIPT

APPENDIX A: DATA TABLES AND STATISTICAL ANALYSES

LIST OF FIGURES

CHAPTER 1: REVIEW OF LITERATURE

CHAPTER 2: MANUSCRIPT

APPENDIX B: SUPPLEMENTAL DATA

LIST OF ABBREVIATIONS

ABCB10	ATP binding cassette subfamily B member 10
Akt	Protein kinase B
AMPK	AMP-activated protein kinase
ASK1	Apoptosis signaling kinase 1
ATF5	Activating transcription factor 5
ATFS-1	Activating transcription factor associated with stress-1
BNIP3	BCL2/adenovirus E1B protein-interacting protein 3
CAMK	Ca^{2+}/calmodulin-dependent kinase
C/EBPβ	CCAAT-enhancer-binding protein β
C. elegans	Caenorhabditis elegans
CHOP	C/EBP homologous protein
c-jun	JUN proto-oncogene, AP-1 transcription factor subunit 1
ClpP	Caseinolytic mitochondrial matrix peptidase proteolytic subunit
ClpX	Caseinolytic mitochondrial matrix peptidase chaperonin subunit
COX IV	Cytochrome c oxidase subunit IV
Cpn10	Chaperonin 10
DCF	2',7'-Dichlorofluorescin
Drp1	Dynamin-related protein 1
DVE-1	Homebox transcription factor
ETC	Electron transport chain
ERRα/β/γ	Estrogen-related receptor α/β/γ
Fis1	Mitochondrial fission protein 1
FLP-2	Neuropeptide
FOXO3	Forkhead box O3 transcription factor
FTR	Fast-twitch red fiber
FTW	Fast-twitch white fiber
GDF15	Growth and differentiation factor 15
GIP	General import pore
HAF-1	HAIF transporter (PGP related)
HO^-	Hydroxyl radical
Hsp60/90	Heat shock protein 60/90
IMF	Intermyofibrillar
IMS	Intermembrane space
ISR	Integrated stress response
JNK	c-Jun N-terminal kinase
KD	Knockdown
LC3-I/II	Microtubule-associated protein 1A/1B-light chain 3-I/II
lin-65	Nuclear co-factor lin-65
LonP	Lon peptidase
MDM	Mitochondrial distribution and morphology
met-2	Histone methyltransferase 2
MFN1/2	Mitofusin 1/2
MHC	Myosin heavy chain
MKP	MAP kinase phosphatase

mtDNA	Mitochondrial DNA
mtHSP70	Mitochondrial heat shock protein 70
MPP	Mitochondrial processing peptidase
MSF	Mitochondrial import stimulating factor
mTORC1	Mammalian target of rapamycin complex 1
mtPTP	Mitochondrial permeability transition pore
MTS	Mitochondrial targeting sequence
MURE	Mitochondrial unfolded protein response element
NAC	N-acetyl-L-cysteine
NIX	BCL2/Adenovirus E1B protein-interacting protein 3-like
NLS	Nuclear localizing sequence
NRF1/2	Nuclear respiratory factor 1/2
NuGEMP	Nuclear gene encoding mitochondrial protein
OCT	Ornithine transcarbamylase
OMI	High temperature requirement A serine protease (HtrA1)
Oxa-1	Oxidase assembly protein-1
OXPHOS	Oxidative phosphorylation
PGC-1α	Peroxisome proliferator-activated receptor gamma coactivator 1-alpha
PIM	Protein import machinery
PINK1	PTEN-induced putative kinase 1
PKA	Protein kinase A
PKR	dsRNA-activated protein kinase
PMF	Proton motive force
PQC	Protein quality control
P38 MAPK	p38 Mitogen-activated kinase
Redox	Reduction-oxidation reaction
RLS	Mitochondrially-released peptides
ROS	Reactive oxygen species
SAM	Sorting and assembly machinery
Sam35/37/50	Sorting and assembly machinery subunit 35/37/50
SatB5	Special AT-rich sequence-binding protein 2
SiRT1/3	Sirtuin 1/3
SS	Subsarcolemmal
STR	Slow-twitch red fiber
Tfam	Mitochondrial transcription factor A
TFEB	Transcription factor EB
TIM	Translocase of the inner membrane
Tim22	Translocase of the inner membrane channel subunit 22
Tim23	Translocase of the inner membrane channel subunit23
TL	Translation lane
TOM	Translocase of the outer membrane
Tom20/70	Translocase of the outer membrane receptor subunits 20/70
Tom40	Translocase of the outer membrane channel subunit 40
Ubl5	Ubiquitin-like protein 5
ULK1	UNC-51-like autophagy activating kinase 1
uORF	Upstream open reading frame

UPR^{mt}	Mitochondrial unfolded protein response
UPR^{mt}E	Mitochondrial unfolded protein response element
UPR^{ER}	Unfolded protein response of the endoplasmic reticulum
VDAC	Voltage-dependent anion channel
$\Delta\Psi$	Membrane potential

CHAPTER 1: REVIEW OF LITERATURE

1.0 SKELETAL MUSCLE PHYSIOLOGY

Skeletal muscle comprises approximately 40-50% of an individual's body mass and is a highly metabolic organ. Apart from its essential role in providing postural support and movement for the organism, it also plays a key role in metabolism (46). In order to understand the maintenance and the plasticity of skeletal muscle, it is important to first examine the constituents that form this complex organ system. Muscle cells are unique in their long cylindrical structure and their multinucleated composition, whereby nuclei are arranged under the sarcolemma in the periphery of the cells. Each muscle cell contains specialized contractile elements such as myosin and actin filaments that are organized into repeating sarcomeres. Through the physical interaction of myosin and actin, skeletal muscle is able to contract in an ATP-dependent manner. Despite these basic properties, there is a vast amount of heterogeneity in skeletal muscle fibers, which are typically classified based on their biochemical, mechanical and metabolic properties. These differences contribute to varying performance capacities as well as the fiber's ability to adapt (24, 68). Overall, skeletal muscle maintenance and plasticity is well characterized, however the underlying mechanisms that mediate this processes have yet to be fully elucidated.

1.1 Skeletal Muscle Fiber Types

Historically, skeletal muscle has been divided into three sub-classes based on the expression of myosin heavy chain isoform, typically determined via histochemical analyses. The standard classification of skeletal muscle is as follows: 1) slow-twitch red (STR) fibers predominately expressing myosin heavy chain (MHC) type I isoform, 2) fast-twitch red (FTR) fibers containing mostly MHC type II isoform, and 3) fast-twitch white (FTW) comprised of either MHC type IIa or IIb, depending on species. Each fiber type contains a distinct profile of

contractile and metabolic properties contributing to their particular phenotype (105). Type I or STR fibers have slower twitch kinetics, meaning longer time to peak tension and longer relaxation times (104, 105). This makes the fiber more economical with the use of ATP and more resistant to fatigue (109). STR fibers are also highly oxidative and rely heavily on mitochondria for their source of ATP (97). Although these fibers have very low force outputs they are, however, well suited for prolonged submaximal exercise (104, 105). Type IIa or FTR fibers have faster twitch kinetics and maintain a fairly oxidative metabolic profile. Type IIb/x or FTW fibers produce the most amount of force due to rapid twitch kinetics however, they also require more ATP (103–105). Type IIb/x fibers are highly glycolytic, which in turn makes them very susceptible to fatigue due to the inefficient generation of ATP and the intramuscular production of lactic acid. The heterogeneity in various biochemical, metabolic and contractile properties contribute to the different phenotypes observed in the three muscle fiber types.

Recently, histology has proven insufficient to fully characterize the complexity of a single muscle fiber. Through the use of single fiber electrophoresis, fiber hybridization has complicated the simple categorization of muscle fibers transforming it into more of a spectrum in which hybrid fibers exist as intermediates of the three traditional sub-classes (48, 53). Fibers expressing all three MHC isoforms have been documented in both human and rodent models (119). It has been proposed that these hybrid fibers are in transition and are in the process of a fiber type switch, however the significance of these fibers is still unclear (91). Muscle groups are not composed of a single fiber type, but rather a mosaic of all fiber types contributing to the complexity and heterogeneity of a single muscle.

1.2 Mitochondrial Subfractions

ATP, the energy currency of the cell, is of the utmost importance for the function and maintenance of the cell and is primarily derived from mitochondrial respiration. Skeletal muscle is no exception, and thus mitochondria are imperative for skeletal muscle performance and are tightly associated with endurance capacity. Mitochondria are structurally unique organelles in that they maintain two intra-organelle sub-compartments separated by phospholipid membranes. The mitochondrial matrix is encapsulated by the inner membrane, and located within are multiple copies of mitochondrial DNA (mtDNA). Encoded within this genome are 22 tRNAs, 2 rRNAs, and 13 components of the electron transport chain, which are transcribed and translated within the mitochondrial matrix (14). The mitochondrial genome provides for less than 1% of all mitochondrial proteins, the vast majority of which are encoded by the nuclear genome. Mitochondria are the only organelle that rely on two genomes and thus require a mechanism for the transport of nuclear-encoded proteins and to maintain proper stoichiometry between both genomes. These processes will be further discussed in a later section.

The inner membrane not only encapsulates the matrix but also houses the five complexes necessary for the electron transport chain. Briefly, the electron transport chain is responsible for carrying out mitochondrial respiration by reducing various substrates such as NADH and $FADH_2$ and moving their electrons through the various complexes. Movement of these electrons through the complexes generates energy that is used to pump protons from the mitochondrial matrix into the intermembrane space creating a proton motive force (PMF) (74). At complex IV, oxygen then acts as the final electron acceptor and combines with hydrogen to produce water. The electrochemical gradient produced by the buildup of protons in the intermembrane space is capitalized on by ATP synthase, which allows a single proton to move back into the matrix (74).

The free energy from the movement of the proton is transformed into chemical energy used to convert ADP into ATP (74). Thus, through various reduction-oxidation (redox) reactions, the mitochondrion is able to exploit this energy to generate large amount of ATP for the cell.

Mitochondria exist as interconnected networks known as the mitochondrial reticulum (57, 83). The reticulum is maintained through highly regulated events of fusion and fission in which mitochondria can combine to promote the expansion of the network, or conversely, dysfunctional areas can be selectively removed through fission (120). Larger, more interconnected mitochondria promote the movement and sharing of substrates along the network thus making the reticulum as a whole more efficient (35). On the other hand, small fragmented mitochondria produce large amounts of reactive oxygen species (ROS), which are toxic to the cell. These smaller, harmful organelles can be removed by the process of mitophagy, which will be discussed later. Thus it is imperative for the mitochondrial reticulum to continuously undergo fusion and fission events in order to maintain a healthy and optimal pool.

Within skeletal muscle, mitochondria exist in two subfractions: subsarcolemmal (SS) and intermyofibrillar (IMF) mitochondria. These two pools of mitochondria are distinguished by their subcellular localization, whereby SS are located along the periphery under the sarcolemmal membrane, and IMF are found between the myofibrils. These separate populations have related, yet distinct functional and biochemical characteristics. Due to their location, it is proposed that SS mitochondria are responsible for providing energy for nuclear and membrane functions. IMF mitochondria are primarily responsible for providing energy for actin and myosin crossbridge cycling and contractions. IMF mitochondria make up about 80-85% of the total mitochondrial volume and exhibit higher rates of mitochondrial respiration, protein synthesis and protein import (20, 117). On the other hand, SS mitochondria tend to produce more reactive oxygen

species (ROS) and display higher membrane potentials. Thus, due to their distinct subcellular localization and differences in biochemical and metabolic properties, these two populations respond differently to external stimuli. In models of exercise training or muscle disuse, SS mitochondria exhibit more robust adaptation and have therefore thought to be more labile (48). The health and maintenance of both pools are required for skeletal muscle health.

1.3 Mitochondrial Turnover

Mitochondria are crucial organelles for their roles in metabolism, calcium handling, regulation of apoptosis and reactive oxygen species production/ signaling. Two opposing processes govern the balance of mitochondria: mitochondrial biogenesis, the synthesis of new organelles, and mitophagy, the selective recycling of these organelles (44). Mitochondrial biogenesis and mitophagy were once thought to be independent and opposing processes, however it has recently been shown that these mechanisms are actually correlated and coordinated in order to maintain a healthy mitochondrial population (106, 123, 125). Both mitochondrial biogenesis and mitophagy are crucial for the overall health of the muscle (13, 15, 28, 70, 71).

1.3.1 Mitochondrial Biogenesis

Mitochondrial biogenesis is broadly described as the synthesis of new mitochondria, however it is important to note that these organelles cannot be formed *de novo* but rather are added to the pre-existing reticulum. Therefore, mitochondrial biogenesis refers to the process through which the nuclear and mitochondrial genomes are coordinated to increase the expression of mitochondrial proteins, which then expand the network (45, 101, 102). Peroxisome proliferator-activated receptor (PPAR)-γ coactivator (PGC-1α) is widely known as the master regulator of mitochondrial biogenesis, this is due to the fact that once activated it promotes the

transcription of nuclear genes encoding mitochondrial proteins (NuGEMPs). PGC-1α concurrently increases the transcription of mitochondrial transcription factor A (TFAM), which then acts on mtDNA to increase the transcription of mitochondrial-encoded components of the electron transport chain (37). However, PGC-1α is incapable of binding DNA directly and thus regulates mitochondrial biogenesis by coactivating transcription factors such as nuclear respiratory factor 1/2 (NRF1/2), the PPAR family, estrogen-related receptors (ERRα/β/γ) and many others (30). Despite its name as the master regulator, PGC-1α does not seem to be required for mitochondrial biogenesis since PGC-1α knockout animals are able to reap similar exercise-mediated mitochondrial adaptations (65, 99, 122). Therefore, the evidence points towards other compensatory mechanisms that may have similar roles as PGC-1α in mediating mitochondrial biogenesis.

Despite being the only organelle aside from the nucleus that contains its own genome, mtDNA encodes for less than 1% of all mitochondrial proteins. Therefore the vast majority of mitochondrial proteins are transcribed from the nuclear genome and thus translated in the cytosol. All products of NuGEMPs contain a mitochondrial targeting sequence (MTS) that is recognized by cytosolic chaperones that unfold and guide the immature protein to the protein import machinery (PIM) (11, 27). The PIM is primarily composed of the translocases of the outer and inner membrane (TOM and TIM complexes, respectively), which rely on ATP and membrane potential to move linearized proteins into the organelle. Once the nuclear-encoded protein arrives in its designated subcompartment, the MTS is cleaved off by mitochondrial processing peptidase (MPP) and refolded by mitochondrial chaperones assuming its mature conformation. All of the complexes of the ETC, besides complex II, require both nuclear and mitochondrial-encoded proteins in order to form a mature holoenzyme. Thus, mitochondrial

biogenesis is not just a matter of transcriptional upregulation, but also a coordinated expression between the two genomes in order to maintain proper ETC stoichiometry.

Mitochondrial biogenesis is not a static process; it is a dynamic and metabolically sensitive pathway that contributes to the overall oxidative capacity of the tissue. It is widely accepted that endurance exercise induces mitochondrial biogenesis, and even one bout can initiate the signals and changes in gene expression (1, 5, 92). Exercise imposes a metabolic demand on the tissue that causes changes in energy status, Ca^{2+} homeostasis, and ROS generation, among many others (12, 16, 25). These alterations to the cellular environment activate AMP-activated protein kinase (AMPK) (29, 49, 50, 128), Ca^{2+}/ calmodulin-dependent kinase (CaMK) (25), and mitogen-activated protein kinase (p38 MAPK) (93, 94), sirtuins (SIRT1/3) (4, 36) which all converge on PGC-1α activation to drive mitochondrial biogenesis. In contrast, there are conditions that suppress mitochondrial biogenesis, such as aging. Although somewhat controversial, aging is associated with lower levels of mitochondrial content and a dampened ability to adapt to stressors such as exercise (69). Understanding the molecular mechanisms that underlie the regulation of mitochondrial biogenesis is imperative, however this process is opposed by the degradation of mitochondria. Thus, it is important to understand both mechanisms independently, as well as how they cooperate to maintain homeostasis.

1.3.2 Mitophagy

The maintenance of mitochondrial quality requires not only the synthesis of new mitochondria but also the degradation of old and damaged organelles. The process of recycling dysfunctional mitochondria is termed mitophagy, meaning a form of mitochondria-specific autophagy (75). Organelles that have lost their viability typically display an elevation in reactive oxygen species (ROS) production and a loss in membrane potential, which serve as signals to

target their sequestration and subsequent degradation (23, 127). Segments of the mitochondrial reticulum that display this loss in membrane potential or elevation in ROS can undergo fission which is the process through which a dysfunctional portion can be excised from the network to ensure the overall health of the reticulum (32). In this process, mitochondrial fission protein 1 (Fis1) recruits and binds dynamin-related protein 1 (Drp1), which pinches off the membrane of the damaged organelle removing it from the network. Once sequestered, the fragmented organelle can be recycled without interfering with the existing reticulum.

Following the budding off of the dysfunctional mitochondrion, the organelle can be targeted for recycling through mitophagy. There are various mechanisms through which mitophagy is thought to be initiated (127). In the canonical pathway, PTEN-induced putative kinase 1 (PINK1), a protein kinase that is regularly imported into the matrix and degraded accumulates on the outer mitochondrial membrane (72, 124). PINK1 accumulation recruits Parkin, an E3 ubiquitin ligase that polyubiquitinates various outer mitochondrial proteins such as MFN1/2 and VDAC (34, 72, 78). Ubiquitin chains act as a flag to signal for the engulfment of the organelle in a lipid membrane containing LC3-II bound via the adaptor protein p62 (34). Once fully engulfed, it is now referred to as the autophagosome, which travels along microtubule tracts to the lysosome. The autophagosome can then fuse with the lysosome, creating the autophagolysosome, which degrades its contents through proteolytic enzymes and a low pH (75). The cargo is subsequently broken down into its basic amino acids and these are released into the cytosol where they can be used for later protein synthesis.

Alternatively, mitophagy can be initiated independent of PINK1 and Parkin, in receptor-mediated pathways. BCL2/ adenovirus E1B interacting protein (BNIP3) and NIX are both receptors found on the outer mitochondrial membrane, previously described for their roles in

apoptosis, have recently been shown to flag dysfunctional organelles for degradation (8, 64). Both BNIP3 and NIX both contain LC3 interacting domains, which allow the engulfment of the damaged organelle by the growing autophagosome (132). Therefore, mitophagy is a complex process that can be initiated by several independent pathways that strives to recycle dysfunctional mitochondria in an attempt to preserve the mitochondrial reticulum.

Similar to mitochondrial biogenesis, mitophagy can be stimulated during various external or environmental stresses. Exercise for example, can induce both mitochondrial biogenesis as well as mitophagy (67). In this context, the depletion of energy alters the ADP:ATP ratio thereby activating AMPK. AMPK has been shown to phosphorylate UNC-51-like kinase 1(ULK1) and inhibit mTORC1 contributing to an increase in autophagy and mitophagy specifically (56, 63). Exercise has also been shown to increase the expression and activation of transcription factor EB (TFEB), the master regulator of lysosomal biogenesis, thus suggesting an increase in capacity for autophagy (77). Recently, it has been proposed that PGC-1α and TFEB are coordinated and may even regulate each other's expression and activity (106, 123, 125). This suggests that the two dichotomous processes that regulate mitochondrial turnover, mitochondrial biogenesis and mitophagy, are highly correlated and coordinated.

2.0 MITOCHONDRIAL PROTEIN IMPORT

As previously discussed, mitochondria are not formed *de novo,* but rather mitochondrial proteins are synthesized from both the nuclear and mitochondrial genomes and expand the preexisting reticulum. The most recent MitoCarta 2.0 posits that these organelles rely on the nuclear genome for 1158 proteins, despite containing their own genomic material (14). Since the vast majority of all mitochondrial proteins are transcribed and translated outside of the organelle, mitochondria require a sophisticated mechanism of targeting these proteins and allowing their

selective passage. Thus, mitochondria rely on their protein import machinery (PIM) to provide passage for products of NuGEMPs through the mitochondrial membranes and into their designated subcompartments (Fig. 1). All nuclear-encoded proteins contain a mitochondrial targeting sequence (MTS) that is recognized by cytosolic chaperones and contains information that facilitates their trafficking to the organelle, and their sublocalization within the mitochondrion (17). In order to efficiently sort and transport all 1158 nuclear-encoded proteins there are several mechanisms for mitochondrial import, which will be outlined in the following sections.

2.1 Canonical Protein Import Pathway

The most widely studied pathway for translocation into the mitochondria is through the translocases of the outer and inner membrane (TOM and TIM complexes, respectively). Translocation through the TOM and TIM complexes is referred to as the canonical import pathway since it was the first discovered and is well characterized. However, it really only illustrates the mechanism through which proteins enter the mitochondria and localize to the matrix and the inner membrane (Fig. 1). Following recognition by cytosolic chaperones such as heat shock protein 90 (Hsp90) and 70 (Hsp70), nascent preproteins are unfolded into their primary structure to reveal the MTS (27, 130). The TOM complex is widely recognized as the general import pore (GIP) and is composed of a β-barrel channel, Tom40, the two primary receptors Tom20 and Tom70, and various other regulatory subunits (10). Generally, Tom20 recognizes MTS found at the N-terminus of nascent proteins in a positively charged α-helix, whereas Tom70 has an affinity for preproteins with internally located targeting sequences (11, 84, 98). Hsp90 is believed to recognize and bind preproteins with internal targeting domains, while Hsp70 can bind proteins with or without N-terminal domains, which is regulated by a

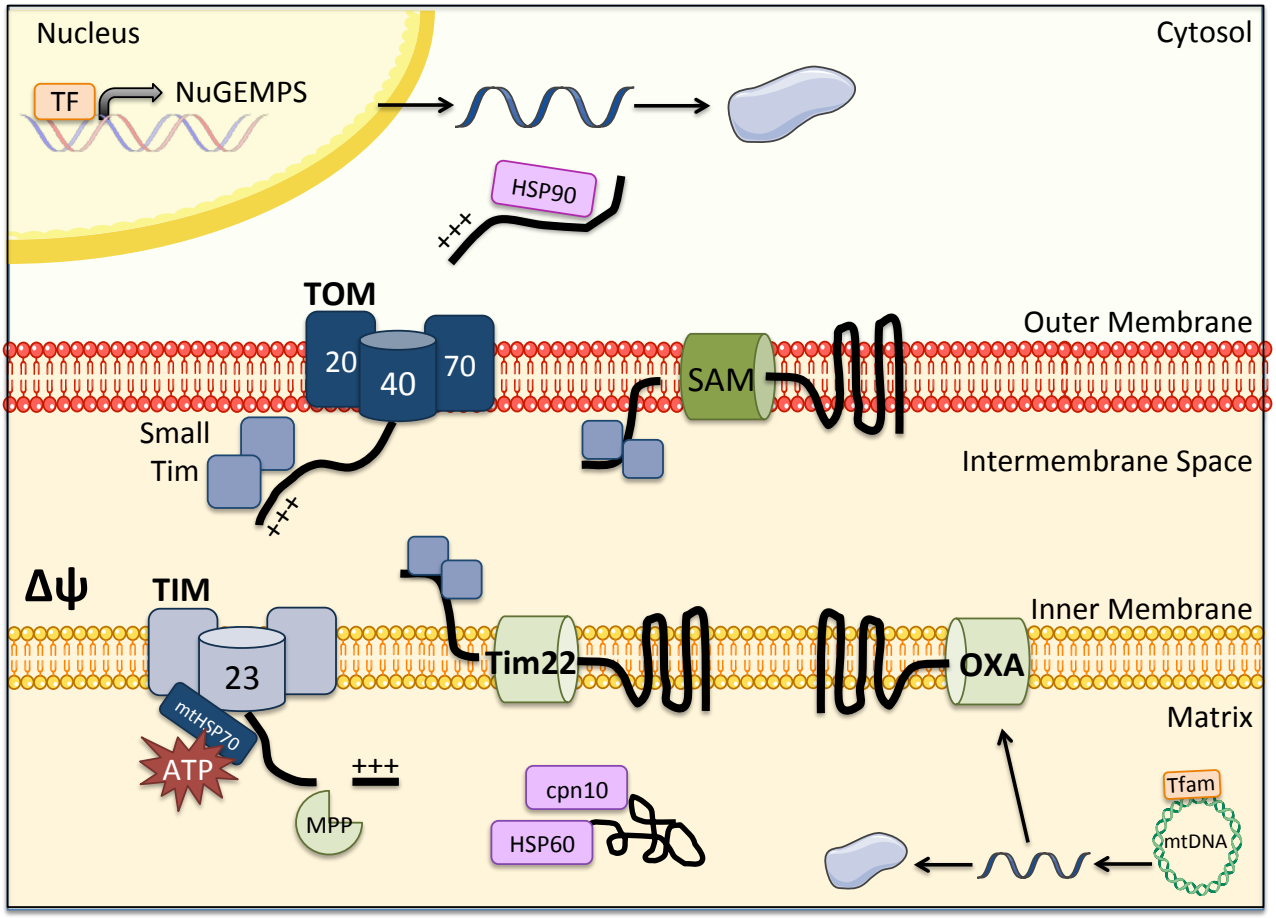

Figure 1: Mitochondrial protein import machinery. Once a NuGEMP is transcribed and translated in the cytosol, it requires a method of entry into the mitochondrion. All products of NuGEMPs contain a MTS that is recognized by cytosolic chaperones such as HSP90, to facilitate it's unfolding and direct it to the TOM complex. Various receptor subunits of the TOM complex, such as Tom20 and Tom70 bind the preprotein and guide it to the general import pore, Tom40. Depending on the transiting protein's final destination, which is encoded by the MTS, small TIM proteins located in the intermembrane space will facilitate their translocation and guide them to the appropriate complex. Proteins destined for the outer mitochondrial membrane will be guided to the SAM complex, which embeds the protein directly into the outer membrane. Similarly, proteins destined for the inner membrane, are guided to Tim22, which embeds the protein directly into the membrane, this channel is thought to operate in conjunction with, and also independently from the TIM complex. Alternatively, transiting proteins destined for the matrix will be guided to the TIM complex. Tim23 is the major channel of this complex and allows the passage through the inner membrane. Closely associated with the TIM complex is the PAM, whose major component, mtHSP70, binds the transiting protein and actively pulls it into the mitochondrial matrix, thus preventing any retrograde movements in the TIM complex. Once in the matrix, the MTS is cleaved by MPP, and the nuclear-encoded protein is refolded by cytosolic chaperones such as HSP60, into its mature conformation. Mitochondria also contain their own genomic material, which encodes 13 components of the electron transport chain. These genes are transcribed and then translated in the matrix and then embedded in the inner membrane and assembled into mature holoenzymes through Oxa1. (Adapted from 38, 85).

series of co-chaperones (43, 121). Hsp70 and Hsp90, have been shown to bind the Tom70 receptor, thereby initiating protein translocation (27, 130).

The receptor subunits then pass on the transiting protein to Tom22, and eventually Tom40, however the mechanism for this interaction is dependent on the receptor (10). Preproteins recognized by Tom20 are passed on to Tom22 through a series of binding events known as the "binding chain hypothesis" (17). In this model, Tom6 and Tom7 play reciprocal roles in stabilizing and destabilizing the interaction between receptor and pore, respectively (26, 42). Alternatively, proteins recognized by the Tom70 receptor are transferred in a manner known as the "translocation in loop formation" where the C- and N-termini are both exposed to the cytosol and the middle section is exposed to the IMS first (26). Both mechanisms rely on membrane potential ($\Delta\Psi$) for translocation through the outer membrane (11). The TOM complex acts as a common gate for all nuclear encoded proteins, from which they are further sorted based on their final destination within the mitochondria.

Proteins destined for the mitochondrial matrix are guided from Tom40 through the IMS by small TIM proteins (114). The TIM complex has a similar organization as the TOM complex. It contains a general pore (Tim23) through which proteins in a linear conformation are able to pass, a receptor (Tim44), and various regulatory subunits (22). Small TIM chaperones in the IMS guide translocating proteins to Tim44. Passage through Tim23 channel is mediated in part by the magnitude of $\Delta\Psi$ and the availability of ATP (38, 115). Following activation or recognition of a preprotein, Tim44 dimerizes on the matrix domain of the complex to recruit mtHSP70, a mitochondrial chaperone, to assemble the presequence translocase-associated motor (PAM) (7, 18). Through the utilization of ATP, mtHSP70 acts as a ratchet to pull preproteins through the channel and prevent retrograde movements into the IMS (51). This is a critical step since Tim23

does not bind translocating proteins tightly and can therefore oscillate when moving through the channel (7). Once inside the mitochondrial matrix, the N-terminus MTS is cleaved off by mitochondrial processing peptidase (MPP) and refolded by various mitochondrial chaperones such as cpn10, into their mature conformation (33).

Translocation through the TIM complex requires not only $\Delta\Psi$, but also the availability of ATP (115). To ensure that these requirements are met, the TIM complex has been shown to associate with complex IV and complex III of the ETC (38). It is thought that this interaction ensures that the $\Delta\Psi$ is maintained in proximity to the channel and also certifies the supply of ATP. Thus the import pathway, though costly and complicated, has evolved in a manner to promote its efficiency.

2.2 Non-Canonical Import Pathways

As described, the TIM complex is mainly responsible for the trafficking of matrix and inner membrane destined proteins, however there are other channels that facilitate the translocation into other subcompartments within the organelle. In this model, the TOM complex acts as a general pore for all nuclear-encoded mitochondrial proteins allowing their transport through the outer mitochondrial membrane (26, 84). From this point, preproteins are targeted to different channels based on their MTS, which contains information about their sublocalization within the organelle. In the following sections, two other methods of protein import will be discussed (Fig. 1).

2.2.1 Sorting and Assembly Machinery (SAM) Complex

The sorting and assembly machinery (SAM) complex is a main constituent of the β-barrel pathway, known for mediating the insertion of nuclear-encoded proteins destined for the mitochondrial outer membrane (10). The SAM complex is integral for the biogenesis and

assembly of the TOM complex because of its role in mediating the insertion of Tom40 (6). It is comprised of two essential subunits, Sam50 and Sam35, which contribute to channel formation (82). Preproteins destined for the mitochondrial outer membrane contain a β-signal that is recognized by Sam35 and initiates the opening of Sam50 channel (62). Concurrent with this recognition, the cytosolic domain of Tom22 physically interacts with the cytosolic domain of a regulatory subunit, Sam37, forming a TOM-SAM supercomplex (114). This interaction facilitates the transition of the preprotein from the TOM complex to the SAM complex by bringing the transiting preprotein and small TIM chaperones in close proximity to the SAM complex (114). Following translocation through the SAM complex, the mitochondrial distribution and morphology (MDM) complex facilitates the insertion and assembly of β-barrel proteins into the outer membrane (11).

2.2.2 Translocase of the Inner Membrane 22 (Tim22)

Similar to the proteins destined for the outer mitochondrial membrane, there exists a distinct pathway for the insertion of carrier proteins destined for the inner membrane. The translocase of the inner membrane 22 (Tim22) is a voltage-gated channel that responds to internal targeting sequences of multitopic proteins destined for the inner membrane (51, 60, 88). Passage through this channel does not require ATP or mtHSP70, but rather, transport is driven primarily by membrane potential (81). In this pathway, preproteins are recognized by Tom70 and translocate through Tom40 into the IMS through the "translocation in loop formation" hypothesis. Within the IMS small TIM chaperones, Tim9 and Tim10, associate with the three positive matrix-facing loop modules found in carrier proteins destined for the inner membrane and guide the protein to Tim22 (51). Tim10 then interacts with a subunit of the TIM22 complex,

Tim12, facilitating the docking of the preprotein to the channel and allowing its voltage-dependent movement into the inner membrane (7).

Tim22 is integral for the translocation and insertion of carrier proteins into the inner membrane, and has also been shown to mediate the insertion of Tim23 and Tim17 (96, 111). However, there do exist other pathways that mediate the integration of nuclear-encoded proteins into the inner membrane (51). The first is the conservative sorting pathway, in which proteins are imported into the mitochondrial matrix through the TIM complex, and then inserted into the membrane through the matrix side via mitochondrial oxidase assembly protein 1 (Oxa1), an export channel (17, 38, 61). The second is the stop-transfer pathway where the hydrophobic region of the transmembrane region arrests its translocation to the matrix and directs its movement laterally into the inner membrane (17, 38). Therefore, there could be some redundancy within the import pathway to ensure efficiency and stoichiometric maintenance.

2.3 Plasticity of Protein Import

Protein import was widely thought to be a static process, and its dynamic ability to sense and respond to the cell's environment and metabolic status went overlooked for quite some time. Evidence predominantly in yeast, and more recently in mammals, has demonstrated that mitochondrial protein import is a regulatory hub for modulating metabolism as well as various stress responses (38). Thus, the following sections will describe how protein import can adapt to environmental stimuli and its role as a mitochondrial status sensor in mediating stress responses.

2.3.1 Differences in Mitochondrial Subfractions

As previously discussed, mitochondrial exist in two related yet functionally and biochemically distinct subfractions within skeletal muscle: subsarcolemmal (SS) and intermyofibrillar (IMF). Based on their subcellular localization, these pools are equipped to

support different subcellular processes. For example IMF are primarly responsible for supplying ATP for actin-myosin crossbridge cycling. A study conducted by Takahashi and Hood, demonstrated that IMF mitochondria have a 3-4 fold higher rate of import into the mitochondrial matrix and that this is surprisingly not related to ATP production rate (117). They also demonstrated that SS have a greater reliance on cardiolipin, a phospholipid present only in the mitochondrial membrane for protein import, therefore the mechanism and capacity for protein import differ in mitochondrial subfractions within skeletal muscle (117). Thus it is proposed that, in part, mitochondria in part derive a portion of their compositional and functional heterogeneity between pools based on differential regulation of the protein import pathway.

2.3.2 Adaptability of the PIM

The ability for the mitochondrial reticulum to adapt and respond to various environmental stimuli is what makes it such a dynamic and metabolically relevant organelle. Protein import plays a large role in mediating the adaptability of the organelle since it mediates the expansion of the reticulum. It is widely known that repeated bouts of endurance exercise result in increased mitochondrial content, and many studies have focused on various transcription factors and coactivators that coordinate changes to gene expression to promote this adaptation. However, chronic contractile activity has also been shown to increase the expression of various PIM components and the assembly of the import complexes, thereby increasing the capacity for protein import and thus, mitochondrial expansion (53, 116). Besides the elevation in PIM content, exercise may also influence the rate of protein import following exercise. Takahashi et al. demonstrated that the addition of a cytosolic fraction from an animal subjected to a model of endurance exercise stimulates the rate of protein import in mitochondria isolated from control animals by 2-fold (116). These findings identified that the increased import rate was in part due

to increased mitochondrial import stimulating factor (MSF) present in the cytosolic fraction of trained animals. However, MSF is not the only factor required for this acceleration, but these stimulants remain to be identified (116). Therefore, the ability of PIM to respond to increased metabolic demand contributes to mitochondrial biogenesis in the context of exercise training.

Conversely, there are various instances that depress protein import in the face of cellular stress. Muscle atrophy as a result of muscle disuse has garnered a lot of attention, especially the mechanisms that underlie this muscle wasting and the concomitant mitochondrial dysfunction. Typically, the stars of muscle atrophy are proteolytic pathways that are increased and promote an exaggerated rate of protein breakdown leading to this phenotype. However, using a denervation model, Singh et al. highlighted a role for protein import in mediating and exacerbating muscle atrophy. In this model, chronic muscle disuse increases reactive oxygen species (ROS) production, which negatively influences the rate of protein import in a dose-dependent manner (110). The reduction in protein import exacerbates the decline in mitochondrial content thereby serving as a positive feedback loop promoting proteolytic pathways and aggravating muscle atrophy (110). The sensitivity of the protein import pathway to ROS suggests a potential mechanism for mitochondrial dysfunction and reduced content in the face of oxidative stress, which has yet to be further explored.

2.4 Role of Import in Metabolism

As outlined in the previous sections, import is a crucial step in the regulation of mitochondrial biogenesis and the maintenance of organelle content during health and disease states. Besides its role in mediating the expansion of the reticulum, import is also vastly intertwined in metabolism and the overall maintenance of the mitochondrion.

Import has widely been studied in yeast, and work from these lower order organisms has outlined a role for protein import during respiration and fermentation based on the availability of glucose. In yeast, protein kinase A (PKA) is inactive in the absence of glucose, allowing import to proceed and to promote respiration. However, when glucose is in high abundance, PKA is activated and phosphorylates Tom40 thereby negatively impacting protein import and limiting mitochondrial biogenesis (38, 85). PKA has also been shown to target the receptor Tom70 to impair the binding of cytosolic chaperones to initiate translocation (38). Work in yeast has highlighted the transient post-translational level of regulation on the PIM, through phosphorylation events that can impact import rate and assembly.

Recently, the understanding of protein import has undergone a paradigm shift where import is now being appreciated for being more than a mere means of entry into the organelle, but also a sensor of mitochondrial status and for communicating this with the cell. An example of this is the PINK1/Parkin-dependent pathway of mitophagy. PINK1 is a kinase with a mitochondrial matrix targeting sequence, which under basal conditions is imported into the mitochondrial matrix and degraded by a mitochondrial protease, presenilins-associated rhomboid-like protein (PARL) (95, 127). However, since protein import into the matrix is dependent on $\Delta\Psi$, when the organelle is dysfunctional, a hallmark characteristic is a loss of membrane potential. PINK1 is no longer imported into the matrix and its translocation is arrested at the outer membrane where it can recruit Parkin, an E3 ubiquitin ligase, from the cytosol (78). Parkin ubiquitinates outer membrane proteins that flag the organelle for degradation through mitophagy (23). Thus the inability for the organelle to import selective proteins can initiate mitochondrial recycling processes to maintain an optimal pool. Therefore, this illustrates that

protein import is in a unique position to rapidly detect changes in potential as a marker for mitochondrial status and communicate this loss of function with the cell (38, 59).

Similarly, in lower order organisms, a role for import in the early signaling events of a protein quality control has recently been discovered. The mitochondrial unfolded protein response (UPR^{mt}) will be discussed in a later section, but briefly it is responsible for removing proteotoxic stress within the mitochondria by either refolding or degrading misfolded proteins (54). In *C. elegans*, activating transcription factor associated with stress-1 (ATFS-1) is normally imported into the mitochondrial matrix and degraded by LonP. However, when the UPR^{mt} is activated, ATFS-1 import into the mitochondrion is blocked and it preferentially translocates into the nucleus. The mechanism for this switch is still poorly understood but is described in detail elsewhere (80). This quality control mechanism is just another example of how protein import serves as a sensor of mitochondrial fitness in an attempt to regain homeostasis. Therefore, import is not merely a means of entry into the organelle, but rather has far-reaching implications in metabolism and cellular homeostasis.

3.0 MITOCHONDRIAL PROTEOSTASIS

Protein conformation dictates structure and function, and for this reason protein folding is a crucial step in protein maturation. Unfortunately, protein folding is an inherently error-prone process and misfolded proteins can be toxic to the cell if left to accumulate. Therefore, protein homeostasis, commonly referred to as "proteostasis" must be maintained by either refolding or degrading misfolded proteins (40). Within the cell, there are various organelles that are more prone to protein misfolding due to their function or structure, such as the endoplasmic reticulum (ER) and the mitochondria. The ER is where a large proportion of proteins are translated and assume their mature conformation; therefore it is equipped with its own unfolded protein

response (UPR^{ER}) (126). As previously discussed, due to the nature of protein import pathway, mitochondrial proteins must be unfolded in order to pass through the β-barrel channels of the outer and inner membrane, and then be refolded upon reaching their destination. Thus protein folding takes place within the various subcompartments of the organelle, making mitochondria susceptible to misfolding. It is therefore equipped with an independent unfolded protein response (UPR^{mt}) (54).

3.1 Mitochondrial UPR in *C. elegans*

The UPR^{mt} is a highly conserved quality control mechanism that was first discovered in mammals, but has since been well characterized in *C.elegans* (3, 47, 89). Similar to mammals, the UPR^{mt} aims to regain proteostasis by refolding or degrading misfolded proteins that may exert toxic effects on the organelle (Fig. 2). Within the mitochondria, the IMS and matrix are both major sites for protein misfolding and are thus equipped with compartment-specific chaperones and proteases to remove proteotoxicity (54). If ever this stress exceeds the capacity of the subcompartment to deal with it, the UPR^{mt} initiates retrograde signaling cascades to increase the expression of protein quality control (PQC) genes (76) (Fig. 2).

In these lower order organisms, misfolded proteins can be degraded by caseinolytic mitochondrial matrix peptidase (ClpP) into 6-30 amino acid protein fragments, which have been shown to be important in the retrograde signaling events (39, 58). These proteolytically-derived peptides are exported from the matrix through a channel in the inner membrane, HAF-1, and are thought to readily diffuse through the outer membrane into the cytosol (41). The presence of these protein fragments in the cytosol influences the tranlocation of activating transcription factor with stress-1 (ATFS-1) (40, 80). ATFS-1 contains both a nuclear localization signal (NLS) and a MTS, allowing for its dynamic regulation (80). Basally, ATFS-1 is imported into the

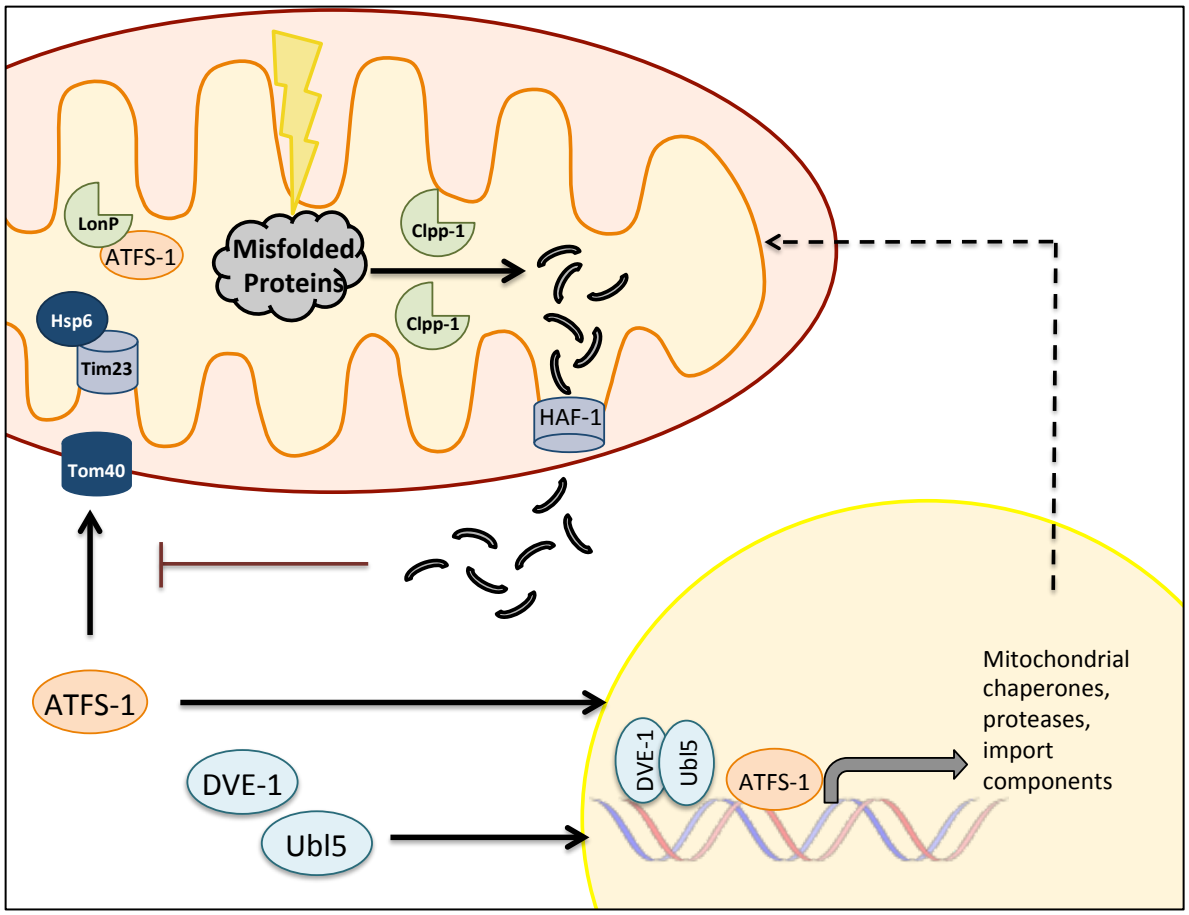

Figure 2: Mitochondrial unfolded protein response in *C. elegans*. Basally, ATFS-1, the homologue of ATF5, is imported into the mitochondrion and degraded by LonP. However, in the presence of proteotoxic stress, Clpp-1 degrades misfolded proteins into peptides. These peptides are then exported into the cytosol by HAF-1. Once in the cytosol, these peptides block the ability of ATFS-1 to translocate into the mitochondrion and therefore force its movement into the nucleus. The mechanism for this is still unknown. The accumulation of misfolded proteins also activates DVE-1 and Ubl5, two transcription factors that heterodimerize upon entry into the nucleus. Together, DVE-1, Ubl5 and ATFS-1 promote the transcription of mitochondrial chaperones, proteases and import components, thereby increasing the organelle's capacity to deal with future proteotoxic insults. (Adapted from 54, 89).

mitochondrial matrix and degraded by LonP, however in the presense of these peptides, ATFS-1 preferentially localizes to the nucleus where it increases the expression of a host of genes to regain proteostasis (55, 80). ATFS-1 is responsible for transcriptionally upregulating mitochondrial chaperones, proteases, import components, detoxification enzymes and autophagy markers as a means of increasing the capacity to deal with future stress (89). However, ATFS-1 is not the only transcriptional regulator activated during the UPR^{mt}. DVE-1 and Ubl5 also translocate into the nucleus to upregulate various chaperones and proteases, some of which are also targets of ATFS-1 thereby providing some redundancy in the system (55).

Work in *C.elegans* has also demonstrated that the UPR^{mt} has other functions besides the maintenance of proteostasis. Activation of the UPR^{mt} has been documented to play a role in metabolism, innate immunity, longevity and the metabolic coordination of distal tissues (9, 66, 73, 79, 90, 118). It was originally thought that under stress conditions ATFS-1 was completely redirected into the nucleus, however it has become clear that a portion of total ATFS-1 is still imported into the mitochondria during stress and can bind to the UPR^{mt} element (UPR^{mt}E) within mtDNA. This redistribution of ATFS-1 limits the accumulation of both nuclear- and mitochondrial-encoded oxidative phosphorylation transcripts, while simultaneously promoting a shift towards glycolysis. Many of the OXPHOS genes do not contain UPR^{mt}E in their promoters, therefore it is thought that this repression may be indirect. This provides an important switch during stress towards a greater glycolytic reliance, thereby providing the organelle with time to repair.

In lower-order organisms activation of the UPR^{mt} has been found to display mitohormetic effects. Mitohormesis is a process through which low levels of mitochondrial stress are actually beneficial in promoting increased lifespan and protection against future insults (131). Recently

various papers have begun to describe how the activation of the UPR^{mt} also promotes chromatin remodeling through the upregulation of histone lysine demethylases, histone methyltransferases and nuclear co-factors (73, 118). These epigenetic modifications promote longevity when activated through the UPR^{mt} as a result of mild mitochondrial stress. It is thought that activation of the histone methyltransferase, met2 and lin-65, a nuclear co-factor, reorganize the chromatin to allow DVE-1 DNA binding. This also promotes persistant reorganization of the chromatin, thereby extending lifespan (118).

This quality control mechanism has garnered attention in neural tissue since its activation is frequently seen in neurodegenerative diseases. Work in neurons of *C.elegans* in 2016 uncovered an endocrine-like function of the UPR^{mt}. In this model, activation of the UPR^{mt} in neurons promotes the release of serotonin, which communicates with distal tissues to activate the UPR and coordinate metabolism, despite no proteotoxic stress in these tissues (9). At around the same time, another group discovered a neuropeptide, FLP-2 that is released from neurons undergoing proteotoxicity and coordinates non-autonomous activation of the UPR^{mt} and metabolism (108). This is intriguing because many neurodegenerative diseases display declines in metabolism in tissues outside of the central nervous system. However, it is unclear if the release of serotonin and FLP-2 is coordinated or if they are independent, and whether or not these are viable targets for treatment in mammals.

3.2 Mitochondrial UPR in Mammals

The mammalian UPR is a highly conserved quality control mechanism that shares many parallels with *c.elegans*, however it is not as well characterized as in invertebrates. Similar to *c.elegans*, the UPR^{mt} is subcompartment specific, and as such it is equipped with chaperones and

proteases specific to either the IMS or the matrix, and stress within each compartment results in activation of compartment specific transcriptional programs (55).

Protein misfolding can occur in any of the subcompartments within the mitochondria due to the nature of the PIM and the organelle's reliance on both genomes (54). When proteins accumulate in the IMS, there are a host of compartment-specific proteases, such as OMI, in place to proteolytically relieve the stress. Proteotoxic stress within the IMS induces an increase in ROS, which culminates in the activation of estrogen-related receptor-α (ERRα) through its phosphorylation by Akt (76). ERRα can act as a transcription factor upon activation to increase an IMS-specific transcriptional program.

Alternatively, proteins that become unfolded or are not incorporated into their holoenzyme (i.e. orphaned subunits) within the matrix activate a different branch of the UPR^{mt} (Fig. 3). Proteotoxicity within the matrix is handled by a variety of chaperones such as Hsp60, and chaperonin 10 (cpn10) and resident proteases such as ClpP, and LonP (55). Perturbation of matrix-specific proteostasis prevents further accumulation by degrading Tim17, a regulatory subunit of the TIM complex, by membrane bound protease Yme1l to reduce protein import into the compartment. Concurrently, dsRNA-activated protein kinase (PKR) phosphorylates eIF2α to inhibit global protein translation similar to the integrated stress response (ISR) (86). Furthermore, JNK2 senses the increased ROS production typically seen with proteotoxic stress, which in turn activates c-jun, a transcription factor that regulates CHOP (3). CHOP heterodimerizes with C/EBPβ to upregulate mitochondrial UPR genes and increase the capacity of the organelle to deal with future proteotoxic stress (76, 133). Interestingly, CHOP is also a regulator of the UPR^{ER}, however the genes that are transcriptionally upregulated are different depending on which compartment the stress originated in (126). The mitochondrial PQC genes

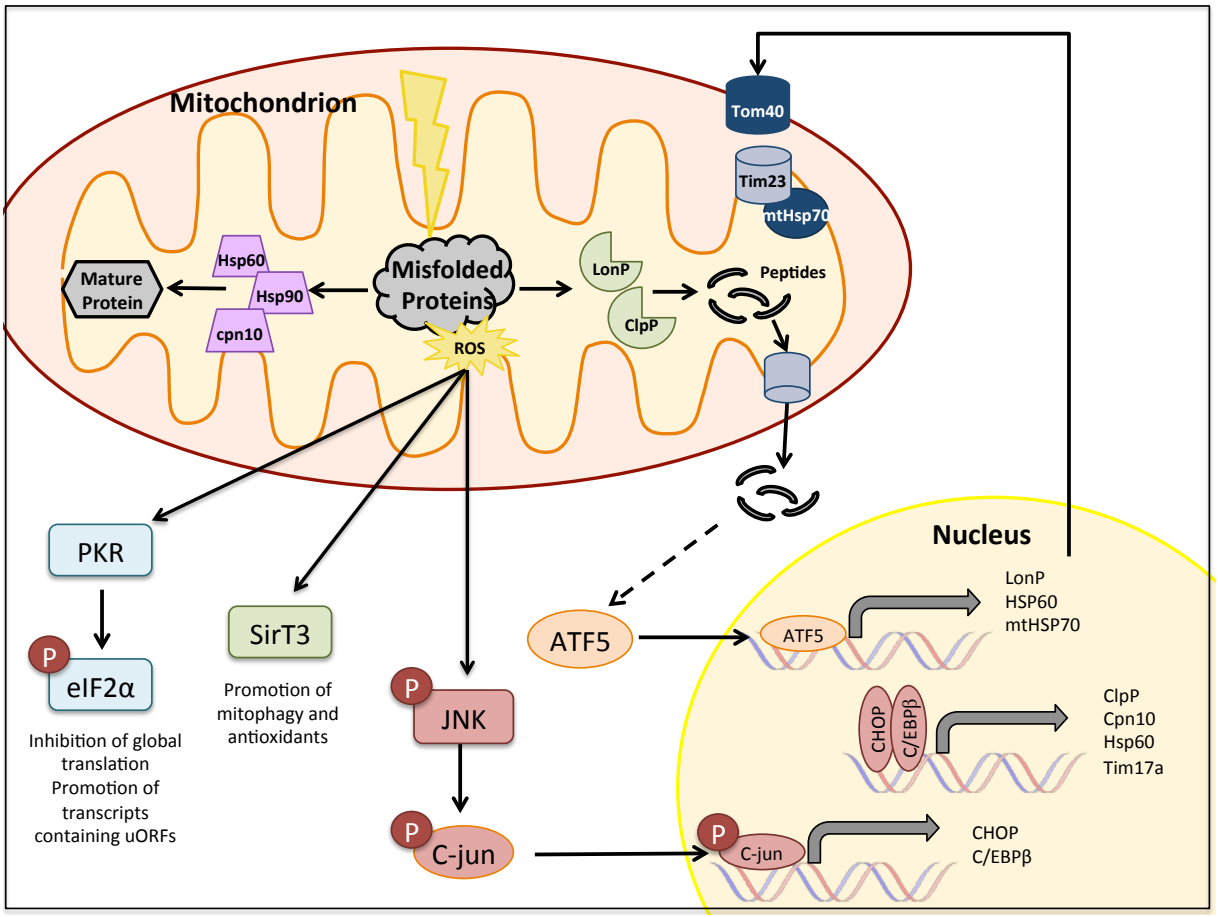

Figure 3: Mammalian mitochondrial unfolded protein response. Under conditions of stress or high volumes of protein synthesis, proteins may become misfolded. In order to combat the toxic effects that are exerted by misfolded proteins, the mitochondrion is equipped with a protein quality control mechanism termed the UPR^{mt}. Misfolded proteins can either be refolded into a mature conformation by resident chaperones, such as cpn10 and HSP60, or degraded by proteases, such as LonP and ClpP. If the stress exceeds the capacity of these quality control proteins, misfolded proteins can accumulate and aggregate. This accumulation is typically associated with an elevation of ROS, which signals the activation of the UPR^{mt}. In response, PKR is activated and phosphorylates eIF2α, which inhibits global translation, while promoting the translation of transcripts that contain uORFs. In order to combat the elevation in ROS, a deacetylase, SirT3 is activated to promote the transcription of mitochondrial antioxidants. However, if the stress is prolonged and unresolved, SirT3 can also promote the recycling of the organelle through mitophagy. JNK, a mitogen-activated protein kinase, can sense the heightened ROS and promote the transcription of CHOP and C/EBPβ, through the phosphorylation of transcription factor c-jun. CHOP and C/EBPβ then heterodimerize to transcriptionally upregulate various mitochondrial chaperones and proteases. ATF5's activation is thought to be dependent on the export of proteolytically-derived peptides, thus promoting its translocation into the nucleus where it acts as a transcription factor to promote the transcription of LonP, HSP60 and mtHSP70. Both ATF5 and CHOP increase the capacity to deal with future mitochondrial proteotoxic stress. (Adapted from 54, 76).

regulated by CHOP all contain a UPR^{mt} response elements (MURE) that flank the CHOP binding site within the promoters of its target genes (3). These MURE sites may provide a level of specificity during CHOP activation, however no transcription factors or co-factors to date have been found to bind these elements.

Concurrent with the activation of CHOP, ROS is also responsible for activating another independent branch of the UPR^{mt}. SirT3, a deacetylase sensitive to the increased oxidative stress typically seen with proteotoxicity, activates forkhead box O3 (FOXO3) promoting its nuclear translocation (87). FOXO3 transcriptionally regulates antioxidant proteins and the activation of mitophagy, thereby increasing antioxidant machinery to combat the elevated ROS. During prolonged exposure to proteotoxicity, mitophagy is able to recycle the damaged organelle through the PINK1-Parkin pathway, if the stress is not dealt with. Interestingly, this recycling does not require the canonical loss of membrane potential, but rather seems to be initiated due to competitive proteolytic degradation whereby PINK1 can no longer be degraded because the mitochondrial proteases are targeting the misfolded proteins (52).

Despite the evolutionary conservation of the UPR^{mt} throughout many species, there are however some differences between invertebrates and mammals. Roles for the mammalian homologues of DVE-1 and Ubl5, SatB2 and Ubl5 respectively, in regulating changes in gene expression have not been identified to date. Furthermore, until recently it was unclear whether or not proteolysis had similar signaling roles in mammals as it does in *c.elegans*. As previously described, in worms the proteolytic byproducts are exported from the matrix into the cytosol where they influence the translocation of ATFS-1 (58, 80). Less than a year ago, ATF5 was identified as the mammalian homologue of ATFS-1, and preliminary evidence suggests that it is

regulated in a similar fashion to its nematode counterparts (31). The exact mechanism of this retrograde signaling has yet to be investigated.

The novel roles for the UPR^{mt} in mediating longevity, coordinating metabolism and non-autonomous regulation of distal tissues in invertebrates, has warranted the question of whether or not these are paralleled in mammals. Unfortunately, activation of the UPR^{mt} and extension of lifespan do not seem to be related phenomena in mammals. This could be due to the complexity of mammals compared to lower-order organisms like *Caenorabditis elegans* and *Drosophila melanogaster*. However activation of quality control mechanisms in mammalian skeletal muscle was shown to promote the release of a myomitokine, GDF15 (19). This growth and differentiation factor then acts in an endocrine fashion to regulate metabolism in distal tissues to protect against obesity and insulin resistance (19). Therefore, although the UPR is a highly conserved mechanism, there are some major differences between species.

3.3 Retrograde Signals in the UPR

Communication between the mitochondrion and the nucleus is mediated by a plethora of signaling molecules. The aim of the UPR is to regain proteostasis in the face of accumulated misfolded proteins, and to protect the organelle from future stress. The latter is achieved through changes in gene expression that drive the synthesis of new chaperones and proteases, thus increasing the capacity to deal with future insults. This communication during the UPR^{mt} is thought to be mediated by two retrograde signaling molecules: ROS and proteolytic byproducts, or peptides.

3.3.1 Reactive Oxygen Species (ROS)

Reactive oxygen species are radical molecules notorious for inducing DNA damage and oxidizing proteins, thereby altering their function by modifying critical amino acid residues. On

the other hand, ROS are indispensible to the cell for its role as a signaling molecule and for mediating adaptations, such as exercise-induced mitochondrial biogenesis (100). Thus, ROS exhibit a mitohormetic effect, whereby up to a theoretical threshold ROS are beneficial to the cell but past this limit they are detrimental due to their role in damaging redox reactions. Mitochondria are a large site for ROS production within the cell. This occurs when electrons prematurely slip from complex I or III leading to the early reduction of oxygen and the generation of superoxides.

Oxidative stress is tightly coupled to protein folding, since the presence of ROS may induce protein misfolding, and proteotoxic stress may itself increase ROS production. Thus, ROS are pivotal signaling molecules during the UPR^{mt}, and they mediate, in part, the communication between the mitochondrion and nucleus in this response (89). Within the organelle ROS are sensed by JNK, a mitogen sensitive kinase that phosphorylates c-jun, a transcription factor, resulting in an increase in CHOP and C/EBPβ expression (76). The exact mechanism through which ROS activate JNK is still poorly understood, but it is thought that they modify upstream regulators of JNK (113). For example, ASK1 is a regulator of JNK basally, held inactive through its interaction with thioredoxin. However in the presence of oxidative stress, thioredoxin is oxidized and released from ASK1, thereby activating JNK (112). ROS have also been shown to directly inhibit MKPs, which maintain the JNK pathway in an inactive state (112). In the context of the UPR^{mt} signaling, the mechanism for ROS sensing has not been studied.

Alongside this, SirT3 is activated in a ROS-dependent manner to induce antioxidant machinery and mitophagy, if necessary. The mechanism through which ROS mediate the

activation of SirT3 is still unclear, however using ROS scavengers such as NAC, ROS have been shown to be critical in the activation of SirT3 in the context of UPR^{mt} (87).

3.3.2 Mitochondrial Proteolysis

During the UPR^{mt}, misfolded proteins are degraded into protein fragments (i.e. peptides) by resident proteases. From a series of experiments conducted in *C.elegans,* a role for peptides in mediating retrograde signaling during the UPR^{mt} was elucidated. In this model, ablation of ClpP, a mitochondrial protease decreased the production of these peptides and reduced the activation of ATFS-1 (39). In mammals, the role of ClpP in mediating UPR^{mt} signaling remains highly controversial in the literature. Work in muscle cells using knockdown of ClpP and the overexpression of its chaperone subunit, ClpX, provide evidence for its role in the UPR^{mt} (2, 21). However, in cardiac muscle in a model of cardiomyopathy, loss of ClpP does not affect the UPR^{mt} (107). In *C. elegans*, knockdown of HAF-1, the channel through which peptides are emitted from the matrix, reduces the ability of the cell to combat proteotoxic stress (41). It is proposed that the proteolytic byproducts are released into the cytosol where they promote the nuclear translocation of ATFS-1 into the nucleus, allowing it to transcriptionally activate PQC genes (58, 80). Although, the mammalian homologue of HAF-1, ABCB10 does not appear to facilitate the export of peptides from the mitochondrion, it may however have a role in UPR^{mt} signaling though the mechanism is still unknown (129).

The mechanism for this retrograde signal has not been elucidated, however there are some proposed theories that have yet to be experimentally tested (58). The first hypothesis is that the peptides are acting directly on a cytosolic peptide receptor that then influences ATFS-1 translocation. Another possibility is that the peptides themselves are not being sensed, but rather the rate at which peptides are exported into the cytosol is a signal for ATFS-1 nuclear

translocation. The third hypothesis is that the presence of peptides in the cytosol influences the PIM to inhibit the translocation of nuclear proteins into the mitochondria. This therefore redirects ATFS-1 translocation from the mitochondrion to the nucleus.

Thus based on the current understanding of the mammalian UPR^{mt} and its activation, we aim to elucidate its relationship with protein import in the stoichiometric maintenance of the mitochondrion. By perturbing the import machinery *in vivo* we can address the effects of a mito-nuclear imbalance on mitochondrial function and proteostasis within skeletal muscle. Furthermore, we wish to address the mechanisms that mediate the communication between the mitochondrion and the nucleus during UPR^{mt} activation. The retrograde signals involved in this process have yet to be elucidated. Understanding the signaling events involved in the UPR^{mt} will promote better understanding of the maintenance of proteostasis since it has been implicated in aging, neurodegenerative disorders and various cancers.

RESEARCH OBJECTIVES

Thus, based on my review of literature, the objectives of my thesis were to:

1. Study the relationship between an import defect and the maintenance of stoichiometry between the nuclear and mitochondrial genomes;
2. Examine the effect of a mito-nuclear protein imbalance *in vivo* on mitochondrial function in skeletal muscle by perturbing the PIM, specifically Tim23;
3. Explore mitochondrial proteolysis and the release of peptides in a mammalian model;
4. Investigate a potential role for peptides in retrograde signaling by mediating protein import during UPR^{mt} activation.

HYPOTHESES

1. A mitochondrial protein import defect will perturb the balance between the nuclear and mitochondrial genomes thereby activating the UPR^{mt} to maintain proteostasis;
2. Partial loss of Tim23 will result in mitochondrial dysfunction, characterized by a deficit in protein import, reduced respiratory capacity and elevated ROS emission;
3. Mitochondria will release protein fragments, and this proteolysis and subsequent export will be susceptible to oxidative stress;
4. Mitochondrially-derived peptides will negatively influence protein import in a dose- and time-dependent manner, thereby serving as a possible mechanism for communicating a loss of proteostasis within the mitochondrion to the nucleus to modify gene expression.

References

1. **Akimoto T**, **Sorg BS**, **Yan Z**. Real-time imaging of peroxisome proliferator-activated receptor- coactivator-1 promoter activity in skeletal muscles of living mice. *AJP Cell Physiol* 287: C790–C796, 2004.

2. **Al-furoukh N**, **Ianni A**, **Nolte H**, **Hölper S**, **Krüger M**, **Wanrooij S**, **Braun T**. ClpX stimulates the mitochondrial unfolded protein response (UPR mt) in mammalian cells. *BBA - Mol Cell Res* 1853: 2580–2591, 2015.

3. **Aldridge JE**, **Horibe T**, **Hoogenraad NJ**. Discovery of genes activated by the mitochondrial Unfolded Protein Response (mtUPR) and cognate promoter elements. *PLoS One* 2, 2007.

4. **Amat R**, **Planavila A**, **Chen SL**, **Iglesias R**, **Giralt M**, **Villarroya F**. SIRT1 controls the transcription of the peroxisome proliferator-activated receptor-γ co-activator-1α(PGC-1α) gene in skeletal muscle through the PGC-1α autoregulatory loop and interaction with MyoD. *J Biol Chem* 284: 21872–21880, 2009.

5. **Baar K**. Adaptations of skeletal muscle to exercise: rapid increase in the transcriptional coactivator PGC-1. *FASEB J* 16: 1879–1886, 2002.

6. **Baker MJ**, **Frazier AE**, **Gulbis JM**, **Ryan MT**. Mitochondrial protein-import machinery: correlating structure with function. *Trends Cell Biol* 17: 456–464, 2007.

7. **Bauer MF**, **Hofmann S**, **Neupert W**, **Brunner M**. Protein translocation into mitochondria: the role of TIM complexes. *Trends Cell Biol* 10: 25–31, 2000.

8. **Bellot G**, **Garcia-Medina R**, **Gounon P**, **Chiche J**, **Roux D**, **Pouyssegur J**, **Mazure NM**. Hypoxia-Induced Autophagy Is Mediated through Hypoxia-Inducible Factor Induction of BNIP3 and BNIP3L via Their BH3 Domains. *Mol Cell Biol* 29: 2570–2581, 2009.

9. **Berendzen KM**, **Durieux J**, **Shao LW**, **Tian Y**, **Kim H eui**, **Wolff S**, **Liu Y**, **Dillin A**. Neuroendocrine Coordination of Mitochondrial Stress Signaling and Proteostasis. *Cell* 166: 1553–1563, 2016.

10. **Bohnert M**, **Pfanner N**, **van der Laan M**. A dynamic machinery for import of mitochondrial precursor proteins. *FEBS Lett* 581: 2802–2810, 2007.

11. **Bolender N**, **Sickmann A**, **Wagner R**, **Meisinger C**, **Pfanner N**. Multiple pathways for sorting mitochondrial precursor proteins. *EMBO Rep* 9: 42–49, 2008.

12. **Brookes PS**. Calcium, ATP, and ROS: a mitochondrial love-hate triangle. *AJP Cell Physiol* 287: C817–C833, 2004.

13. **Calvo JA**, **Daniels TG**, **Wang X**, **Paul A**, **Lin J**, **Spiegelman BM**, **Stevenson SC**, **Rangwala SM**. Muscle-specific expression of PPAR coactivator-1 improves exercise performance and increases peak oxygen uptake. *J Appl Physiol* 104: 1304–1312, 2008.

14. **Calvo SE**, **Clauser KR**, **Mootha VK**. MitoCarta2.0: an updated inventory of mammalian mitochondrial proteins. *Nucleic Acids Res* 44: D1251-1257, 2015.

15. **Cannavino J**, **Brocca L**, **Sandri M**, **Bottinelli R**, **Pellegrino MA**. PGC1-α over-expression prevents metabolic alterations and soleus muscle atrophy in hindlimb unloaded mice. *J Physiol* 592: 4575–4589, 2014.

16. **Carroll S**, **Nicotera P**, **Pette D**. Calcium transients in single fibers of low-frequency stimulated fast-twitch muscle of rat. *Am J Physiol* 277: C1122–C1129, 1999.

17. **Chacinska A**, **Koehler CM**, **Milenkovic D**, **Lithgow T**, **Pfanner N**. Importing mitochondrial proteins: machineries and mechanisms. *Cell* 138: 628–644, 2009.

18. **Chen D**, **Wilkinson CRM**, **Watt S**, **Penkett CJ**, **Toone WM**, **Jones N**, **Bähler J**. High-resolution crystal structure and in vivo function of a kinesin-2 homologue in giardia intestinalis. *Mol Biol Cell* 19: 308–317, 2007.

19. **Chung HK**, **Ryu D**, **Kim KS**, **Chang JY**, **Kim YK**, **Yi HS**, **Kang SG**, **Choi MJ**, **Lee SE**, **Jung SB**, **Ryu MJ**, **Kim SJ**, **Kweon GR**, **Kim H**, **Hwang JH**, **Lee CH**, **Lee SJ**, **Wall CE**, **Downes M**, **Evans RM**, **Auwerx J**, **Shong M**. Growth differentiation factor 15 is a myomitokine governing systemic energy homeostasis. *J Cell Biol* 216: 149–165, 2017.

20. **Cogswell AM**, **Stevens RJ**, **Hood DA**. Properties of skeletal muscle mitochondria from subsarcolemmal and intermyofibrillar isolated regions. *Am J Physiol Cell Physiol* 264: C383–C389, 1993.

21. **Deepa SS**, **Bhaskaran S**, **Ranjit R**, **Qaisar R**, **Nair BC**, **Liu Y**, **Walsh ME**, **Fok WC**, **Van Remmen H**. Down-regulation of the mitochondrial matrix peptidase ClpP in muscle cells causes mitochondrial dysfunction and decreases cell proliferation. *Free Radic Biol Med* 91: 281–292, 2015.

22. **Demishtein-Zohary K**, **Azem A**. The TIM23 mitochondrial protein import complex: function and dysfunction. *Cell Tissue Res* 367: 33–41, 2017.

23. **Ding WX**, **Yin XM**. Mitophagy: Mechanisms, pathophysiological roles, and analysis. *Biol Chem* 393: 547–564, 2012.

24. **Dudley GA**, **Abraham WM**, **Terjung RL**. Influence of exercise intensity and duration on biochemical adaptations in skeletal muscle. *J Appl Physiol* 53: 844–850, 1982.

25. **Erlich AT**, **Tryon LD**, **Crilly MJ**, **Memme JM**, **Moosavi ZSM**, **Oliveira AN**, **Beyfuss**

K, **Hood DA**. Function of specialized regulatory proteins and signaling pathways in exercise-induced muscle mitochondrial biogenesis. *Integr Med Res* 5: 187–197, 2016.

26. **Esaki M**, **Shimizu H**, **Ono T**, **Yamamoto H**, **Kanamori T**, **Nishikawa SI**, **Endo T**. Mitochondrial protein import. Requirement of presequence elements and TOM components for precursor binding to the TOM complex. *J Biol Chem* 279: 45701–45707, 2004.

27. **Fan ACY**, **Bhangoo MK**, **Young JC**. Hsp90 functions in the targeting and outer membrane translocation steps of Tom70-mediated mitochondrial import. *J Biol Chem* 281: 33313–33324, 2006.

28. **Fan J**, **Kou X**, **Jia S**, **Yang X**, **Yang Y**, **Chen N**. Autophagy as a potential target for sarcopenia. *J Cell Physiol* 231: 1450–1459, 2016.

29. **Fentz J**, **Kjøbsted R**, **Kristensen CM**, **Hingst JR**, **Birk JB**, **Gudiksen A**, **Foretz M**, **Schjerling P**, **Viollet B**, **Pilegaard H**, **Wojtaszewski JFP**. AMPKα is essential for acute exercise-induced gene responses but not for exercise training-induced adaptations in mouse skeletal muscle. *Am J Physiol - Endocrinol Metab* 309: E900–E914, 2015.

30. **Finck BN**, **Kelly DP**. PGC-1 coactivators: Inducible regulators of energy metabolism in health and disease. *J Clin Invest* 116: 615–622, 2006.

31. **Fiorese CJ**, **Schulz AM**, **Lin Y**, **Rosin N**, **Pellegrino MW**, **Haynes CM**. The transcription factor ATF5 mediates a mammalian mitochondrial UPR. *Curr Biol* 26: 2037–2043, 2016.

32. **Frank M**, **Duvezin-Caubet S**, **Koob S**, **Occhipinti A**, **Jagasia R**, **Petcherski A**, **Ruonala MO**, **Priault M**, **Salin B**, **Reichert AS**. Mitophagy is triggered by mild oxidative stress in a mitochondrial fission dependent manner. *Biochim Biophys Acta - Mol Cell Res* 1823: 2297–2310, 2012.

33. **Gakh O**, **Cavadini P**, **Isaya G**. Mitochondrial processing peptidases. *Biochim Biophys Acta - Mol Cell Res* 1592: 63–77, 2002.

34. **Geisler S**, **Holmström KM**, **Skujat D**, **Fiesel FC**, **Rothfuss OC**, **Kahle PJ**, **Springer W**. PINK1/Parkin-mediated mitophagy is dependent on VDAC1 and p62/SQSTM1. *Nat Cell Biol* 12: 119–131, 2010.

35. **Glancy B**, **Hartnell LM**, **Malide D**, **Yu Z-X**, **Combs CA**, **Connelly PS**, **Subramaniam S**, **Balaban RS**. Mitochondrial reticulum for cellular energy distribution in muscle. *Nature* 523: 617–620, 2015.

36. **Gurd BJ**. Deacetylation of PGC-1α by SIRT1: importance for skeletal muscle function and exercise-induced mitochondrial biogenesis. *Appl Physiol Nutr Metab* 36: 589–597, 2011.

37. **Handschin C**, **Spiegelman BM**. Peroxisome proliferator-activated receptor γ coactivator 1 coactivators, energy homeostasis, and metabolism. *Endocr Rev* 27: 728–735, 2006.

38. **Harbauer AB**, **Zahedi RP**, **Sickmann A**, **Pfanner N**, **Meisinger C**. The protein import machinery of mitochondria—A regulatory hub in metabolism, stress, and disease. *Cell Metab* 19: 357–372, 2014.

39. **Haynes CM**, **Petrova K**, **Benedetti C**, **Yang Y**, **Ron D**. ClpP mediates activation of a mitochondrial unfolded protein esponse in C. elegans. *Dev Cell* 13: 467–480, 2007.

40. **Haynes CM**, **Ron D**. The mitochondrial UPR - protecting organelle protein homeostasis. *J Cell Sci* 123: 3849–3855, 2010.

41. **Haynes CM**, **Yang Y**, **Blais SP**, **Neubert TA**, **Ron D**. The matrix peptide exporter HAF-1 signals a mitochondrial UPR by activating the transcription factor ZC376.7 in C. elegans. *Mol Cell* 37: 529–40, 2010.

42. **Hönlinger A**, **Bömer U**, **Alconada A**, **Eckerskorn C**, **Lottspeich F**, **Dietmeier K**, **Pfanner N**. Tom7 modulates the dynamics of the mitochondrial outer membrane translocase and plays a pathway-related role in protein import. *EMBO J* 15: 2125–37, 1996.

43. **Hood DA**, **Joseph A-M**. Mitochondrial assembly: protein import. *Proc Nutr Soc* 63: 293–300, 2004.

44. **Hood DA**, **Tryon LD**, **Vainshtein A**, **Memme J**, **Chen C**, **Pauly M**, **Crilly MJ**, **Carter H**. Exercise and the regulation of mitochondrial turnover. *Prog Mol Biol Transl Sci* 135: 99–127, 2015.

45. **Hood DA**, **Zak R**, **Pette D**. Chronic stimulation of rat skeletal muscle induces coordinate increases in mitochondrial and nuclear mRNAs of cytochrome-c-oxidase subunits. *Eur J Biochem* 179: 275–280, 1989.

46. **Hoppeler H**. Molecular networks in skeletal muscle plasticity. *J Exp Biol* 219: 205–213, 2016.

47. **Horibe T**, **Hoogenraad NJ**. The Chop gene contains an element for the positive regulation of the mitochondrial unfolded protein response. *PLoS One* 2, 2007.

48. **Howald H**, **Hoppeler H**, **Claassen H**, **Mathieu O**, **Straub R**. Influences of endurance training on the ultrastructural composition of the different muscle fiber types in humans. *Eur J Physiol* 403: 369–376, 1985.

49. **Irrcher I**, **Ljubicic V**, **Kirwan AF**, **Hood DA**. AMP-activated protein kinase-regulated activation of the PGC-1α promoter in skeletal muscle cells. *PLoS One* 3, 2008.

50. **Jäger S**, **Handschin C**, **St-Pierre J**, **Spiegelman BM**. AMP-activated protein kinase

(AMPK) action in skeletal muscle via direct phosphorylation of PGC-1alpha. *Pnas* 104: 12017–12022, 2007.

51. **Jensen RE**, **Dunn CD**. Protein import into and across the mitochondrial inner membrane: role of the TIM23 and TIM22 translocons. *Biochim Biophys Acta - Mol Cell Res* 1592: 25–34, 2002.

52. **Jin SM**, **Youle RJ**. The accumulation of misfolded proteins in the mitochondrial matrix is sensed by PINK1 to induce PARK2/Parkin-mediated mitophagy of polarized mitochondria. *Autophagy* 9: 1750–1757, 2013.

53. **Joseph A-M**, **Hood DA**. Plasticity of skeletal muscle mitochondria in response to contractile activity. *Exp Physiol* 88: 99–107, 2003.

54. **Jovaisaite V**, **Auwerx J**. The mitochondrial unfolded protein response—synchronizing genomes. *Curr Opin Cell Biol* 33: 74–81, 2015.

55. **Jovaisaite V**, **Mouchiroud L**, **Auwerx J**. The mitochondrial unfolded protein response, a conserved stress response pathway with implications in health and disease. *J Exp Biol* 217: 137–143, 2014.

56. **Kim J**, **Kundu M**, **Viollet B**, **Guan K-L**. AMPK and mTOR regulate autophagy through direct phosphorylation of Ulk1. *Nat Cell Biol* 13: 132–141, 2011.

57. **Kirkwood SP**, **Munn EA**, **Brooks GA**. Mitochondrial reticulum in limb skeletal muscle. *Am J Physiol* 251: C395-402, 1986.

58. **Kirstein-Miles J**, **Morimoto RI**. Peptides Signal Mitochondrial Stress. *Cell Metab* 11: 177–178, 2010.

59. **Kotiadis VN**, **Duchen MR**, **Osellame LD**. Mitochondrial quality control and communications with the nucleus are important in maintaining mitochondrial function and cell health. *Biochim Biophys Acta - Gen Subj* 1840: 1254–1265, 2014.

60. **Kovermann P**, **Truscott KN**, **Guiard B**, **Rehling P**, **Sepuri NB**, **Müller H**, **Jensen RE**, **Wagner R**, **Pfanner N**. Tim22, the essential core of the mitochondrial protein insertion complex, forms a voltage-activated and signal-gated channel. *Mol Cell* 9: 363–373, 2002.

61. **Krüger V**, **Deckers M**, **Hildenbeutel M**, **Van Der Laan M**, **Hellmers M**, **Dreker C**, **Preuss M**, **Herrmann JM**, **Rehling P**, **Wagner R**, **Meinecke M**. The mitochondrial oxidase assembly protein1 (Oxa1) insertase forms a membrane pore in lipid bilayers. *J Biol Chem* 287: 33314–33326, 2012.

62. **Kutik S**, **Stojanovski D**, **Becker L**, **Becker T**, **Meinecke M**, **Krüger V**, **Prinz C**, **Meisinger C**, **Guiard B**, **Wagner R**, **Pfanner N**, **Wiedemann N**. Dissecting Membrane Insertion of Mitochondrial β-Barrel Proteins. *Cell* 132: 1011–102, 2008.

63. **Lee JW**, **Park S**, **Takahashi Y**, **Wang HG**. The association of AMPK with ULK1 regulates autophagy. *PLoS One* 5: 1–9, 2010.

64. **Lee Y**, **Lee H-Y**, **Hanna RA**, **Gustafsson AB**. Mitochondrial autophagy by Bnip3 involves Drp1-mediated mitochondrial fission and recruitment of Parkin in cardiac myocytes. *AJP Hear Circ Physiol* 301: H1924–H1931, 2011.

65. **Leick L**, **Wojtaszewski J**, **Johansen S**, **Kiilerich K**, **Comes J**, **Hellsten Y**, **Hidalgo J**, **Pilegaard H**. PGC-1α is not mandatory for exercise-and training-induced adaptive gene responses in mouse skeletal muscle. *Am J Physiol Endocrinol Metab* 294: 463–474, 2008.

66. **Lin YF**, **Haynes CM**. Metabolism and the UPRmt. *Mol Cell* 61: 677–682, 2016.

67. **Lira VA**, **Okutsu M**, **Zhang M**, **Greene NP**, **Laker RC**, **Breen DS**, **Hoehn KL**, **Yan Z**. Autophagy is required for exercise training-induced skeletal muscle adaptation and improvement of physical performance. *FASEB J* 27: 4184–4193, 2013.

68. **Ljubicic V**, **Hood DA**. Kinase-specific responsiveness to incremental contractile activity in skeletal muscle with low and high mitochondrial content. *Am J Physiol Endocrinol Metab* 295: E195-204, 2008.

69. **Ljubicic V**, **Joseph AM**, **Adhihetty PJ**, **Huang JH**, **Saleem A**, **Uguccioni G**, **Hood DA**. Molecular basis for an attenuated mitochondrial adaptive plasticity in aged skeletal muscle. *Aging (Albany NY)* 1: 818–830, 2009.

70. **Masiero E**, **Agatea L**, **Mammucari C**, **Blaauw B**, **Loro E**, **Komatsu M**, **Metzger D**, **Reggiani C**, **Schiaffino S**, **Sandri M**. Autophagy is required to maintain muscle mass. *Cell Metab* 10: 507–515, 2009.

71. **Masiero E**, **Sandri M**. Autophagy inhibition induces atrophy and myopathy in adult skeletal muscles. *Autophagy* 6: 307–309, 2010.

72. **Matsuda N**, **Sato S**, **Shiba K**, **Okatsu K**, **Saisho K**, **Gautier CA**, **Sou YS**, **Saiki S**, **Kawajiri S**, **Sato F**, **Kimura M**, **Komatsu M**, **Hattori N**, **Tanaka K**. PINK1 stabilized by mitochondrial depolarization recruits Parkin to damaged mitochondria and activates latent Parkin for mitophagy. *J Cell Biol* 189: 211–221, 2010.

73. **Merkwirth C**, **Jovaisaite V**, **Durieux J**, **Matilainen O**, **Jordan SD**, **Quiros PM**, **Steffen KK**, **Williams EG**, **Mouchiroud L**, **Tronnes SU**, **Murillo V**, **Wolff SC**, **Shaw RJ**, **Auwerx J**, **Dillin A**. Two conserved histone demethylases regulate mitochondrial stress-induced longevity. *Cell* 165: 1209–1223, 2016.

74. **Mitchell P**. Coupling of phosphorylation to electron and hydrogen transfer by a chemi-osmotic type of mechanism. *Nature* 191: 144–148, 1961.

75. **Mizushima N**, **Levine B**, **Cuervo AM**, **Klionsky DJ**. Autophagy fights disease through cellular self-digestion. *Nature* 451: 1069–1075, 2008.

76. **Mottis A**, **Jovaisaite V**, **Auwerx J**. The mitochondrial unfolded protein response in mammalian physiology. *Mamm Genome* 25: 424–433, 2014.

77. **Napolitano G**, **Ballabio A**. TFEB at a glance. *J Cell Sci* 129: 2475–2481, 2016.

78. **Narendra DP**, **Jin SM**, **Tanaka A**, **Suen DF**, **Gautier CA**, **Shen J**, **Cookson MR**, **Youle RJ**. PINK1 is selectively stabilized on impaired mitochondria to activate Parkin. *PLoS Biol* 8, 2010.

79. **Nargund AM**, **Fiorese CJ**, **Pellegrino MW**, **Deng P**, **Haynes CM**. Mitochondrial and nuclear accumulation of the transcription factor ATFS-1 promotes OXPHOS recovery during the UPR(mt). *Mol Cell* 58: 123–133, 2015.

80. **Nargund AM**, **Pellegrino MW**, **Fiorese CJ**, **Baker BM**, **Haynes CM**. Mitochondrial import efficiency of ATFS-1 regulates mitochondrial UPR activation. *Science (80-)* 337: 587–590, 2012.

81. **Neupert W**. Protein import into mitochondria. *Annu Rev Biochem* 66: 863–917, 1997.

82. **Neupert W**, **Herrmann JM**. Translocation of Proteins into Mitochondria. *Annu Rev Biochem* 76: 723–749, 2007.

83. **Ogata T**, **Yamasaki Y**. Ultra-high-resolution scanning electron microscopy of mitochondria and sarcoplasmic reticulum arrangement in human red, white, and intermediate muscle fibers. *Anat Rec* 248: 214–223, 1997.

84. **Omura T**. Mitochondria-targeting sequence, a multi-role sorting sequence recognized at all steps of protein import into mitochondria. *J Biochem* 1016: 1010–1016, 1998.

85. **Opalińska M**, **Meisinger C**. Metabolic control via the mitochondrial protein import machinery. *Curr Opin Cell Biol* 33: 42–48, 2015.

86. **Pakos-Zebrucka K**, **Koryga I**, **Mnich K**, **Ljujic M**, **Samali A**, **Gorman AM**. The integrated stress response. *EMBO Rep* 17: 1374–1395, 2016.

87. **Papa L**, **Germain D**. SirT3 regulates the mitochondrial unfolded protein response. *Mol Cell Biol* 34: 699–710, 2014.

88. **Peixoto PM V**, **Graña F**, **Roy TJ**, **Dunn CD**, **Flores M**, **Jensen RE**, **Campo ML**. Awaking TIM22, a dynamic ligand-gated channel for protein insertion in the mitochondrial inner membrane. *J Biol Chem* 282: 18694–18701, 2007.

89. **Pellegrino MW**, **Nargund AM**, **Haynes CM**. Signaling the mitochondrial unfolded protein response. *Biochim Biophys Acta - Mol Cell Res* 1833: 410–416, 2013.

90. **Pellegrino MW**, **Nargund AM**, **Kirienko N V.**, **Gillis R**, **Fiorese CJ**, **Haynes CM**.

Mitochondrial UPR-regulated innate immunity provides resistance to pathogen infection. *Nature* 516: 414–417, 2014.

91. **Pette D**, **Staron RS**. Myosin isoforms, muscle fiber types, and transitions1. *MicroscResTech* 50: 500–509, 2000.

92. **Pilegaard H**, **Saltin B**, **Neufer PD**. Exercise induces transient transcriptional activation of the PGC-1α gene in human skeletal muscle. *J Physiol* 546: 851–858, 2003.

93. **Pogozelski AR**, **Geng T**, **Li P**, **Yin X**, **Lira VA**, **Zhang M**, **Chi JT**, **Yan Z**. P38Γ Mitogen-Activated Protein Kinase Is a Key Regulator in Skeletal Muscle Metabolic Adaptation in Mice. *PLoS One* 4, 2009.

94. **Puigserver P**, **Rhee J**, **Lin J**, **Wu Z**, **Yoon JC**, **Zhang CY**, **Krauss S**, **Mootha VK**, **Lowell BB**, **Spiegelman BM**. Cytokine stimulation of energy expenditure through p38 MAP kinase activation of PPARgamma coactivator-1. *Mol Cell* 8: 971–982, 2001.

95. **Quirós PM**, **Langer T**, **López-otín C**. New roles for mitochondrial proteases in health , ageing and disease. *Nat Publ Gr* 16: 345–359, 2015.

96. **Rehling P**, **Pfanner N**, **Meisinger C**. Insertion of hydrophobic membrane proteins into the inner mitochondrial membrane - A guided tour. *J Mol Biol* 326: 639–657, 2003.

97. **Rivero JLL**, **Talmadge RJ**, **Edgerton VR**. Fibre size and metabolic properties of myosin heavy chain-based fibre types in rat skeletal muscle. *J Muscle Res Cell Motil* 19: 733–742, 1998.

98. **Roise D**, **Schatz G**. Mitochondrial presequences. *J Biol Chem* 263: 4509–4511, 1988.

99. **Rowe GC**, **El-Khoury R**, **Patten IS**, **Rustin P**, **Arany Z**. PGC-1α is dispensable for exercise-induced mitochondrial biogenesis in skeletal muscle. *PLoS One* 7, 2012.

100. **Ryan MT**, **Hoogenraad NJ**. Mitochondrial-Nuclear Communications. *Annu Rev Biochem* 76: 701–722, 2007.

101. **Safdar A**, **Little JP**, **Stokl AJ**, **Hettinga BP**, **Akhtar M**, **Tarnopolsky MA**. Exercise increases mitochondrial PGC-1α content and promotes nuclear-mitochondrial cross-talk to coordinate mitochondrial biogenesis. *J Biol Chem* 286: 10605–10617, 2011.

102. **Scarpulla R**. Transcriptional paradigms in mammalian mitochondrial biogenesis and function. *Physiol Rev* 88: 611–638, 2008.

103. **Schiaffino S**, **Ausoni S**, **Gorza L**, **Saggin L**, **Gundersen K**, **Lomo T**. Myosin heavy chain isoforms and velocity of shortening of type 2 skeletal muscle fibres. *Acta Physiol Scand* 134: 575–576, 1988.

104. **Schiaffino S**, **Reggiani C**. Myosin isoforms in mammalian skeletal muscle. *J Appl Physiol* 77: 493–501, 1994.

105. **Schiaffino S**, **Reggiani C**. Fiber types in mammalian skeletal muscles. *Physiol Rev* 91: 1447–1531, 2011.

106. **Scott I**, **Webster BR**, **Chan CK**, **Okonkwo JU**, **Han K**, **Sack MN**. GCN5-like protein 1 (GCN5L1) controls mitochondrial content through coordinated regulation of mitochondrial biogenesis and mitophagy. *J Biol Chem* 289: 2864–2872, 2014.

107. **Seiferling D**, **Szczepanowska K**, **Becker C**, **Senft K**, **Hermans S**, **Maiti P**, **König T**, **Kukat A**, **Trifunovic A**. Loss of CLPP alleviates mitochondrial cardiomyopathy without affecting the mammalian UPR mt. 17: 953–964, 2016.

108. **Shao L-W**, **Niu R**, **Liu Y**. Neuropeptide signals cell non-autonomous mitochondrial unfolded protein response. *Cell Res* 26: 1182–1196, 2016.

109. **Sieck GC**, **Zhan W-Z**, **Prakash YS**, **Daood MJ**, **Watchko JF**. SDH and actomyosin ATPase activities of different fiber types in rat diaphragm muscle. *J Appl Physiol* 79: 1629–1639, 1995.

110. **Singh K**, **Hood DA**. Effect of denervation-induced muscle disuse on mitochondrial protein import. *Am J Physiol Cell Physiol* 300: C138–C145, 2011.

111. **Sirrenberg C**, **Bauer MF**, **Guiard B**, **Neupert W**, **Brunner M**. Import of carrier proteins into the mitochondrial inner membrane mediated by Tim22. *Nature* 384: 582–585, 1996.

112. **Son Y**, **Cheong Y-K**, **Kim N-H**, **Chung H-T**, **Kang DG**, **Pae H-O**. Mitogen-activated protein kinases and reactive oxygen species: how can ROS activate MAPK pathways? *J Signal Transduct* 2011: 1–6, 2011.

113. **Son Y**, **Kim S**, **Chung H-T**, **Pae H-O**. Reactive oxygen species in the activation of MAP kinases. 1st ed. Elsevier Inc.

114. **Straub SP**, **Stiller SB**, **Wiedemann N**, **Pfanner N**. Dynamic organization of the mitochondrial protein import machinery. *Biol Chem* 397: 1097–1114, 2016.

115. **Stuart RA**, **Gruhler A**, **van der Klei I**, **Guiard B**, **Koll H**, **Neupert W**. The requirement of matrix ATP for the import of precursor proteins into the mitochondrial matrix and intermembrane space. *Eur J Biochem* 220: 9–18, 1994.

116. **Takahashi M**, **Chesley A**, **Freyssenet D**, **Hood DA**. Contractile activity-induced adaptations in the mitochondrial protein import system. *Am J Physiol* 274: C1380-7, 1998.

117. **Takahashi M**, **Hood DA**. Protein import into subsarcolemmal and intermyofibrillar skeletal muscle mitochondria. *J Biol Chem* 271: 27285–27291, 1996.

118. **Tian Y**, **Garcia G**, **Bian Q**, **Steffen KK**, **Joe L**, **Wolff S**, **Meyer BJ**, **Dillin A**. Mitochondrial stress induces chromatin reorganization to promote longevity and UPRmt. *Cell* 165: 1197–1208, 2016.

119. **Trappe S**, **Gallagher P**, **Harber M**, **Carrithers J**, **Fluckey J**, **Trappe T**. Single muscle fibre contractile properties in young and old men and women. *J Physiol* 552: 47–58, 2003.

120. **Twig G**, **Hyde B**, **Shirihai OS**. Mitochondrial fusion, fission and autophagy as a quality control axis: The bioenergetic view. *Biochim Biophys Acta - Bioenerg* 1777: 1092–1097, 2008.

121. **Tzankov S**, **Wong MJH**, **Shi K**, **Nassif C**, **Young JC**. Functional divergence between Co-chaperones of Hsc70. *J Biol Chem* 283: 27100–27109, 2008.

122. **Uguccioni G**, **Hood DA**. The importance of PGC-1 in contractile activity-induced mitochondrial adaptations. *AJP Endocrinol Metab* 300: E361–E371, 2011.

123. **Vainshtein A**, **Desjardins EM**, **Armani A**, **Sandri M**, **Hood DA**. PGC-1α modulates denervation-induced mitophagy in skeletal muscle. *Skelet Muscle* 5: 1–17, 2015.

124. **Vainshtein A**, **Hood DA**. The regulation of autophagy during exercise in skeletal muscle. *J Appl Physiol* 120: 664–673, 2016.

125. **Vainshtein A**, **Tryon LD**, **Pauly M**, **Hood DA**. Role of PGC-1α during acute exercise-induced autophagy and mitophagy in skeletal muscle. *Am J Physiol - Cell Physiol* 308: C710–C719, 2015.

126. **Wang M**, **Kaufman RJ**. Protein misfolding in the endoplasmic reticulum as a conduit to human disease. *Nature* 529: 326–335, 2016.

127. **Wei H**, **Liu L**, **Chen Q**. Selective removal of mitochondria via mitophagy: Distinct pathways for different mitochondrial stresses. *Biochim Biophys Acta - Mol Cell Res* 1853: 2784–2790, 2015.

128. **Winder WW**, **Holmes BF**, **Rubink DS**, **Jensen EB**, **Chen M**, **Holloszy JO**. Activation of AMP-activated protein kinase increases mitochondrial enzymes in skeletal muscle. *J Appl Physiol* 88: 2219–2226, 2000.

129. **Yano M**. ABCB10 depletion reduces unfolded protein response in mitochondria. *Biochem Biophys Res Commun* 486: 465–469, 2017.

130. **Young JC**, **Hoogenraad NJ**, **Hartl FU**. Molecular chaperones Hsp90 and Hsp70 deliver preproteins to the mitochondrial import receptor Tom70. *Trends Biochem Sci* 30: 41–50, 2005.

131. **Yun J**, **Finkel T**. Mitohormesis. *Cell Metab* 19: 757–766, 2014.

132. **Zhang J**, **Ney PA**. Role of BNIP3 and NIX in cell death, autophagy, and mitophagy. *Cell Death Differ* 16: 939–946, 2009.

133. **Zhao Q**, **Wang J**, **Levichkin I V**, **Stasinopoulos S**, **Ryan MT**, **Hoogenraad NJ**. A mitochondrial specific stress response in mammalian cells. *EMBO J* 21: 4411–4419, 2002.

CHAPTER 2: MANUSCRIPT

EFFECT OF TIM23 KNOCKDOWN *IN VIVO* ON PROTEIN IMPORT INTO MITOCHONDRIA AND RETROGRADE SIGNALING TO THE UPR^{MT} IN MUSCLE

Ashley N. Oliveira, and David A. Hood

Muscle Health Research Centre, School of Kinesiology and Health Science, York University, Toronto, Ontario, M3J 1P3, Canada

MANUSCRIPT AUTHOR CONTRIBUTIONS

Ashley N. Oliveira: performed all In-Vivo Morpholino treatments, mitochondrial isolations, mitochondrial function experiments, qPCR, western blotting, peptide isolation and experiments; data analysis and interpretation; and wrote the manuscript.

Dr. David A. Hood: supervised this project and is the principal investigator.

ABSTRACT

The mitochondrial unfolded protein response (UPR^{mt}) is a compartment-specific protein quality control mechanism that strives to achieve proteostasis in the face of misfolded or misassembled proteins. Due to the mitochondrion's reliance on both the nuclear and mitochondrial genomes, a perturbation of the coordination of these genomes results in a mito-nuclear imbalance in which holoenzymes are unable to assume their mature stoichiometry and thereby activates the UPR^{mt}. Thus, we sought to perturb this genomic coordination by using a systemic anti-sense oligonucleotide (*in-vivo* Morpholino) targeted to Tim23, the major channel of the inner membrane. This resulted in a 40% reduction in Tim23 protein content, and a corresponding 60% reduction in protein import into the matrix, but not to other subcompartments. This matrix-specific import defect was sufficient to activate the CHOP-branch of the UPR^{mt}, as evident from increases in ClpP and cpn10, but not the ATF5 arm. This demonstrated that, in the face of proteotoxic stress, CHOP and ATF5 could be activated independently to regain proteostasis. Our second aim was to investigate the role of proteolytically-derived peptides in mediating retrograde signaling. To do so, peptides released from the mitochondrion following basal proteolysis were isolated and incubated with import reactions. A dose- and time-dependent effect of peptides on protein import was observed. Our data suggest that mitochondrial proteolytic byproducts exert an inhibitory effect on the protein import pathway, possibly to reduce excessive protein import as a potential negative feedback mechanism. The inhibition of import into the organelle may also serve as a retrograde function, to modify nuclear gene expression and ultimately improve organelle folding capacity.

INTRODUCTION

Proteostasis refers to the maintenance of proper protein synthesis, maturation and degradation to ensure a functional proteome (1, 2). Proteins that are unable to assume their tertiary or quaternary structures exert toxic effects on the cell, referred to as proteotoxicity (29, 34). Within the mitochondrion, the goal of achieving protein homeostasis is complex since it is the only organelle that contains its own genome, and therefore generates its own gene products. There, the maintenance of a functional stoichiometry relies on the coordination of both nuclear and mitochondrial genomes, as well as proper protein handling and maturation (5).

Despite containing their own genetic material, mitochondria rely heavily on the nuclear genome for over 99% of all mitochondrial proteins, while mtDNA encodes for 13 proteins that are transcribed and translated within the organelle (7). Furthermore, due to the double-membrane structure of the mitochondrion, products of nuclear genes encoding mitochondrial proteins (NuGEMPs) require a sophisticated mechanism for mediating their sorting and translocation. Mitochondrial protein import is a complex mechanism through which proteins are recognized via their mitochondrial targeting sequence (MTS) by cytosolic chaperones and delivered to the protein import machinery (PIM) within the organelle (6, 8). Products of NuGEMPs are recognized by cytosolic chaperones that guide proteins to the translocases of the outer membrane, the TOM complex. These chaperones are also responsible for unfolding their cargo into a linear structure to faciliate their passage through the β-barrel channel of the TOM complex, and subsequently through the translocase of the inner membrane, the TIM complex (4). Once in its final destination, such as in the matrix, the MTS is cleaved by mitochondrial processing peptidase (MPP) the protein is refolded by mitochondrial chaperones to assume its mature conformation (18). Many of these nuclear products can then combine with

mitochondrially-encoded subunits to form mature holoenzymes. Previous research has shown that protein import is a dynamic process that can respond to the metabolic status of the cell, thereby promoting the balance between the nuclear and mitochondrial genomes (9, 14). However, this process is laden with potential points for protein misfolding or misassembly, which may exert proteotoxic stress on the organelle.

To combat proteotoxicity, mitochondria are equipped with a protein quality control mechanism, the unfolded protein response (UPR^{mt}). The UPR^{mt} is a compartment-specific response that detects misfolded proteins and either refolds them through the use of chaperones (cpn10, Hsp60), or degrades them via proteases (LonP, ClpP) to eliminate the proteotoxic stress that they exert on the organelle (26). When the stress exceeds the capacity of resident quality control proteins, a retrograde signal is initiated through various mechanisms including an increase in reactive oxygen species (ROS) to indirectly activate CHOP and C/EBPβ, which transcriptionally regulate various mitochondrial chaperones and proteases (19). ATF5, a recently discovered transcription factor, is also activated, however the mechanism involved in this activation are currently unknown in mammalian cells (12). Work in *C. elegans* originally led to a proposed role for proteolytically-derived peptides in mediating the nuclear translocation of ATF5. In these organisms, the byproducts of proteolysis within the mitochondrion are released into the cytosol, and this is required for the activation and nuclear translocation of the homologue of ATF5, ATFS-1, where it can promote a compensatory gene expression response (15, 16, 27). Based on this research, the UPR^{mt} appears to be designed to selectively promote the transcription of protein quality control genes, while transiently arresting other sources of proteotoxic stress (11).

However, since its discovery in 2002, our understanding of the UPR^{mt} is primarily

derived from work in lower order organisms, and our knowledge regarding its mammalian counterpart is still lacking (2, 26). Therefore, the first purpose of this study was to investigate the consequence of UPR^{mt} induction in skeletal muscle by inducing a mito-nuclear imbalance. This was achieved by knocking down Tim23, the major channel of the TIM complex with an injectable anti-sense oligonucleotide. Our second purpose was to investigate the effect of peptides on the import process, and their potential role as a retrograde signal. We expected that mitochondrially-derived peptides would negatively influence import in a dose- and time-dependent manner.

METHODS

Animal Care and In-Vivo Morpholino Treatment- C57BL/6 mice (3 months) were housed in the vivarium and given food and water *ad libitum* under a 12hr light/dark cycle. In-Vivo Morpholinos (GeneTools, OR, USA) were designed to target Tim23 and were dissolved in phosphate-buffered saline at a concentration of 5mM as recommended by the manufacturer. Animals were administered a dose of 12mg/kg per day via intraperitoneal injection for three consecutive days (10). Control animals were treated with a standard control oligo offered through GeneTools at the same dose. Mice were sacrificed 48hr following their last injection by cervical dislocation and tissues were promptly harvested. Tibialis anterior, extensor digitorum longus, quadriceps, and triceps were collected from both hindlimbs and used immediately for mitochondrial isolations. Gastrocnemius muscles, heart and liver were frozen in liquid nitrogen and stored at -80°C for later analysis.

Mitochondrial Isolation- Fresh tissues were minced and homogenized using an Ultra-Turrex Polytron (IKA, Staufen, Germany) at 9.8 Hz and subjected to differential centrifugation to separate intermyofibrillar (IMF) and subsarcolemmal (SS) mitochondria, as was done previously

(25). IMF mitochondria were treated with Nagarse, a proteinase from *Bacillus lichenformis,* to liberate the mitochondrial population. Fractions were subjected to a final centrifugation at 9000 rpm to pellet mitochondria and were resuspended in resuspension buffer containing 100mM KCl, 10mM MOPS and 0.2% BSA (pH 7.4). Concentrations were determined using Bradford method.

Mitochondrial Respiration- Using a Clark Electrode (Strathkelvin Instruments, North Lanarkshire, Scotland), oxygen consumption was measured over time. Briefly, 50µL of mitochondria were incubated with 250µL of VO_2 buffer (250mM sucrose, 50mM KCl, 25mM Tris base, 10mM K_2HPO_4 and pH 7.4) and continuously stirred at 30°C. Mitochondrial O_2 consumption was measured in the presence of 10mM glutamate to assess basal (state 4) respiration, followed by the addition of 0.44mM ADP for maximal (state 3) respiration. Integrity of the inner membrane was assessed through the addition of NADH during state 3 respiration. Respiratory rates were corrected for the total amount of protein.

Mitochondrial ROS Emission- Mitochondria (75µg) were incubated in a 96-well plate with VO2 buffer and 50uM 2'7' dichlorofluorescin (DCF) at 37°C for 30 min. ROS emission was measured under state 3 and 4 respiratory conditions through the addition of ADP and glutamate or glutamate respectively. Fluorescence (excitation 480nm, emission 520 nm) was measured using a Synergy HT microplate reader (BioTek Instruments,VT, USA) and KC4 software (v.3.0), and was directly proportional to ROS emission.

In Vitro Transcription, Translation and Protein Import- As previously described (32), plasmid DNA containing the ornithine transcarbamylase (OCT) cDNA and competent DH5α cells were transformed and grown on agar plates. Bacterial colonies were then amplified overnight in lysogeny broth (LB) media and treated with ampicillin. Plasmid DNA was then isolated using a HiSpeed Plasmid Maxi Kit (Qiagen, Hilden, Germany). The DNA was then linearized using

Sca1 and subsequently purified using phenol and precipitated using ethanol. OCT was transcribed *in vitro* using SP6 polymerase for 90 min at 40°C. Translation was then carried out at 37°C by combining rabbit reticulocyte lysate, mRNA, a cocktail of amino acids minus methionine, radio-labeled ^{35}S methionine and water for 25 minutes.

As previously described (32), 75µg of freshly isolated mitochondria and 18µL of the translation mix were incubated for 30 min at 30°C to allow protein import. Mitochondria were then centrifuged through a sucrose gradient at 16,000g for 15 min at 4°C and resuspended in breaking buffer (0.6M sorbitol and 20mM HEPES) and lysis buffer (10% glycerol, 2.3% SDS, 62.5mM Tris-HCl and 5% mercaptoethanol). Samples were denatured at 95°C for 5 min and then resolved through a 12% SDS-polyacrylamide gel for ~2 hr. Gels were then boiled for 5 min in 5% TCA, briefly washed with ddH_2O, incubated with 10mM Tris for 5 min, followed by 30 min in 1M salicyclic acid. Gels were then dehydrated at 80°C for 1hr and radiolabelled bands were captured on a Fujifilm Multipurpose Storage Phospho film and visualized using a Typhoon Scanner (GE Healthcare, Little Chalfont, UK).

Protein Release Assay and Peptide Isolation- IMF mitochondria (150µg) from untreated C57BL/6 mice were incubated for 1hr at 30°C with or without the presence of 5mM H_2O_2, and $FeSO_4$ to perturb the organelle and promote apoptosis. To assess whether or not peptides were being released from the mitochondrial permeability transition pore (mtPTP) basally and under stress, under the same conditions 200uM of cyclosporin A was added to block the opening of the mtPTP. Following incubation, mitochondria were pelleted by centrifugation (5 min at 14,000g at 4°C) to collect all released material. Finally, the released fraction was separated based on size using a Spin-X Concentrator (Corning, MA, USA) collecting everything under 3kDa in size. Concentrations were determined spectrophotometrically using a NanoDrop 2000 (Thermo

Fisher, MA, USA).

This protocol was also used to isolate peptides for the import reactions with the exception that H_2O_2 and $FeSO_4$ were not used to perturb the mitochondrion. Peptides were isolated under basal conditions in the presence of up to 600µg of mitochondria to increase peptide yield.

Total RNA and Reverse Transcription- Approximately 100mg of pulverized gastrocnemius tissue was combined with 1mL of TRIzol Reagent (Invitrogen, CA, USA) and homogenized at 6Hz (3x 10 sec) then mixed with chloroform. Samples were centrifuged at 16,000g for 15 min at 4°C. The aqueous phase was then transferred to a new tube and precipitated using isopropanol at -80°C for 1hr. Samples were then once again centrifuged at 16,000g for 15 min at 4°C and pellets were resuspended in 30µL of molecular grade sterile water (Wisent Bio Products, QC, Canada). The concentration and purity of RNA were determined by spectrophotometer (NanoDrop 2000, Thermo Fisher, MA, USA). Superscript III reverse transcriptase (Invitrogen, CA, USA) was used according to manufacturer directions to convert 1.5µg of RNA into cDNA.

Real-Time PCR- Primers were designed using sequences from GenBank, Primer 3 (v.0.4.0) software (Massachusetts Institute of Technology, MA, USA) and OligoAnalyzer 3.1 (Integrated DNA Technologies, ON, Canada) for genes of interest. mRNA expression was determined by combining SYBR Green Supermix (Quanta Biosciences, MD, USA), forward and reverse primers (20uM), stH_2O and cDNA (10ng) in a 96-well plate. PCR amplification was carried out in a StepOnePlus Real-Time PCR System (Applied Biosystems, CA, USA) including a final melt-stage to check for nonspecific amplification. Results were corrected using two house-keeping genes: β-actin and 18S ribosomal RNA.

Protein Isolation- Frozen gastrocnemius muscle was pounded into a fine powder, of which 15-20mg were diluted in 10x Sakamoto Buffer with the addition of protease and phosphatase

Table 1: A. *In-vivo* Morpholino sequences purchased from GeneTools, designed according to company guidelines targeted for Tim23 knockdown. **B.** List of primer sequences used for real-time PCR analysis. All primers are designed for *mus musculus.*

A

Gene	In-Vivo Morpholino Sequence
Tim23	5'-TCT TCC GCC ACC TTC CAT GAG GTC-3'
Control	5'-CCT CTT ACC TCA GTT ACA ATT TAT A-3'

B

Gene	**Primer**	
	Forward	**Reverse**
Ddit3 (CHOP)	5'-CAC CAC ACC TGA AAG CAG AA-3'	5'-AGG TGA AAG GCA GGG ACT CA-3'
ATF5	5'-TGG AGC GGG AGA TCC AGT A-3'	5'-GAC GCT GGA GAC AGA CGT ACA-3'
Hspa9 (mtHsp70)	5'-TGG CTA TTA CTG CGG GTT CT-3'	5'-CAT CTG CTC CAC CTC CTC T-3'
Hspd1 (Hsp60)	5'-CTG GGT GCA AGA GCC ATA TA-3'	5'-GAA AGG CTG CTT CTG AAC TCT-3'
Hspe1 (cpn10)	5'-GGA GTG CTG CTG CCG AAA CTG TA-3'	5'-TCA CAC TGA CAG GCT CAA TCT-3'
Lonp1 (LonP)	5'-CGA CTT GCA CAG CCC TAT GT-3'	5'-CGA ATG TTC CCG TAT GGT AGA T-3'
Timm23 (Tim23)	5'-CCCGAGGCAGATTTGAACTA-3'	5'-AAAGCCAGGGAGCCTAGAGTAT-3'
B-actin	5'-TGT GAC GTT ACA TCC GTA A-3'	5'-GCT AGG AGC CAG AGG AGT AA-3'
18S rRNA	5'-GTAACCCGTTGAACCCCATT-3'	5'-CCATCCAATCGGTAGTAGCG-3'

inhibitors (Sigma, MO, USA). Samples were then rotated at 4°C for 1hr and then sonicated (3x 3 sec at 30% power). Samples underwent centrifugation at 14,000g at 4°C and the supernate was collected and stored at -80°C.

Western Blotting- As previously described (24), whole muscle protein extracts were prepared and separated in polyacrylamide SDS-PAGE gels. Proteins were then transferred onto nitrocellulose membranes and blocked in 5%-10% milk in TBS-T. Subsequently, membranes were incubated with the appropriate concentration of primary antibodies overnight at 4°C, and then with HRP-conjugated secondary antibodies for 1hr at room temperature. Membranes were then visualized with enhanced chemiluminesence and a Carestream Model imaging system and Image J software was used for quantifications and corrected for with the appropriate loading control.

Statistical Analysis- Unpaired t-tests were used to detect differences between Tim23 knockdown and control mice using GraphPad Prism 6.0. When comparing the effect of peptides on the import reaction or in the proteolysis experiments, paired t-tests or two-way ANOVA were used when appropriate. The critical value was set at $p<0.05$. All error bars represent the SEM.

Table 2: List of antibodies and concentrations used for Western blotting. All antibodies are prepared in 5% milk unless otherwise specified.

Protein	Manufacturer	Catalog No.	Concentration	
			Primary	Secondary
Tim23	BD Transduction Laboratories	611222	1:1000	1:2000 (M)
COX IV	Abcam	ab140643	1:4000	1:4000 (M)
Tfam	In house	---	1:3000	1:5000 (R)
mtHsp70	Enzo Life Sciences	ADI-SPA-810	1:1000	1:2000 (M)
Hsp60	Enzo Life Sciences	ADI-SPA-806	1:1000	1:2000 (M)
cpn10	Enzo Life Sciences	ADI-SPA-110	1:4000	1:4000 (R)
ClpP	Abcam	ab124822	1:1000	1:1000 (R)
LonP	Cell Signaling	28020S	1:1000	1:2000 (R)
ATF5	Abcam	ab60126	1:750 (5% BSA)	1:3000 (R)
CHOP	Santa Cruz	sc-7351	1:500	1:2500 (M)
VDAC	Abcam	ab14734	1:5000	1:5000 (M)
Aciculin	In house	---	1:3000	1:3000 (M)

RESULTS

Consequence of Tim23 Knockdown- Following In-Vivo Morpholino treatment, Tim23 protein content was significantly reduced in the IMF fraction by an average 40% (Figs. 1A, B). This corresponded to a 60% reduction in OCT import into the mitochondrial matrix *in vitro* (Fig. 1C). As expected the degree of Tim23 knockdown was strongly correlated to the level of impairment of import into the matrix (R^2=0.533, p=0.01, Fig. 1D). Nuclear-encoded mitochondrial proteins were measured to assess whether or not this reduction in protein import affected the delivery of proteins to the organelle *in vivo*. COX IV, a subunit of the electron transport chain (ETC) located within the inner membrane was not changed in the IMF fraction (Fig. 1A). However, mitochondrial transcription factor A (Tfam) was significantly reduced by 25% (Fig. 1B) suggesting that partial loss of Tim23 selectively impairs protein import into the matrix both *in vivo* and *in vitro*.

Maintenance of Mitochondrial Function Despite an Import Defect- Since Tim23 is the major channel of the TIM complex and is an integral part of the protein import process, we speculated that mitochondrial function would be impaired. In order to ascertain whether there was any mitochondrial dysfunction, mitochondrial respiration and ROS emission were assessed. Mitochondrial oxygen consumption both during state IV (basal) and state III (maximal) conditions were unchanged in the IMF fraction (Fig. 2A) of Tim23 knockdown animals. Similarly, during state IV respiration there was no difference found in ROS emission (Fig. 2B), a marker of oxidative stress, suggesting that mitochondrial function was maintained basally, despite a significant impairment in matrix-specific import. However, under maximal respiratory conditions there was a strong trend for increased ROS production (p=0.059; Fig. 2B). Suggesting that maximal mitochondrial function may be more susceptible to oxidative stress in the face of

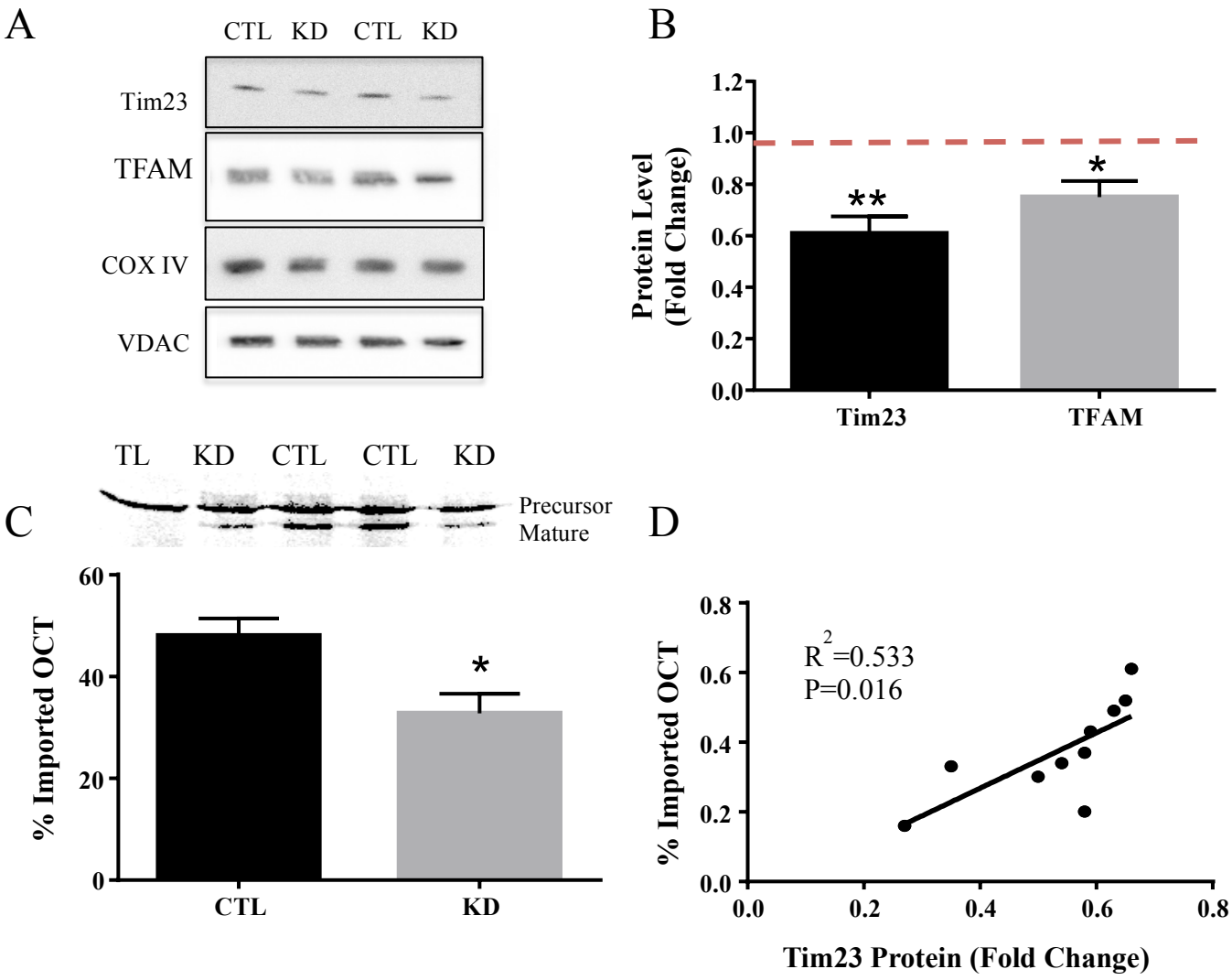

Figure 1: Consequence of Tim23 knockdown. Representative western blots for Tim23, Tfam, COX IV and the loading control, VDAC in IMF fractions **(A)**. Graphical representation for Tim23 and Tfam protein content following In-Vivo Morpholino treatment **(B).** Graphical representation of OCT import into the mitochondrial matrix with a corresponding blot **(C)**. Correlation between Tim23 protein content and OCT import into the mitochondrial matrix (**D;** R^2=0.533). (n=5-11. *, p<0.05; **, p<0.001). CTL, control; KD, knockdown; TL, OCT translation product alone.

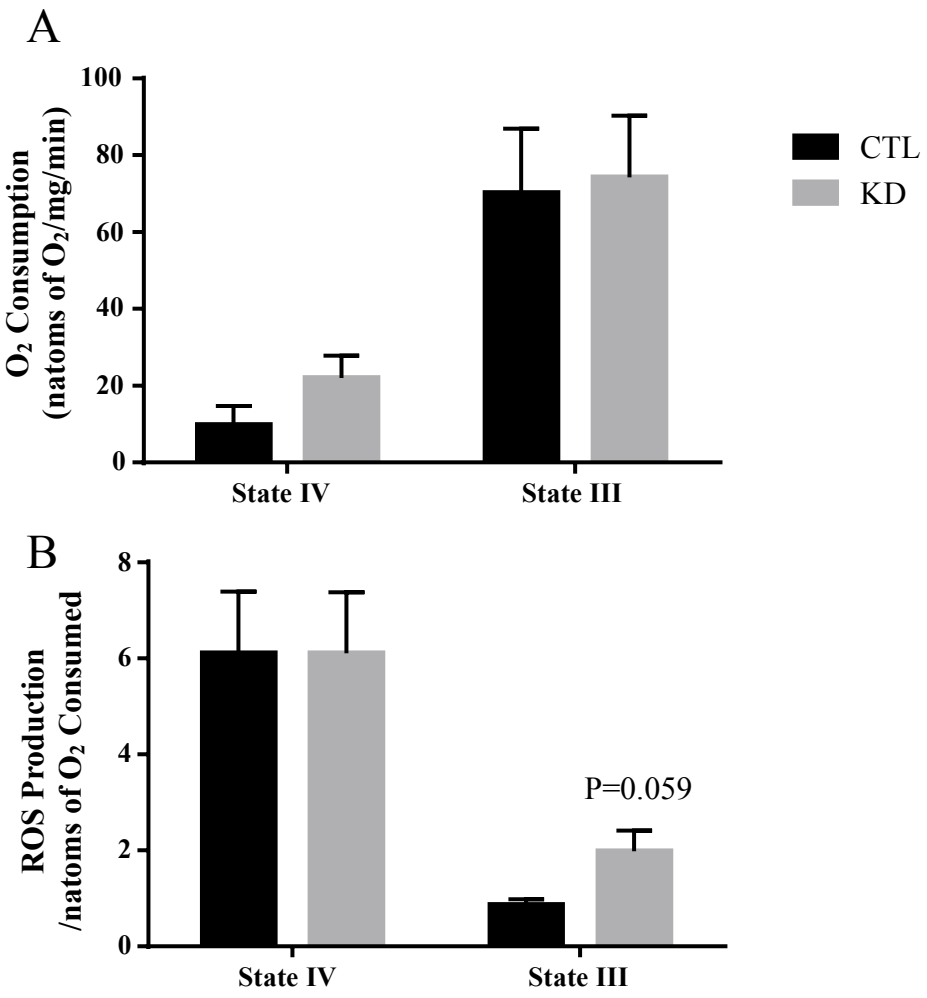

Figure 2: Maintenance of mitochondrial function despite import defect. Graphical representation of mitochondrial respiration during both state IV (basal) and state III (maximal) respiratory states **(A).** ROS production under the same respiratory conditions, corrected for oxygen consumption **(B)**. (n=4-6) CTL, control IMF mitochondria; KD, knockdown IMF mitochondria.

an import defect.

Activation of the UPR^{mt} Following Tim23 Knockdown- To assess whether partial loss of Tim23 resulted in a perturbation of protein homeostasis, markers of the UPR^{mt} were measured. To our surprise, ATF5, a novel proteolytic-dependent transcription factor, was unchanged (Fig. 3A). However, CHOP was elevated by 2.7-fold in the knockdown animals (Fig. 3B). Mitochondrial chaperones, mtHSP70 and HSP60, were unchanged in Tim23 knockdown animals (Fig. 3A), but chaperonin 10 (cpn10) was elevated by 40% (Fig. 3C). Similarly, of the resident proteases, LonP showed no change (Fig. 3A), however ClpP was increased by 1.8-fold (Fig. 3D). Taken together, it appears that a CHOP-dependent branch of the UPR^{mt} may have been activated, following inhibition of protein import into the matrix.

Next, we sought to investigate whether partial loss of Tim23 resulted in changes in mRNA expression. We had hypothesized that various protein quality control proteins would be upregulated in similar fashion to the protein data. However, both *ATF5* and *CHOP* transcripts remained unchanged following Tim23 knockdown, and similarly no differences were observed in their downstream targets (Fig. 4).

Understanding Proteolysis Within the Mitochondrion- To assess peptide release, mitochondria were isolated and incubated at 30°C for 30 minutes to allow basal proteolysis to occur with or without the presence of 5mM H_2O_2 to induce oxidative stress. These results demonstrate that proteolysis does occur basally and that the byproducts are exported into the cytosol. Thus, we sought to further perturb the organelle and assess how these protein fragments were exiting the mitochondrion. Mitochondria were incubated in the presence of H_2O_2 and $FeSO_4$, to produce a hydroxyl radical (HO^-). Under these conditions there was a significant increase in released peptides demonstrating an increased rate of proteolysis (Fig. 5). The addition of 200uM

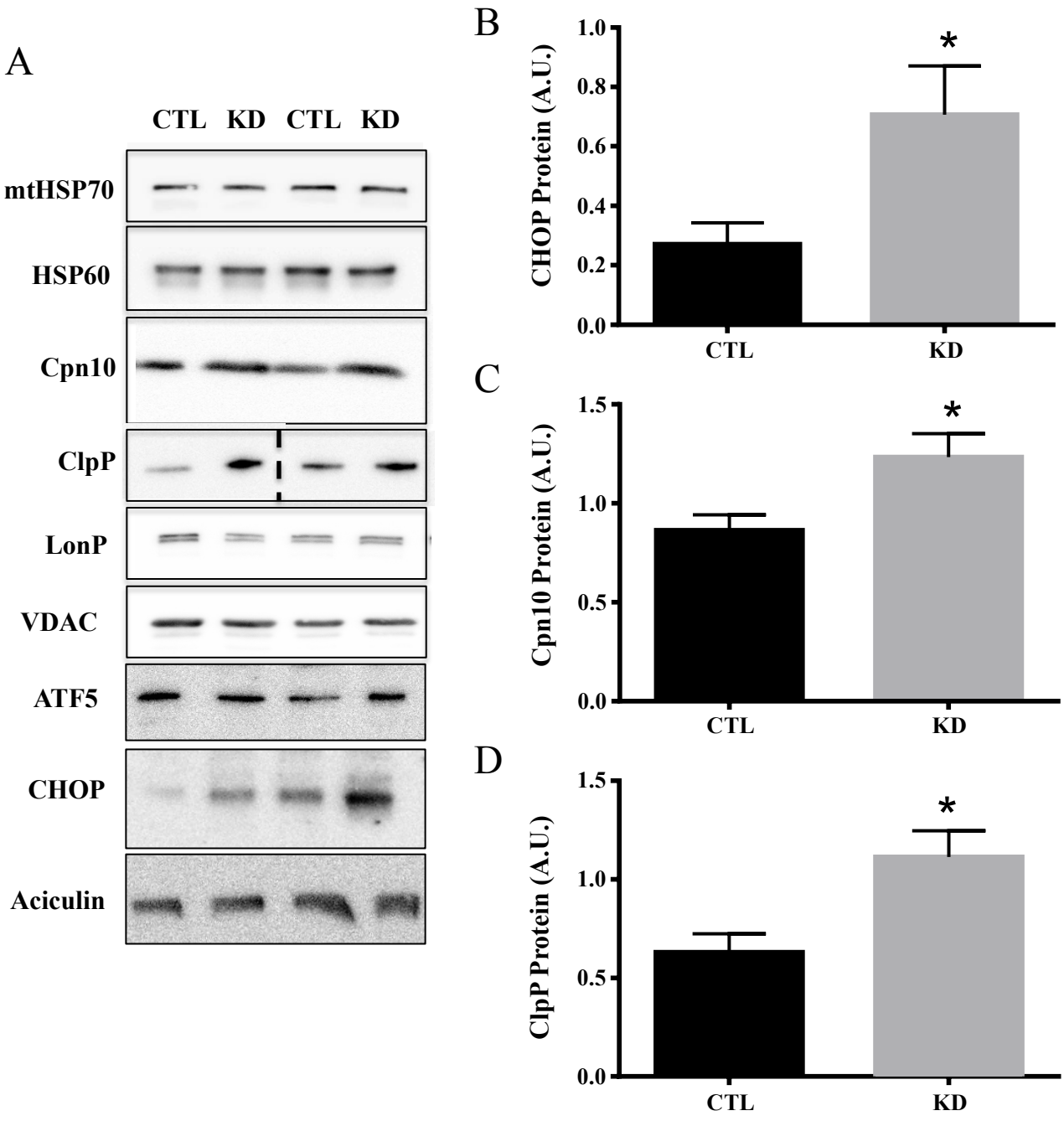

Figure 3: Activation of the UPR^{mt} following Tim23 knockdown. Representative western blots for mtHSP70, HSP60, cpn10, ClpP, LonP, in isolated IMF mitochondria; CHOP, and ATF5 in whole muscle extracts with their respective loading controls, VDAC and aciculin (**A**). Graphical representation of CHOP protein content in whole muscle extracts **(B,** $p=0.05$**),** Cpn10 (**C,** *, $p<0.05$) and ClpP in IMF mitochondria (**D,** $p<0.05$). Dashed line in ClpP blot indicates images taken from two separate blots. (CTL, n=7; KD, n=11). CTL, control; KD, knockdown.

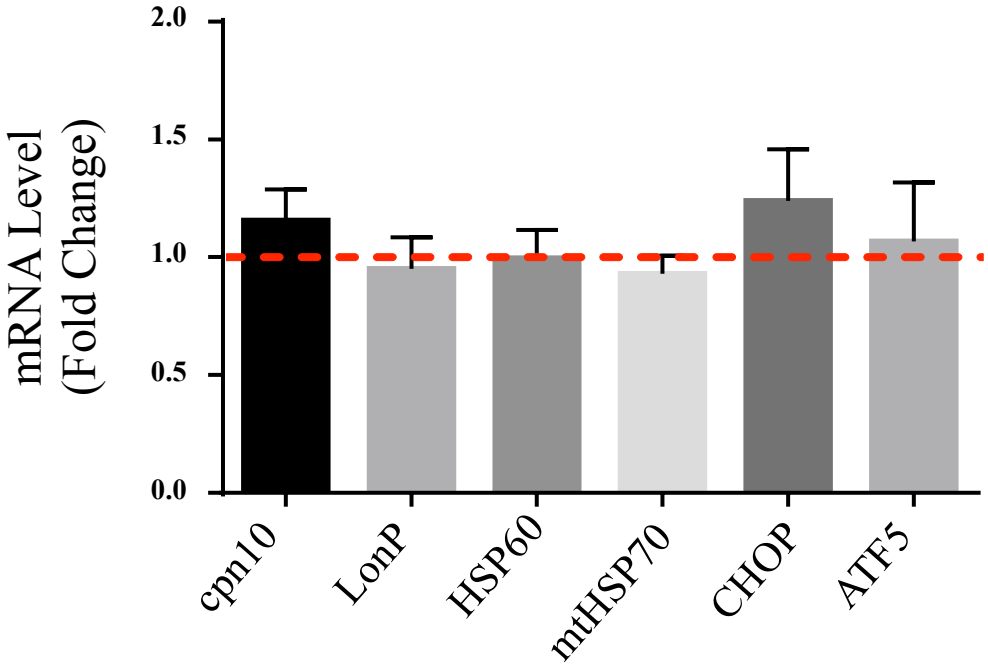

Figure 4: Changes in gene expression following Tim23 knockdown. mRNA expression of various UPR^{mt} markers are expressed as fold changes over control values (n=6-8).

Cyclosporin A was used under these same conditions to block the opening of the mitochondrial permeability transition pore (mtPTP), a nonselective channel on the outer membrane. The addition of cyclosporin A did not block the release of peptides from the mitochondria, thus eliminating the mtPTP as the channel through which the peptides were exported (Fig. 5).

Role of Mitochondrially-Derived Peptides in Modulating Protein Import- The mechanism through which peptides influence retrograde signaling during the activation of the UPR^{mt} is currently unknown. Thus, we investigated whether peptides may be influencing the UPR^{mt} by modulating protein import. To test this hypothesis, peptides were isolated following basal proteolysis from mitochondria and incubated with radiolabeled OCT and freshly isolated mitochondria. Peptides were added to the import reaction in increasing doses (2, 4, and 6μg) with volume-matched controls. No effect of peptides on protein import was observed at 2 and 4ug, however 25% ($p<0.05$) decrease in import was apparent using 6ug of peptides (Fig. 6A). Next we asked if this relationship was also time-dependent by incubating 6μg of peptides for various time points (10, 20 and 30 min) since import itself is a time-dependent process. The inhibitory effect was not apparent at early times, but became evident after 30min of incubation (Fig. 6B). These data suggest that with increasing concentrations of peptides present this impairs protein import into the mitochondrial matrix.

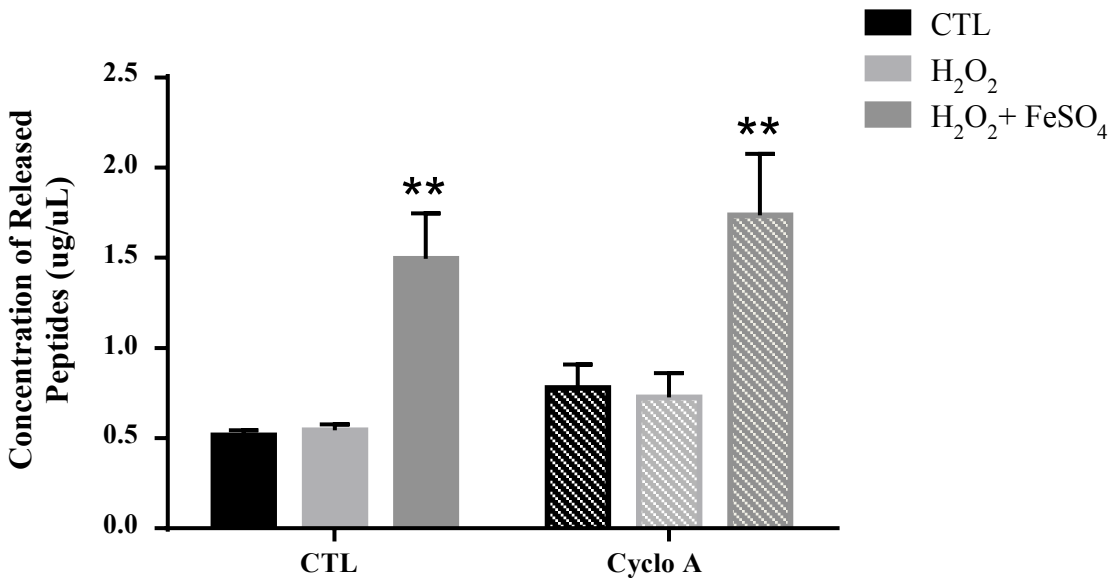

Figure 5: Understanding proteolysis within the mitochondrion. Mitochondrial peptide release in the presense of H_2O_2 and $FeSO_4$ with or without Cyclosporin A. CTL, control; Cyclo A, cyclosporin A. (**, $P<0.001$; n=6)

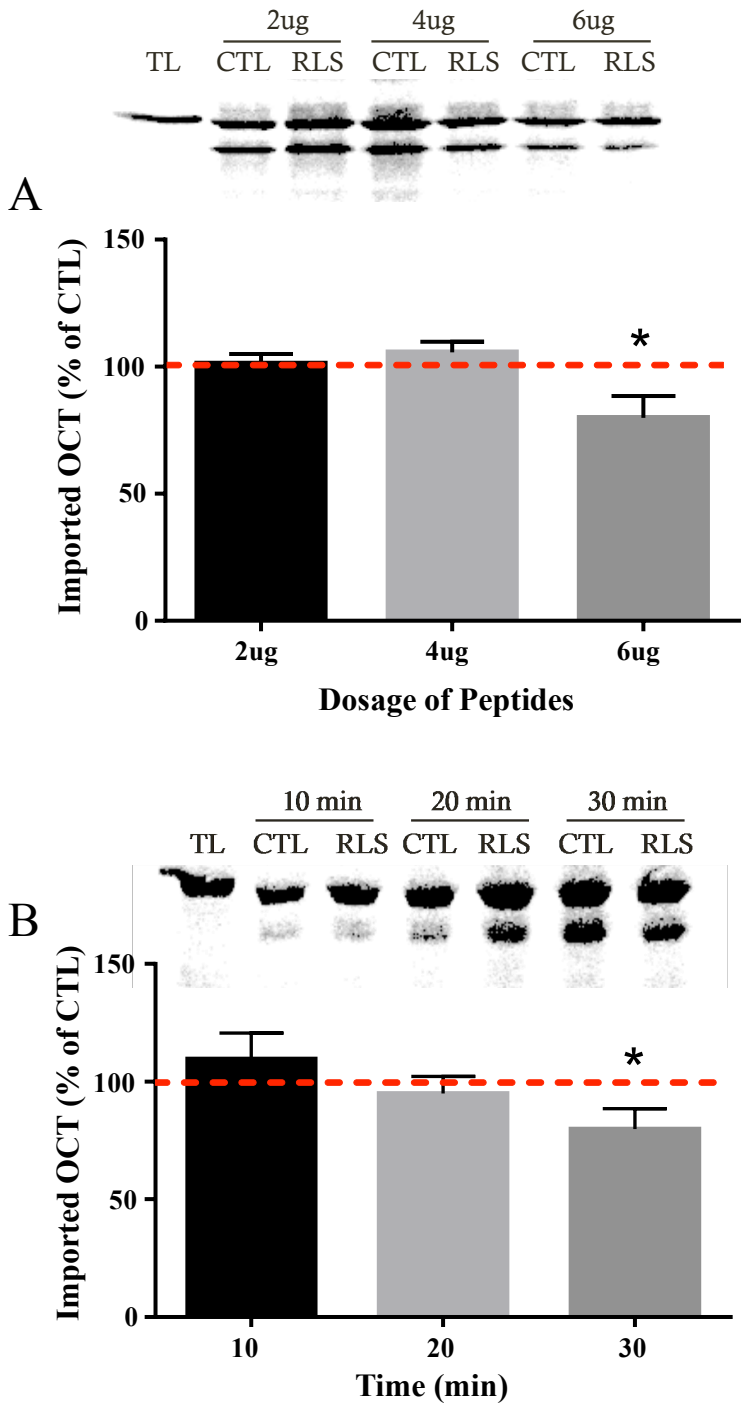

Figure 6: Role of mitochondrially-derived peptides on protein import. Peptides incubated with import reactions at various doses, graph represents import rates as a percentage of their respective controls (**A;** p=0.06; 2, 4ug, n=6; 6ug, n=12**).** Import reactions in the presence of 6ug of peptides for various time points (10, 20 and 30 minutes) shown as a percentage of control (**B;** 10, 20 min**,** n=5; 30 min, n=12**)**. TL, translation product alone; CTL, control; RLS, mitochondrially-released peptides.

DISCUSSION

The maintenance of proteostasis is integral for the health of the cell(22, 34). Proteins that are misfolded or misassembled exert negative effects referred to as proteotoxicity, and this is combatted by compartment-specific protein quality control mechanisms known as the unfolded protein response (UPR) (28, 30). Mitochondrial biogenesis requires the contribution of protein products from both the nuclear and mitochondrial genomes. Thus, a mitochondrion must coordinate the expression of the nuclear genome, while also supporting the transcription and translation of its own gene products. Mitochondria are equipped with a protein import machinery (PIM) that facilitates the translocation of nuclear-encoded proteins (31), as well as a mitochondrion-specific UPR (UPR^{mt}) that strives to maintain proteostasis (26, 36).

In this study, we sought to better understand the UPR^{mt} by inducing an imbalance between the two genomes. To achieve this, we knocked down the expression of Tim23, the major channel of the translocase of the inner membrane (TIM complex), using a systemically injectable anti-sense oligonucleotide, In-Vivo Morpholino. This treatment successfully reduced Tim23 protein in skeletal muscle IMF mitochondria to 60% of normal levels. We were not seeking a complete depletion of Tim23 levels, since homozygous deletion of Tim23 is embryonic lethal and thus critical for development (1). The consequence of this depletion was a functional impairment of protein import into the matrix, but not to other sub-compartments such as the inner membrane. This specificity is undoubtedly due to the complex nature of the PIM in which Tim23 mediates matrix-destined import but is not essential for translocation to other sub-compartments (18). Tim22 is thought to operate in conjunction with, and independently from Tim23, to facilitate the passage of proteins directly into the inner membrane (23). In our experiments, this could also explain how mitochondrial respiration and ROS emission were

maintained basally despite this matrix import defect, since the electron transport chain (ETC) is found within the inner membrane. These data are in accordance with previous literature from the liver of Tim23 heterozygous and wildtype mice in which no differences in mitochondrial respiration were found (29). However, we did observe a tendency for elevated ROS emission during ADP-stimulated maximal respiration in mitochondria in which import was impaired. Thus, it appears that compositional changes brought upon by the import defect may only become evident during maximal respiration, leading to elevated ROS production. We had hypothesized that there would be an elevation in ROS in these animals because of the induction of structural imbalances in the stoichiometry of Krebs' Cycle and electron transport chain subunits in the presence of an import defect. ROS are thought to mediate retrograde signaling to the nucleus through JNK, a mitogen-activated protein kinase. Work by Horibe *et al*. demonstrated that JNK activation was required for CHOP activation during UPR^{mt}, however ROS were never measured in that study (31). Thus, the elevated ROS levels observed during state III respiration may, in part, explain the 2.7-fold increase in CHOP seen following Tim23 knockdown.

We also hypothesized that Tim23 knockdown *in vivo* would result in UPR^{mt} activation. This was based on the research by Fiorese *et al.* who knocked down Tim23 in *C. elegans* to induce the UPR^{mt}. This robustly activated ATFS-1, the homologue of ATF5 (12). Interestingly, they also demonstrated that Tim23 knockdown also activates ATF5 when expressed in *C. elegans* (12). However, in our study no detectable changes in mRNAs encoding ATF5, CHOP, or their downstream targets were observed in the tissues collected 48hr following the last injection. Alterations in mRNA levels are transient events, and it is possible that these changes were occurring at an earlier timepoint. Thus, we sought to examine the protein level of various UPR^{mt} markers via immunoblotting. This analysis revealed an increase in CHOP, the stress-

induced transcription factor associated with UPR activation. ClpP and cpn10, a resident protease and chaperone respectively, were also both upregulated following Tim23 knockdown. Both ClpP and cpn10 are targets of CHOP, suggesting that the CHOP branch of the UPR^{mt} was activated following Tim23 knockdown (17). However ATF5, a proteolytic-dependent transcription factor was not elevated, and neither were its downstream targets LonP, HSP60 and mtHSP70. These results provide evidence that the various branches of the UPR^{mt} can act independently, and thus both transcription factors may not be needed for the maintenance of mitochondrial proteostasis. This appears to be different from stimuli that induce ER stress, where CHOP transcriptionally activates ATF5 to promote apoptosis (33). Taken together, our results suggest that Tim23 knockdown *in vivo* produces an import defect that results in modest mitochondrial dysfunction. This is likely involved in inducing proteotoxic stress, leading to the activation of the CHOP branch of the UPR^{mt}, independent of ATF5. Therefore, even though Tim23 knockdown in *C. elegans* activates ATFS-1, our findings and those of others demonstrate that the activation of the UPR^{mt} in mammalian models may differ from its counterpart in *C. elegans*.

Much of what we know about ATF5 is through work done on ATFS-1. It is thought that similar to ATFS-1, ATF5 is imported into the mitochondrion under basal conditions, and degraded. However, in the face of proteotoxicity, proteolytically-derived peptides are exported into the cytosol, thereby redirecting ATFS-1 into the nucleus where it acts as a transcription factor (17). However, it remains unclear how these peptides may influence the translocation of ATFS-1, or of other transcription factors, in the face of proteotoxicity. Thus, we sought to investigate potential mechanisms through which retrograde signaling may be activated, and we chose to focus on the role of mitochondrial proteolysis.

Freshly isolated mitochondria left unperturbed will continue to proteolytically degrade

resident proteins and release the byproducts of this catabolism into the cytosol (4). Therefore, we incubated mitochondria to allow this basal proteolysis to occur, and then we collected all products released from the organelle that were under 3kDa. This includes all peptides that are 6-30 amino acids in length, and therefore about 1kDa in size (15). Our data support previous literature that shows that peptides are released from mitochondria basally (4), and we demonstrated that excessive induction of oxidative stress promotes proteolysis and the subsequent release of peptides from the organelle. Next, we asked whether the mitochondrial permeability transition pore (mtPTP) could facilitate this export, since it is a channel that is opened during oxidative stress. However, treatment of mitochondria with Cyclosporin A, a known inhibitor of pore formation had no impact on peptide release (13). In *C. elegans* the mitochondrial channel, HAF-1, is necessary for the release of peptides from the organelle. Recently, Yano provided evidence for a mammalian homologue, ABCB10, and demonstrated its role in mediating UPR^{mt} activation in HepG2 cells, however this channel does not seem to regulate peptide release (36). Therefore, it remains unclear which channel mediates the export of these proteolytically-derived peptides into the cytosol.

How could released peptides mediate retrograde signaling? Even in *C. elegans* this remains unknown, but a few possible mechanisms have been proposed. The first possibility is that peptides are being "sensed" by ATFS-1, or its mammalian homologue ATF5 (16, 21, 27). The second is that peptide efflux rate or volume is being monitored to influence ATF5 translocation (21). We propose that peptides are influencing the import machinery to redirect the translocation of proteins from the mitochondrion to the nucleus. Work in yeast, and more recently in mammals, has demonstrated the dynamic nature of protein import and its ability to be modulated in response to its metabolic environment. This positions the PIM as a sensor of

mitochondrial health status, and a means of communicating this throughout the cell (14). An example of this is during the process of mitophagy, where PINK1 is regularly imported into the matrix, but under stress is arrested on the outer membrane, thereby initiating mitophagy. Thus, we asked whether proteolytic byproducts could modulate protein import as a potential retrograde signal to communicate proteotoxic stress. We incubated peptides at various doses and found that import capacity was reduced in the presence of peptides in a dose- and time-dependent manner. These findings fit with the idea that low concentrations of peptides, which are continuously exported from mitochondria due to basal proteolysis, would remain innocuous. However, higher concentrations of peptides representing stress-induced elevations in protein breakdown would exert signaling consequences. For example, peptide-dependent import inhibition could serve to redirect ATF5 or other proteins to the nucleus to induce compensatory gene expression, while at the same time reducing new sources of proteotoxic stress directed toward the organelle's PIM. It remains to be addressed whether peptides could in fact influence ATF5 directly, or through some intermediary signaling step.

In summary, these results demonstrate that Tim23 knockdown *in vivo* disrupts protein import resulting in a mito-nuclear imbalance that selectively activates the CHOP-branch of the UPR^{mt}, independent of ATF5. In addition, our data highlight a potential mechanism in which protein import is modulated by the presence of mitochondrially-derived peptides in the cytosol to communicate proteotoxic stress within the mitochondrion to the nucleus. Better understanding of the UPR^{mt} and its retrograde signals would provide much needed insight into the mitochondrial stress response, which has been implicated in a variety of cancers, neurodegenerative diseases and aging.

ACKNOWLEDGMENTS

This work was supported by funding from the Natural Sciences and Engineering Research Council of Canada (NSERC) to D. A. Hood. D. A. Hood is also the holder of a Canada Research Chair in Cell Physiology. A. N. Oliveira was a recipient of CIHR-Canada Graduate Scholarship

REFERENCES

1. **Ahting U**, **Floss T**, **Uez N**, **Schneider-lohmar I**, **Becker L**, **Kling E**, **Iuso A**, **Bender A**, **Hrabé M**, **Angelis D**, **Gailus-durner V**, **Fuchs H**, **Meitinger T**, **Wurst W**, **Prokisch H**, **Klopstock T**. Neurological phenotype and reduced lifespan in heterozygous Tim23 knockout mice, the first mouse model of defective mitochondrial import. *BBA - Bioenerg* 1787: 371–376, 2009.

2. **Aldridge JE**, **Horibe T**, **Hoogenraad NJ**. Discovery of genes activated by the mitochondrial Unfolded Protein Response (mtUPR) and cognate promoter elements. *PLoS One* 2, 2007.

3. **Amico DD**, **Sorrentino V**, **Auwerx J**. Cytosolic proteostasis networks of the mitochondrial stress response. *Trends Biochem Sci* xx: 1–14, 2017.

4. **Augustin S**, **Nolden M**, **Muller S**, **Hardt O**, **Arnold L**, **Langer T**. Characterization of peptides released from mitochondria: Evidence for constant proteolysis and peptide efflux. *J Biol Chem* 280: 2691–2699, 2005.

5. **Bohnert M**, **Pfanner N**, **van der Laan M**. A dynamic machinery for import of mitochondrial precursor proteins. *FEBS Lett* 581: 2802–2810, 2007.

6. **Bolender N**, **Sickmann A**, **Wagner R**, **Meisinger C**, **Pfanner N**. Multiple pathways for sorting mitochondrial precursor proteins. *EMBO Rep* 9: 42–49, 2008.

7. **Calvo SE**, **Clauser KR**, **Mootha VK**. MitoCarta2.0: an updated inventory of mammalian mitochondrial proteins. *Nucleic Acids Res* 44: D1251-1257, 2015.

8. **Chacinska A**, **Koehler CM**, **Milenkovic D**, **Lithgow T**, **Pfanner N**. Importing mitochondrial proteins: machineries and mechanisms. *Cell* 138: 628–644, 2009.

9. **Erlich AT**, **Tryon LD**, **Crilly MJ**, **Memme JM**, **Moosavi ZSM**, **Oliveira AN**, **Beyfuss K**, **Hood DA**. Function of specialized regulatory proteins and signaling pathways in exercise-induced muscle mitochondrial biogenesis. *Integr Med Res* 5: 187–197, 2016.

10. **Ferguson DP**, **Dangott LJ**, **Lightfoot JT**. Lessons learned from vivo-morpholinos: How to avoid vivo-morpholino toxicity. *Biotechniques* 56: 251–6, 2014.

11. **Fiorese CJ**, **Haynes CM**. Integrating the UPR into the mitochondrial maintenance network. *Crit Rev Biochem Mol Biol* 9238, 2017.

12. **Fiorese CJ**, **Schulz AM**, **Lin Y**, **Rosin N**, **Pellegrino MW**, **Haynes CM**. The transcription factor ATF5 mediates a mammalian mitochondrial UPR. *Curr Biol* 26: 2037–2043, 2016.

13. **Gutiérrez-aguilar M**, **Baines CP**. Structural mechanisms of cyclophilin D-dependent

control of the mitochondrial permeability transition pore. *BBA - Gen Subj* 1850: 2041–2047, 2015.

14. **Harbauer AB**, **Zahedi RP**, **Sickmann A**, **Pfanner N**, **Meisinger C**. The protein import machinery of mitochondria—A regulatory hub in metabolism, stress, and disease. *Cell Metab* 19: 357–372, 2014.

15. **Haynes CM**, **Petrova K**, **Benedetti C**, **Yang Y**, **Ron D**. ClpP mediates activation of a mitochondrial unfolded protein esponse in C. elegans. *Dev Cell* 13: 467–480, 2007.

16. **Haynes CM**, **Yang Y**, **Blais SP**, **Neubert TA**, **Ron D**. The matrix peptide exporter HAF-1 signals a mitochondrial UPR by activating the transcription factor ZC376.7 in C. elegans. *Mol Cell* 37: 529–40, 2010.

17. **Horibe T**, **Hoogenraad NJ**. The Chop gene contains an element for the positive regulation of the mitochondrial unfolded protein response. *PLoS One* 2, 2007.

18. **Jensen RE**, **Dunn CD**. Protein import into and across the mitochondrial inner membrane: role of the TIM23 and TIM22 translocons. *Biochim Biophys Acta - Mol Cell Res* 1592: 25–34, 2002.

19. **Jovaisaite V**, **Auwerx J**. The mitochondrial unfolded protein response—synchronizing genomes. *Curr Opin Cell Biol* 33: 74–81, 2015.

20. **Kaushik S**, **Cuervo AM**. Proteostasis and aging. *Nat Med* 21: 1406–1415, 2015.

21. **Kirstein-Miles J**, **Morimoto RI**. Peptides Signal Mitochondrial Stress. *Cell Metab* 11: 177–178, 2010.

22. **Koga H**, **Kaushik S**, **Cuervo AM**. Protein homeostasis and aging: The importance of exquisite quality control. *Ageing Res Rev* 10: 1–11, 2010.

23. **Kovermann P**, **Truscott KN**, **Guiard B**, **Rehling P**, **Sepuri NB**, **Müller H**, **Jensen RE**, **Wagner R**, **Pfanner N**. Tim22, the essential core of the mitochondrial protein insertion complex, forms a voltage-activated and signal-gated channel. *Mol Cell* 9: 363–373, 2002.

24. **Memme JM**, **Oliveira AN**, **Hood DA**. Chronology of UPR activation in skeletal muscle adaptations to chronic contractile activity. *Am J Physiol Cell Physiol* 310: 1024–1036, 2016.

25. **Menzies KJ**, **Singh K**, **Saleem A**, **Hood DA**. Sirtuin 1-mediated Effects of Exercise and Resveratrol on Mitochondrial Biogenesis. *J Biol Chem* 288: 6968–6979, 2013.

26. **Mottis A**, **Jovaisaite V**, **Auwerx J**. The mitochondrial unfolded protein response in mammalian physiology. *Mamm Genome* 25: 424–433, 2014.

27. **Nargund AM**, **Pellegrino MW**, **Fiorese CJ**, **Baker BM**, **Haynes CM**. Mitochondrial import efficiency of ATFS-1 regulates mitochondrial UPR activation. *Science (80-)* 337: 587–590, 2012.

28. **Pellegrino MW**, **Nargund AM**, **Haynes CM**. Signaling the mitochondrial unfolded protein response. *Biochim Biophys Acta - Mol Cell Res* 1833: 410–416, 2013.

29. **Sandri M**, **Robbins J**. Proteotoxicity : An underappreciated pathology in cardiac disease. *J Mol Cell Cardiol* 71: 3–10, 2014.

30. **Schröder M**, **Kaufman RJ**. The mammalian unfolded protein response. *Annu Rev Biochem* 74: 739–789, 2005.

31. **Straub SP**, **Stiller SB**, **Wiedemann N**, **Pfanner N**. Dynamic organization of the mitochondrial protein import machinery. *Biol Chem* 397: 1097–1114, 2016.

32. **Takahashi M**, **Hood DA**. Protein import into subsarcolemmal and intermyofibrillar skeletal muscle mitochondria. *J Biol Chem* 271: 27285–27291, 1996.

33. **Teske BF**, **Fusakio ME**, **Zhou D**, **Shan J**, **Mcclintick JN**. CHOP induces activating transcription factor 5 (ATF5) to trigger apoptosis in response to perturbations in protein homeostasis. 24, 2013.

34. **Wang M**, **Kaufman RJ**. Protein misfolding in the endoplasmic reticulum as a conduit to human disease. *Nature* 529: 326–335, 2016.

35. **Yano M**. ABCB10 depletion reduces unfolded protein response in mitochondria. *Biochem Biophys Res Commun* 486: 465–469, 2017.

36. **Zhao Q**, **Wang J**, **Levichkin I V**, **Stasinopoulos S**, **Ryan MT**, **Hoogenraad NJ**. A mitochondrial specific stress response in mammalian cells. *EMBO J* 21: 4411–4419, 2002.

FUTURE WORK

1. Our data indicate that the CHOP-branch of the UPR^{mt} can be activated independently from ATF5. During the activation of the UPR^{mt}, CHOP and ATF5 respond to different stress signals to transcriptionally regulate a wide variety of mitochondrial chaperones and proteases. Future work should address whether these transcription factors are able to act in a compensatory fashion, or if they rely on one another for the complete maintenance of proteostasis.
2. Our model of mitochondrial proteotoxic stress resulted in the selective activation of CHOP and elevations in its downstream targets. Previous work identified mitochondrial unfolded protein response elements (MURE) that flank the CHOP binding site within the promoters of its targets. Mutation of these MURE sites blunts their response to mitochondrial stress, however it is still unknown what factors bind to these elements. By performing a CHIP assay or an electromobility shift assay, we could test the binding of transcription factors that are thought to be associating with the UPR^{mt} such as SatB5 and UBL5. These transcription factors were originally discovered in *C. elegans* but their role in the mammalian UPR^{mt} has not been assessed.
3. In contrast to our findings, Tim23 knockdown in *C. elegans* has been shown to activate the homologue of ATF5, ATFS-1. Therefore despite the evolutionary conservation of the UPR^{mt} there appears to be some discrepancy between species. Other groups have also described this inconsistency, and it appears that this may be due to the fact that the mammalian UPR^{mt} lies in the midst of an interconnected stress network. Therefore in order to understand the maintenance of proteostasis in mammals, it would be beneficial to understand how other stress responses, such as the integrated stress response, ATF4-

dependent mitochondrial stress pathway and others, may be coordinated to maintain cellular health.

4. For the isolation of peptides our current study employed a technique that allowed the collection of released products under 3kDa. Previous studies have used peptide columns and HPLC to selectively isolate mitochondrially-released peptides. Our methodology provided a cost- and time-efficient alternative and provided some preliminary data to guide future experimentation. However, it is possible that our released fraction may contain other factors besides peptides. Therefore, future experiments will incorporate the use of HPLC to specifically isolate peptides of 6-30 amino acids. This will help definitively address the role of peptides in modulating protein import.
5. Our study on the role of proteolysis and retrograde signaling addressed but one hypothesis, however there are other proposed mechanisms that have yet to be tested. For instance, it is possible that the peptides may directly influence ATF5, thereby redirecting its translocation from the mitochondrion to the nucleus.
6. Our model of proteotoxic stress involved perturbing the expression import machinery. However, this resulted only in the activation of the CHOP-branch of the UPR^{mt}. Future work could attempt to induce proteotoxicity without genetic manipulation. For example, exercise has been shown to activate both the UPR of the mitochondria and the endoplasmic reticulum. It is thought that the UPR is activated to support the heightened exercise-induced volume of protein synthesis and ensure their proper folding and maturation.

APPENDIX A: DATA TABLES AND STATISTICAL ANALYSES

Table 1A: Tim23 protein data of control and knockdown animals.

Tim23 Protein Data (A.U.)		
N	CTL	KD
1	0.9709826	0.2412409
2	0.8816105	0.3072163
3	0.7520235	0.4386753
4		0.5208293
5	0.7073644	0.4778115
6	1.026959	0.5134783
7	0.9541969	0.5589802
8	-	0.5159158
9	-	0.5794561
10	-	0.8611497
11	-	0.8873845
AVG	0.8822	0.5366
SEM	0.0521	0.0592

Unpaired T-Test	
P value	0.0015
P value Summary	**
Significantly Different? (P≤0.05)	Yes

Table 1B: Tfam protein data of control and knockdown animals.

Tfam Protein Data (A.U.)		
N	CTL	KD
1	1.150407	
2	1.181901	0.9389503
3	0.6448731	
4	0.7689064	0.4469627
5	0.7000248	0.5118412
6	0.9533582	0.5207944
7	1.043469	0.7216239
8	-	0.8199509
9	-	0.6279679
10	-	0.8812299
11	-	0.7413225
AVG	0.9204	0.6901
SEM	0.0824	0.0580

Unpaired T-Test	
P value	0.0336
P value Summary	*
Significantly Different? (P≤0.05)	Yes

Table 1C: COX IV protein data from control and knockdown animals.

COX IV Protein Data (A.U.)		
N	CTL	KD
1	0.8553003	0.90185
2	0.9331461	0.9648626
3	0.5881978	0.8622854
4	0.5616511	1.047629
5	1.031318	1.121172
6	-	0.9603741
7	-	0.7705699
8	-	0.4620712
9	-	0.8923979
10	-	0.6910083
AVG	0.7939	0.8674
SEM	0.0938	0.0598

Unpaired T-Test	
P value	0.5048
P value Summary	NS
Significantly Different? (P≤0.05)	No

Table 1D: OCT import into the mitochondrial matrix of control and knockdown animals.

OCT Protein Import (% of Imported OCT)		
N	CTL	KD
1		16
2	41	33
3	57	30
4	49	43
5	45	34
6	-	20
7	-	49
8	-	37
9	-	
10	-	
AVG	48.0000	32.7500
SEM	3.4160	3.8720

Unpaired T-Test	
P value	0.0306
P value Summary	*
Significantly Different? (P≤0.05)	Yes

Table 1E: Correlation between Tim23 protein content and OCT protein import.

Correlation		
N	Tim23 Protein	OCT Import
1	0.27	0.16
2	0.35	0.33
3	0.5	0.3
4	0.59	0.43
5	0.54	0.34
6	0.58	0.2
7	0.63	0.49
8	0.58	0.37
9	0.65	0.52
10	0.66	0.61

Linear Regression	
R^2 value	0.5331
P value	0.0165
P value Summary	*
Significantly Different? (P≤0.05)	Yes

Table 2A: Mitochondrial oxygen consumption during state III and state IV respiration in IMF mitochondria of control and knockdown animals.

O_2 Consumption State III (natoms of O_2/mg/min)		
N	CTL	KD
1	26.344	128.89
2	69.55	127.92
3	107.04	36.26
4	78	16.71
5	-	64.53
6	-	80.86
7	-	65.01
AVG	70.23	74.31
SEM	16.69	16.07

Unpaired T-Test	
P value	0.8734
P value Summary	NS
Significantly Different? (P≤0.05)	No

O_2 Consumption State IV (natoms of O_2/mg/min)		
N	CTL	KD
1	4.884	34.91
2	3.16	50.63
3	24.24	13.55
4	7.04	5.56
5	-	14.45
6	-	16.34
7	-	18.77
AVG	9.83	22.03
SEM	4.87	5.83

Unpaired T-Test	
P value	0.1918
P value Summary	NS
Significantly Different? (P≤0.05)	No

Table 2B: ROS emission during state III and IV respiration in IMF mitochondria of control and knockdown animals.

ROS Emission State III (ROS/ natoms O_2 consumed)		
N	CTL	KD
1	1.16	3.48
2	1.04	3.51
3	0.65	0.83
4	0.93	2.33
5	0.55	1.38
6	-	1.02
7	-	1.31
AVG	0.87	1.98
SEM	0.11	0.43

ROS Emission State IV (ROS/ natoms O_2 consumed)		
N	CTL	KD
1	7.43	11.73
2		8.520001
3	3.53	2.69
4	7.35	6.95
5	-	6.64
6	-	3.2
7	-	3.01
AVG	6.10	6.11
SEM	0.11	0.43

Unpaired T-Test	
P value	0.0598
P value Summary	ns
Significantly Different? (P≤0.05)	No

Unpaired T-Test	
P value	0.9991
P value Summary	ns
Significantly Different? (P≤0.05)	No

Table 3A: mtHSP70 protein data from control and knockdown animals.

mtHSP70 Protein Data (A.U.)		
N	CTL	KD
1	0.833247	0.773398
2	0.8547752	0.7959417
3	1.064442	1.084773
4	0.9361669	1.412059
5	1.38914	2.117404
6	0.9280701	1.175649
7	1.053496	0.9443448
8	-	1.058178
9	-	0.9780438
10	-	1.230151
11	-	0.9541746
AVG	1.0085	1.1386
SEM	0.0717	0.1128

Unpaired T-Test	
P value	0.4098
P value Summary	NS
Significantly Different? (P≤0.05)	No

Table 3B: HSP60 protein data from control and knockdown animals.

HSP60 Protein Data (A.U.)		
N	CTL	KD
1	0.5397548	0.4589969
2	0.6180008	0.8974862
3	0.6849582	0.6328499
4	0.6082724	1.04916
5	0.8928078	0.9006587
6	1.057783	0.4796593
7	-	0.8257073
8	-	0.7353758
9	-	1.117737
10	-	0.9781952
AVG	0.7336	0.8076
SEM	0.0815	0.0719

Unpaired T-Test	
P value	0.5216
P value Summary	NS
Significantly Different? (P≤0.05)	No

Table 3C: cpn10 protein data from control and knockdown animals.

cpn10 Protein Data (A.U.)		
N	CTL	KD
1		1.504431
2	0.6228833	2.025082
3	0.7957519	0.8345317
4	0.784143	1.232726
5	1.183278	1.421117
6	0.9724378	1.430972
7	0.8189973	0.9539758
8	-	0.7813434
9	-	1.122589
10	-	1.022741
11	-	
AVG	0.8629	1.2330
SEM	0.0717	0.1128

Unpaired T-Test	
P value	0.4098
P value Summary	NS
Significantly Different? (P≤0.05)	No

Table 3D: LonP protein data from control and knockdown animals.

LonP Protein Data (A.U.)		
N	CTL	KD
1	0.6195474	0.3061144
2	0.6195693	0.9700184
3	0.4513356	0.7766681
4	0.6662512	0.8779618
5	0.6959335	0.9626596
6	-	0.2159032
7	-	0.4266551
8	-	0.5309769
9	-	0.6353779
AVG	0.6105	0.6336
SEM	0.0717	0.1128

Unpaired T-Test	
P value	0.8643
P value Summary	NS
Significantly Different? (P≤0.05)	No

Table 3E: ATF5 protein data from control and knockdown animals.

ATF5 Protein Data (A.U.)		
N	CTL	KD
1	0.7743397	1.385935
2		1.023056
3	1.592352	0.6377682
4	0.6868413	0.8388594
5	0.7338548	0.8105195
6	1.114785	1.462193
7	0.9051485	1.380047
8	-	0.7651758
9	-	1.428164
10	-	0.8455867
AVG	0.9679	1.0577
SEM	0.0717	0.1128

Unpaired T-Test	
P value	0.6053
P value Summary	NS
Significantly Different? (P≤0.05)	No

Table 3F: CHOP protein data from control and knockdown animals.

CHOP Protein Data (A.U.)		
N	CTL	KD
1		0.3450447
2	0.2838199	0.5536446
3	0.5661022	0.8984315
4	0.1711907	1.545068
5	0.1776699	1.035631
6	0.0622094	
7	0.363386	
8	-	0.1504418
9	-	0.2806712
10	-	0.8399679
AVG	0.2707	0.7061
SEM	0.0717	0.1128

Unpaired T-Test	
P value	0.05
P value Summary	*
Significantly Different? (P≤0.05)	Yes

Table 4A: *cpn10* mRNA data from control and knockdown animals.

cpn10 mRNA Data (ΔCT)		
N	CTL	KD
1	2.171846	1.87155
2	1.712675	3.336012
3	1.609414	2.400604
4	0.8588074	1.205472
5	2.301737	1.717492
6	3.185344	2.76584
7	2.758926	3.623366
8		3.784026
9	-	3.120884
AVG	2.0855	2.6472
SEM	0.2923	0.3019

Unpaired T-Test	
P value	0.2116
P value Summary	NS
Significantly Different? (P≤0.05)	No

Table 4B: *LonP* mRNA data from control and knockdown animals.

***LonP* mRNA Data**		
N	CTL	KD
1	0.7548169	
2	0.9568937	0.9602019
3	1.101486	0.54255
4	0.5024896	0.6155571
5	1.685142	1.2605
6	1.124732	1.745178
7	0.764742	0.8029145
8	1.336282	1.078348
9	-	0.8123369
AVG	1.0283	0.9772
SEM	0.1314	0.1374

Unpaired T-Test	
P value	0.7919
P value Summary	NS
Significantly Different? (P≤0.05)	No

Table 4C: *HSP60* mRNA data from control and knockdown animals.

***Hsp60* mRNA Data (ΔCT)**		
N	CTL	KD
1	1.722142	1.314453
2	0.9785895	0.923695
3	1.424187	2.068885
4	0.726134	1.091315
5	2.167586	1.513709
6	2.125198	2.505007
7	2.141938	2.556027
8	3.651004	2.714573
9	-	2.043776
AVG	1.8671	1.8590
SEM	0.3197	0.2234

Unpaired T-Test	
P value	0.9835
P value Summary	NS
Significantly Different? (P≤0.05)	No

Table 4D: mtHSP70 mRNA data from control and knockdown animals.

***mtHSP70* mRNA Data (ΔCT)**		
N	CTL	KD
1	1.907764	1.030411
2	0.713637	0.9519883
3	1.001654	1.703628
4	0.5558497	0.8947718
5	1.514157	1.087605
6	1.644336	1.684619
7	1.289915	1.336527
8	2.364284	1.420414
9	-	1.407776
AVG	1.3739	1.2797
SEM	0.2159	0.1012

Unpaired T-Test	
P value	0.6873
P value Summary	NS
Significantly Different? (P≤0.05)	No

Table 4E: *CHOP* mRNA data from control and knockdown animals.

***CHOP* mRNA Data (ΔCT)**		
N	CTL	KD
1	0.9654048	1.215488
2	0.5072798	1.654349
3	0.483783	0.6409809
4	0.283044	
5	1.131608	0.551734
6	0.821074	0.971155
7	0.414419	0.62835
8	0.772394	0.521684
9	-	0.483822
AVG	0.6724	0.8334
SEM	0.1044	0.1474

Unpaired T-Test	
P value	0.3875
P value Summary	NS
Significantly Different? (P≤0.05)	No

Table 4F: *ATF5* mRNA data from control and knockdown animals.

***ATF5* mRNA Data (ΔCT)**		
N	CTL	KD
1	0.3281052	
2	1.030194	1.32043
3	1.253029	0.4327194
4	0.5011962	0.4422385
5	1.770217	1.138875
6	1.390195	2.2088
7	1.645271	3.463086
8	2.232759	1.699408
9	-	1.280162
AVG	1.2689	1.4982
SEM	0.2263	0.3501

Unpaired T-Test	
P value	0.5909
P value Summary	NS
Significantly Different? (P≤0.05)	No

Table 5: Peptide Release from IMF mitochondria under oxidative stress conditions, H_2O_2 and $FeSO_4$.

Peptide Release Data (ug/uL)						
N	**CTL**			**Cyclosporin A**		
	CTL	H_2O_2	H_20_2+$FESO_4$	CTL	H_2O_2	H_20_2+$FESO_4$
1	0.44	0.56	1.3	0.8	0.97	2.05
2	0.64	0.62	1.85	1.4	1.29	2.95
3	0.53	0.39	2.14	0.74	0.48	2.15
4	0.45	0.57	2.08	0.6	0.52	1.67
5	0.51	0.51	0.7	0.53	0.56	0.83
6	0.518	0.615	0.9	0.605	0.535	0.77
AVG	0.5147	0.5442	1.4950	0.7792	0.7258	1.7367
SEM	0.2923	0.3019	0.3019	0.3019	0.3019	0.3019

Repeated Measures 2-Way ANOVA			
Source of Variation	P value	P value Summary	Significant?
Interaction	0.7575	NS	No
Cyclosporin A	0.1883	***	Yes
Oxidative Stress	0.0008	NS	No

Bonferroni Post Hoc Test-Contol vs. Oxidative Stress				
Condition	Difference	T	P value	Summary
H_20_2	0.01192	0.05922	P>0.05	NS
H_2O_2+$FeSO_4$	-0.9689	4.815	P<0.001	**

Table 6A: OCT protein import into the matrix of IMF mitochondria in the presence of 2ug of peptides.

Protein Import with 2ug Peptides (Imported OCT/ Total OCT)		
N	CTL	2ug PEP
1	0.32	0.31
2	0.39	0.4
3	0.39	0.37
4	0.37	0.44
5	0.51	0.5
6	0.51	0.49
AVG	0.4150	0.4183
SEM	0.0318	0.0298

Paired T-Test	
P value	0.822
P value Summary	NS
Significantly Different? (P≤0.05)	No

Table 6B: OCT protein import into the matrix of IMF mitochondria in the presence of 4ug of peptides.

Protein Import with 4ug Peptides (Imported OCT/ Total OCT)		
N	CTL	4ug PEP
1	0.38	0.45
2	0.37	0.44
3	0.45	0.43
4	0.44	0.45
5	0.48	0.46
6	0.44	0.45
AVG	0.4267	0.4467
SEM	0.0175	0.0042

Paired T-Test	
P value	0.2856
P value Summary	NS
Significantly Different? (P≤0.05)	No

Table 6C: OCT protein import into the matrix of IMF mitochondria in the presence of 6ug of peptides for 10 minutes.

Protein Import with 6ug Peptides-10 min (Imported OCT/ Total OCT)		
N	CTL	6ug PEP
1	0.13	0.15
2	0.38	0.4
3	0.38	0.4
4	0.43	0.33
5	0.31	0.45
AVG	0.3260	0.3460
SEM	0.0526	0.0526

Paired T-Test	
P value	0.626
P value Summary	NS
Significantly Different? (P≤0.05)	No

Table 6D: OCT protein import into the matrix of IMF mitochondria in the presence of 6ug of peptides for 20 minutes.

Protein Import with 6ug Peptides-20 min (Imported OCT/ Total OCT)		
N	CTL	6ug PEP
1	0.32	0.39
2	0.49	0.48
3	0.47	0.42
4	0.47	0.39
5	0.4	0.33
AVG	0.4300	0.4020
SEM	0.0315	0.0244

Paired T-Test	
P value	0.3627
P value Summary	NS
Significantly Different? (P≤0.05)	No

Table 6E: OCT protein import into the matrix of IMF mitochondria in the presence of 6ug of peptides for 30 minutes.

Protein Import with 6ug Peptides-30 min (Imported OCT/ Total OCT)		
N	CTL	6ug PEP
1	0.35	0.39
2		
3	0.5	0.34
4	0.34	0.15
5	0.42	0.33
6	0.23	0.09
7	0.45	0.39
8	0.47	0.41
9	0.47	0.32
10	0.4	0.29
11	0.32	0.36
12	0.3	0.35
AVG	0.3864	0.3109
SEM	0.0256	0.0306

Paired T-Test	
P value	0.0157
P value Summary	*
Significantly Different? (P≤0.05)	Yes

APPENDIX B: SUPPLEMENTAL DATA

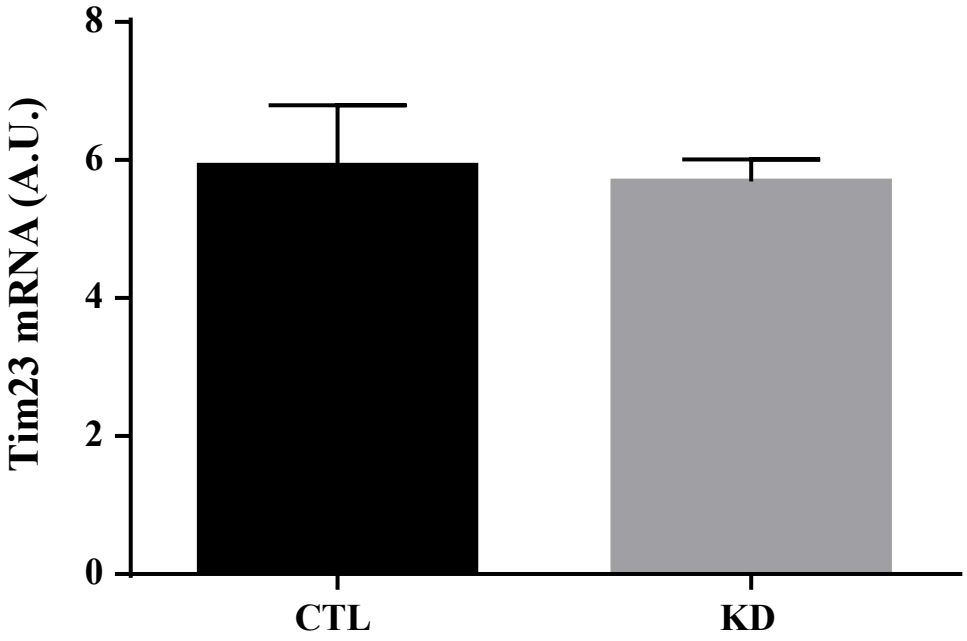

Figure S1: *Tim23* mRNA levels following In-Vivo Morpholino treatment. (n=8-9) CTL, control; KD, knockdown.

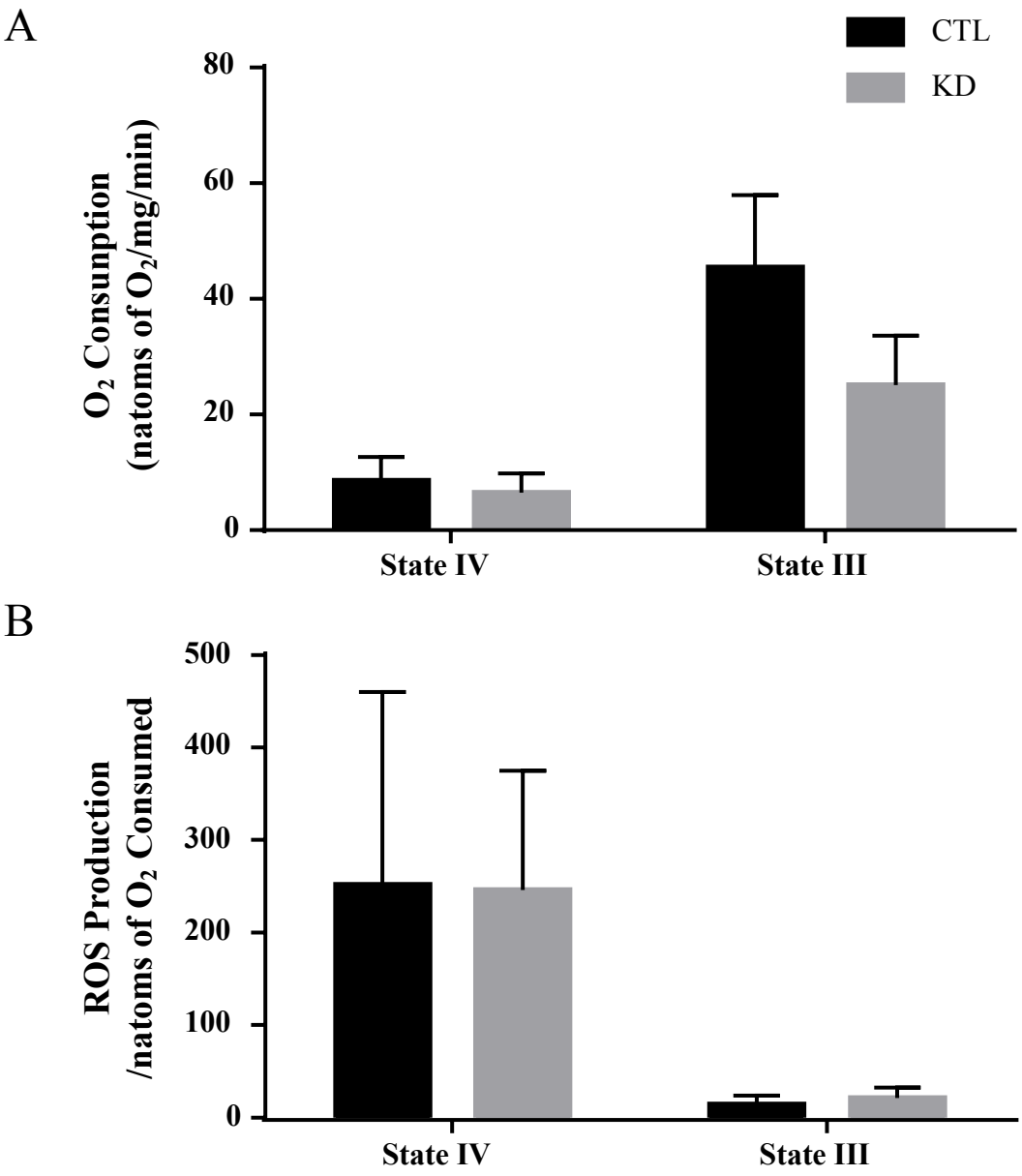

Figure S2: Graphical representation of mitochondrial respiration from SS mitochondria during both state IV (basal) and state III (maximal) respiratory states **(A).** ROS production under the same respiratory conditions, corrected for oxygen consumption **(B)**. (n=3-5) CTL, control SS mitochondria; KD, knockdown SS mitochondria

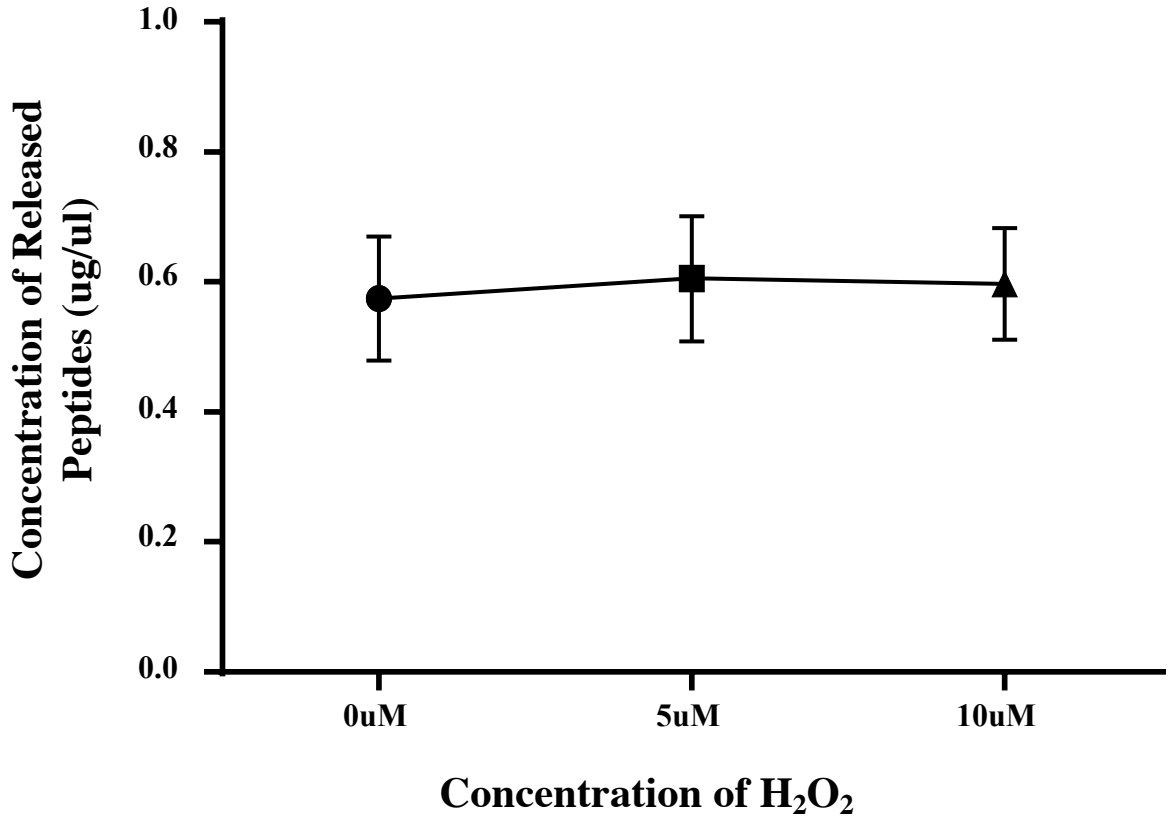

Figure S3: Concentration of peptides released from the mitochondria following 30 minutes incubation with various doses of H_2O_2 at 30ºC. (n=4).

APPENDIX C: LABORATORY METHODS AND PROTOCOLS

IN-VIVO MORPHOLINO TREATMENT

Reference: Ferguson DP, et al. Biotech, 2015, 56:251-256.

In-Vivo Morpholinos are shipped as a sterile lyophilized solid and can be diluted with either sterile water or phosphate-buffered saline (PBS) as per the company's recommendation. Stock may be kept at room temperature for about a year. You may autoclave the stock after a year and continue using.

Stock solutions of Morpholino oligos		
Amount of Morpholino (Amount of Vivo-Morpholino)	Volume of sterile water	Resulting stock concentration
100 nanomoles	0.10 mL	1.0 milliMolar (mM)
(100 nanomoles Vivo-MO)	0.20 mL	0.5 milliMolar (mM)
300 nanomoles	0.30 mL	1.0 milliMolar (mM)
(400 nanomoles Vivo-MO)	0.80 mL	0.5 milliMolar (mM)
1000 nanomoles	1.00 mL	1.0 milliMolar (mM)
(2000 nanomoles Vivo-MO)	4.00 mL	0.5 milliMolar (mM)

GeneTools will provide a product sheet containing information such as molecular weight, and weight of the product. Each oligo will differ in these values based on the sequence synthesized.

In-Vivo Morpholino can be used locally or systemically, with good delivery to most major organs (liver, small intestine, colon, muscle, lung, and stomach tissues) via an intravenous or intraperitoneal injection. Delivery has been demonstrated to a lesser extent in the spleen, heart, skin and brain.

For systemic delivery:

1. Weigh mouse prior to the first injection
2. Prepare injection at a dose of 12.5mg/kg of body in a sterile 29 G x1/2 syringe
3. Restrain the mouse by holding them by the scruff of the neck and the base of the tail, thus exposing the belly. Or by using a cloth, create a small pocket for the mouse to crawl into, hold the animals back and raise the tail, exposing the intraperitoneal cavity.
4. Locate the intraperitoneal space, just medial to the thigh, and inject the animal. Minimal resistance should be felt when piercing this cavity.
5. Monitor the animal for a while after, typically there are little to no signs of discomfort.
6. Injections are given once daily for 3 consecutive days, following steps 2-5. Tissues may be harvested 48hrs following the last injection.

MITOCHONDRIAL ISOLATIONS FROM MUSCLE

References: Cogswell et al. Am J Physiol, 1993, 264: C388-C389
Krieger et al. J Appl Physiol, 1980, 48: 23-28

Reagents:

All buffers are set to pH 7.4 and stored at 4 °C

- Buffer 1
  100 mM KCl
- Buffer 1 + ATP
  Add 1 mM ATP to Buffer 1

5 mM MgSO4
5 mM EDTA
50 mM Tris base

- Buffer 2
  100 mM KCl
  5 mM MgSO4
  5 mM EGTA
  50 mM Tris base
  1 mM ATP
- Nagarse protease (Sigma, P-4789)
  10 mg/ml in Buffer 2
  Make fresh for each isolation, keep on ice

- Resuspension medium
  100 mM KCl
  10 mM MOPS
  0.2% BSA

Procedure:

1. Remove various muscles from mouse and place in a scintillation vial containing ice cold buffer 1.
2. Place muscles on a watch glass that is also on ice and trim away fat and connective tissue. Proceed to thoroughly mince the muscle sample with forceps and scissors, until no large pieces are remaining.
3. Place the minced tissue in a plastic centrifuge tube and record the exact weight of tissue.
4. Add a 10-fold dilution of Buffer 1 + ATP to the tube.
5. Homogenize the samples using the Ultra-Turrax polytron with 40% power output (9.8 Hz) and 10 sec exposure time.
6. Using a Beckman JA 25.50 rotor, spin the homogenate at a centrifuge setting of 800 g for 10 min. This step divides the IMF and SS mitochondrial subfractions. The supernate will contain the SS mitochondria and the pellet will contain the IMF mitochondria.

SS mitochondrial isolation:

7. Filter the supernate through a single layer of cheesecloth into a second set of 50 ml plastic centrifuge tubes.
8. Spin tubes at 9000 g for 10 min. Upon completion of the spin discard the supernate and gently resuspend the pellet in 3.5 ml of Buffer 1 + ATP. Since the mitochondria are easily damaged, it is important that the resuspension of the pellet is done carefully.
9. Repeat the centifugation of the previous step (9000 g for 10 min) and discard the supernate.
10. Resuspend the pellet in 100 µl of Resuspension medium, being gentle so as to prevent damage to the SS mitochondria. Some extra time is needed during this final resuspension to ensure the SS pellet is completely resuspended.
11. Keep the SS samples on ice while proceeding to islolate the IMF subfraction.

IMF mitochondrial isolation:

7. Gently resuspend the pellet (from step 6) in a 10-fold dilution of Buffer 1 + ATP using a teflon pestle.
8. Using the Ultra-Turrax polytron set at 40% power output, polytron the resuspended pellet for 10 s. Rinse the shaft with 0.5 ml of Buffer 1 + ATP.
9. Spin at 800 g for 10 min and discard the resulting supernate.
10. Resuspend the pellet in a 10-fold dilution of Buffer 2 using a teflon pestle.

11. Add the appropriate amount of nagarse. The calculation for the appropriate volume is 0.025 ml/g of tissue. Mix gently and let stand exactly 5 min.
12. Dilute the nagarse by adding 20 ml of Buffer 2.
13. Spin the diluted samples at 5000 g for 5 min and discard the resulting supernate.
14. Resuspend the pellet in a 10-fold dilution of Buffer 2. Gentle resuspension is with a teflon pestle.
15. Spin the samples at 800 g for 10 min. Upon the completion of the spin, the supernate is poured into another set of 50 ml plastic tubes (on ice), and the pellet is discarded.
16. Spin the supernate at 9000 g for 10 min. The supernate is discarded and the pellet is resuspended in 3.5 ml of Buffer 2.
17. Spin samples at 9000 g for 10 min and discard the supernate.
18. Gently resuspend the pellet in 200 µl of Resuspension medium.

MITOCHONDRIAL RESPIRATION

Reference: Estabrook, R.W., Meth. Enzymol., **10**: 41-47 (1967)

The rate of mitochondrial respiration is an important consideration in the biochemical analysis of mitochondria. There are three phases of interest in analyzing the respiratory ability of mitochondria. Mitochondria produce ATP in the presence of oxygen. The respiratory ability of the freshly isolated IMF and SS mitochondrial fractions and the homogenates can be illustrated by measuring the rate of oxygen consumption using a Clark oxygen electrode in the presence of a) the substrate alone (e.g. glutamate for state 4 or resting respiration); b) ADP, (state 3 or active respiration); and c) $NADH^+$, which is used to measure the amount of damage that has occurred to the mitochondria, since the inner membrane is impermeable to $NADH^+$.

Reagents:

1. VO_2 Buffer for **muscle** mitochondria:

   250 mM **Sucrose** 42.8 g/500 ml
   50 mM **KCl** 1.86 g/500ml
   25 mM **Tris-HCl *** 1.97 g/500ml
   10 mM **K_2HPO_4** 0.871 g/500ml
   pH to 7.4

   * In place of 25mM Tris-HCl you can use 25 mM Tris (aka Tris (hydroxymethyl) methylamine). This works out to 1.5125 g/500ml (FW=121.4). Using Tris in place of Tris-HCl means that you will have to add more HCl to get the pH down to 7.4
2. **Glutamate** - final conc. of 11.1 mM.....**2.0 M initial conc**. (406.4 mg/ml)
3. **ADP** - Final conc of 0.44 mM ..... **20 mM initial conc.** (8.54 mg/ml)
4. **NADH** - Final conc.: 2.8 mM.....**0.5 M initial conc.** (354.7 mg/ml)

Procedure:

1. Set water bath at 30°C -- clean out chambers (Clark oxygen electrode; Yellow Springs Inst. Co., Yellow Springs, OH) and stir bars.

2. Add 250uL of VO_2 Buffer to each chamber.

3. Insert electrode # 2 into the chamber.

4. Remove all bubbles in the chamber and allow it to reach equilibrium temperature (30^oC) while spinning.

5. Set recorder for chamber # 2 and paper speed for 3 cm/min.

6. Set monitor and recorder to 100 %.

7. Remove electrode. Add 50 µl of mitochondria into the chamber.

8. Allow a steady state to be reached.

9. Add 12.5 µl of pyruvate and 12.5 µl of malate (heart) or 12.5 µl glutamate (muscle).

10. Wait approximately 3 minutes then add ADP: 50 µl for muscle, 100 µl for heart.

11. Wait (about 2-3 minutes) for a steady rate of state 3 respiration before adding 12.5 µl of NADH. Prepare the next chamber while the respiration recordings are being made.

12. Clean out the chamber in the following manner : Remove the electrode and aspirate, remove the magnetic stir bar and aspirate, and finally, clean the electrode by rinsing with distilled water and pat dry.

13. Put electrode in the next chamber (which should already have the buffer and sample in it).

14. Prepare the next chamber while the measuring the respiration of the current chamber (ie. add 2 ml of VO_2 Buffer and allow to equilibrate).

15. Calculate the state 4, state 3 and $NADH^+$ rates for each sample. Remember that the chart speed is 3 cm/sec and full scale is 100 %. (slope=rate=blocks/min)

16. Calculate the rates of state 3 and state 4 respiration per mg of mitochondrial protein by dividing the state 3 and 4 rates by the amount of protein (mg) added to the VO_2 Buffer.

Calculate the Respiratory Control Ratio (RCR):

RCR = state 3 rate/ state 4 rate

For the above ratio you need only use slopes from the graph. However, for exact calculations of the state 3 and state 4 rates follow the method below:

References: Biological Oxygen Monitor Instruction Manual (table 1, p.13).
Chappel, J.B. Biochem. J. (1964) 90:225-237

- Assume a barometric pressure of 1 atm. (760 mmHg). At 1 atm. the amount of oxygen dissolved in medium equals 5.47 µl O_2/ml (value taken from Biological Oxygen Monitor Instruction Manual). Since 2 ml are being used in the chamber, total O_2 is equal to 2 x 5.47 = 10.94 µl. The rate of change from 100% O_2 can then be used to calculate the amount of O_2 consumed per unit time:

$$\frac{\text{State 3 or 4 /mg protein x 10.94 µl } O_2}{100\%}$$

- But the units of O_2 consumed are now typically expressed in units of natoms O_2. Thus,

$$\frac{\text{State 3 or 4 /mg prot. x 968 natoms } O_2}{100\%} = x \text{ natoms } O_2\text{/mg prot./min.}$$

ROS EMISSION

Background: Mitochondria are the primary source of reactive oxygen species (ROS) to the cell. It is estimated that about 2% of total cellular oxygen is converted ROS by the inappropriate reduction of molecular oxygen by intermediate members of the electron transport chain (ETC). ROS are damaging molecules that are capable of compromising the integrity of macromolecules within the mitochondria and may lead to overall organelle dysfunction. In particular, mtDNA may be prone to attack by ROS because 1) mtDNA is located in close proximity to the ETC, 2) mtDNA lacks the protective sheath of histones compared to nuclear DNA and, 3) mitochondria have an insufficient repair system for mtDNA mutations. ROS can exist in a variety of molecular permutations such as superoxide (O_2^-), hydroxyl radical (OH^-) and hydrogen peroxide (H_2O_2).

DCF (2,7,-dichloro-fluorescein; Fig.1) is a reagent that is non-fluorescent until the acetate groups are removed by intracellular esterases and oxidation occurs within the mitochondria (Fig.1). DCF is oxidized by all of the different forms of ROS and this can be detected by monitoring the increase in fluorescence with a fluorometric plate reader. The appropriate plate reader filter settings for fluorescein are the following: **Excitation 485/20 and Emission 528/20** (Fig.2).

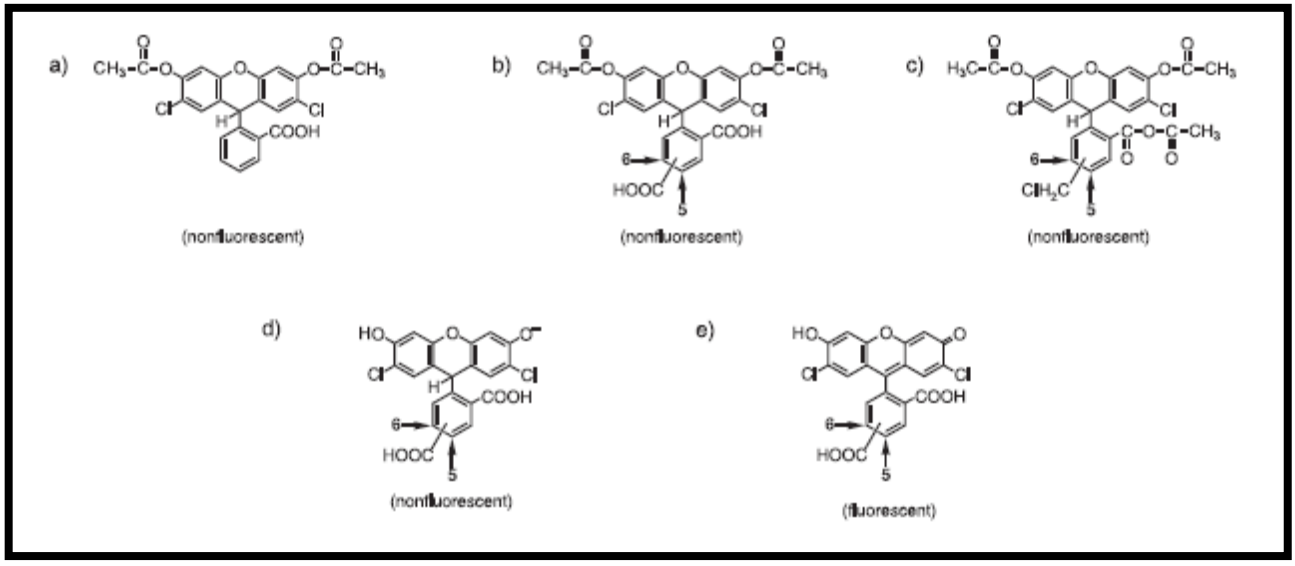

Fig.1-DCF molecule and oxidation of DCF resulting in fluorescence

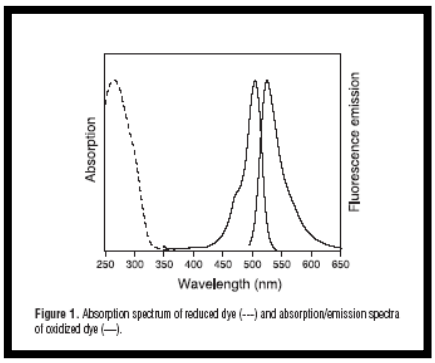

Figure 1. Absorption spectrum of reduced dye (---) and absorption/emission spectra of oxidized dye (—).

Fig.2-Absorption and Emission Spectra of oxidized dye

KC4 Software Settings: The Settings icon in the upper left corner allows the alteration of various parameters. Once clicked, another window appears, click on the Wizard Icon. In this window there will be a variety of components that can be altered. The following are the parameters that need to be changed in order to utilize the DCF and measure time-dependent ROS production from isolated mitochondria:

1) Top Middle Panel- Absorbance, Fluorescence, Luminescence- choose **Fluorescence**
2) Top Left Panel- End Point, Kinetic, Spectrum- choose **Kinetic**
3) Top Middle Panel- Click on larger box labeled Kinetic to set parameters- **Run Time 1:20:00, Interval 5:00 (takes a measure every 5 minutes),** click on box labeled **Allow Well Zoom during Read,** and also click on box labeled **Individual Well Auto Scaling**- The Well Zoom and Auto scaling allows for monitoring each individual well during the experiment and scales it appropriately.
4) Middle Panel-***Filter Set***- Choose #1, then set the **excitation to 485/20**, and **emission to 528/20** as described above. The optics position should be set to the **TOP** (i.e. readings are taken from the top of the well) and the sensitivity is set at **50** (depending upon the amount and/or nature of the sample).
5) Plate-Type-choose **96-well plate**, choose which wells are to be read i.e. **A1-C12.**
6) Shaking-**Intensity** set at **1, Duration** set at **15s** and then click the box that is labeled **before every reading** (it shakes the samples for 15 s before every reading).
7) Temperature Control- Click on the box indicating **YES,** also click on box labeled pre-heating, and put 37°C into the temperature box.

Reagents:

DCF (2,7,-dichlorodihydrofluorescein diacetate) reagent MW=487.29 (Molecular Probes D-399/ 100mg)

1° STOCK- Make up **50mM** Stock Solution in EtOH- 24 mg/ml- only make about 500ul i.e. 14 mg per 500ul EtOH. Wrap stock solution in aluminum foil and limit exposure to light since DCF is light-sensitive.

Working Stock Solution-2° STOCK- Dilute 50mM by 100-fold by taking 10ul and adding 990 ul of EtOH to attain a **500uM DCF Stock Solution**. This will be the DCF concentration used to add to the reaction mixture.

VO_2 Buffer- refer to mitochondrial respiration protocol

Procedure:

1. SS and IMF mitochondria are isolated as described in the mitochondrial isolation protocol. Alternatively, frozen mitochondrial extracts can also be used.
2. Determine the volume necessary for 50ug of mitochondria. Typical volumes should range between 5-40ul depending upon concentration of mitochondrial extracts.

3. Final concentration of DCF is 50uM. The total volume of the reaction mixture is 250ul. Thus, 25ul of DCF is used in the reaction mixture since this represents a 10-fold dilution. Set up table (***as shown below***) and determine the amount of VO_2 buffer necessary to make each of the reaction mixtures equal to 250 ul. (Remember to include a ***control*** with only VO2 buffer and DCF reagent as in Well #1 shown below)

	SS			
	Control	Mar.23	Mar.25	Mar.29
	Well #1	Well #2	Well #3	Well #4
ug mito	0	50	50	50
ul mito	0.00	11.77	9.80	17.24
VO2 Buff	225.00	213.23	215.20	207.76
DCF (50uM)	25	25	25	25
Total Volume	250	250	250	250

4. Once table is complete and volumes for all samples have been determined, place the frozen (already thawed) or fresh mitochondria, VO_2 buffer and DCF (500uM) into a 37°C circulating water bath for 5-10 min.
5. Pipette the volume of VO_2 buffer required for each of the samples followed by the mitochondrial samples into the appropriate wells of a 96-well plate. In addition, include a well (usually in the corner well) with only 250 ul of VO_2 buffer to monitor temperature (see below). Place the 96-well plate with the VO_2 buffer and mitochondria into a 37°C incubator. Using the YSI temperature probe, place the recording electrode into the well with buffer only and monitor the temperature until 37°C is reached. During this time, be sure that the KC4 software is set up and that the Biotek plate reader is pre-heating to 37°C.
6. Once mitochondria and buffer have reached temperature (37°C), take the DCF out of the circulating water bath (37°C) and quickly add the DCF to each of the reaction mixtures. Following addition of DCF, promptly place the plate into the Biotek plate reader for fluorescence measurement and start the KC4 program by pressing **READ** plate on the upper left portion of the computer screen. Kinetic program will operate for 1 h and 20 min.

MITOCHONDRIAL PROTEIN IMPORT

Reference: Takahashi and Hood, J. Biol. Chem. (1996) 271, 27285-27291

The majority of nuclear-encoded mitochondrial proteins require a mechanism of import. Proteins destined for this organelle also require a presequence. This will provide a "passport" containing instructions for the final destination for that protein. Once the protein has reached its final destination, the presequence is cleaved, leaving a "mature" protein. By taking advantage of this change in protein size, we are able to establish a means by which imported proteins can be discerned. This can be accomplished by radiolabelling the precursor proteins in vitro then allowing them to be imported. The

samples can be electrophoresed on a polyacrylamide gel and will appear as two bands (precursor and mature) when the gel is exposed to film.

A. <u>In Vitro Transcription And Translation</u>

Note: Steps 1-7 are usually done on the same day.

1. Linearize DNA

- Combine the following in an eppendorf:
  - 40 µl DNA at 5 µg/µl (200 µg)
  - 5 µl 10x Enzyme buffer
  - 5 µl Restriction enzyme
- incubate for 1 hour at 37°C.

2. Proteinase K- only to be carried out if using miniprep DNA, otherwise skip to step 3

- Combine the following:
  - 50 µl above
  - 6.7 µl 10X Proteinase K buffer
  - 6.7 µl 5% SDS
  - 7.0 µl PK [1 µg/µl] -- to a final [ ] of 100 µg/ml

Note: 1 µg/µl PK should be made on day of experiment by diluting the stock; 20 µg/µl stock PK is kept at in the -20 °C freezer.

- Incubate for 1 hour at 37°C.

3. Phenol extraction / ethanol precipitation

a) Add appropriate volume of sterile dH_2O so that the final volume equals 400 µl.
b) Add 400 µl phenol.
c) Mix by inversion and spin in microfuge for 30 sec.
d) Withdraw and save upper phase.
e) Add 400 µl Phenol:Chloroform:Isoamylalcohol (25:24:1, v:v:v).
f) Mix by inversion and spin in microfuge for 30 sec.
g) Withdraw and save the upper phase.
h) Add 400 µl Chloroform:Isoamylalcohol (24:1, v:v).
i) Mix by inversion and spin.
j) Withdraw and save the upper phase.
k) Add 40 µl 3 M Na Ac (1/10 vols) and 1 ml of -20 °C 100% ethanol (2.5 vols).
l) Mix by inversion and precipitate at -70 °C for 30 min (can be left overnight).
m) Spin 10 min. at 4 °C and discard the supernate.
n) Gently wash pellet with 400 µl 70% ethanol.
o) Spin 3 min. at 4°C, discard the supernate.
p) Dessicate pellet.
q) Resuspend the pellet in 30-50 µl TE, pH 8.0.

4. Measure [DNA]

- Read the O.D. at A_{260} to determine the concentration of DNA.
- Dilute the DNA to 0.8 µg/µl in TE (pH 8.0).

5. Transcription

- Combine the following in the order indicated:
  - 60.8 µl plasmid (0.8 µg/µl in TE)

8.4 µl dH_2O
5.2 µl NTP (10 mM)
10.0 µl ATP (10 mM)
11.6 µl 7-MGG (1 mM)
15.6 µl Mix
5.2 µl RNA guard
4.8 µl of appropriate RNA polymerase
121.6 µl total volume

- Incubate for 90 min. at the optimum temperature for the polymerase (37 °C for T7, 40 °C for SP6).
- Note: the reaction can be scaled up or down in volume, provided proportions are maintained.

6. Phenol extraction / ethanol precipitation

- Bring volume up to 400 µl with sterile dH_2O (using 280 µl)
- Proceed exactly as described in step 3, above.
- Resuspend the pellet in 25-40 µl sterile dH_2O

7. Measure [mRNA]

- Read the O.D. at A260 to determine the concentration of mRNA
- Dilute mRNA to 2.8 µg/µl in sterile dH_2O. Store at -20 °C in 50 µl aliquots

B. In Vitro Translation

Reference: Promega Technical Manual: "Rabbit Reticulocyte Lysate System" Part # TM232.

1. Combine the following:

Promega lysate		(For 1 reaction -- in µl)	For 10µl of final "lysate"
Lysate	64.1%	11.8	6.38
AA(-met)	2.2%	0.4	0.22
st. dH_2O	21.6%	3.97	2.15
^{35}S-met	7.2%	1.33	0.72
mRNA	5.4%	1.0	0.54
		18.5 µl	

Notes: i) The Promega manual suggests that lysate should be thawed slowly on ice. It also suggests that the number of freeze/thaw cycles be limited to two.
ii) The volume of mRNA can be adjusted to optimize translational efficiency by altering the dH_2O volume accordingly.

2. Incubate for 25-60 min. at 30 °C (note: time may vary with mRNA)
3. Record ^{35}S use (15 µCi/µl).

C. Protein Import

Isolated mitochondria (see protocol "MITOISO") should be resuspended in a resuspension buffer. A sample pipette plan is provided below: (typically 13 lanes can be run on SDS-PAGE gels)

			SS					IMF		
Lane	1	2	3	4	5	6	7	8	9	10	11
time (min)		0	1.5	3	6	10	0	1.5	3	6	10
mito (µg)		50---------->					20---------->				

lysate (µl)	5	12---------->
TOTAL	62---------->	32---------->

- preincubate both the mitochondria and lysate for 10 minutes @ 30^0C, then combine lysate and mitochondria to initiate import reaction.
- incubate @ 30^0C for the times indicated.
- to recover the mitochondria following import, spin the entire volume through a sucrose gradient (600 µl) for 15 min at 4^0C.
- remove the supernate with pasteur pipette into the radioactive waste.
- resuspend pellets in 25 µl breaking buffer.
- add 25 µl lysis buffer and 10 µl BPB.
- denature samples for 5 min. at 95°C, then quick cool on ice.
- apply the samples to an 8% SDS polyacrylamide gel (see "Gel" on disk) and electrophorese overnight at approximately 45 volts.

D. Fluorography

1. Remove gel from chamber and cut out the appropriate section of the gel. Identify the orientation of the gel.
2. Boil the gel in approximately 200 ml of 5% TCA for 5 min. in metal container, over the Bunsen burner in the fume hood.
3. Using a spatula, transfer the gel to a radioactive tupperware container and rinse the gel briefly in dH_2O (approximately 30 seconds).
4. Wash in 10 mM Tris-base for 5 min. on shaker (approxiamtely 100 ml).
5. Wash in 1 M salicylic acid for 30 min. on shaker (approximately 100 ml).
6. Dry the gel for 1 hr at 80°C.
7. Combine all wash solutions in the metal container and boil down the liquid. Let cool and then dispose of in ^{35}S waste.

E. Solutions for Transcription and Translation

Note: because mRNA is involved in both transcription and translation, sterile conditions should be adhered to at all times. Use sterile glassware, eppendorfs, dH_2O, etc. Autoclave or sterile filter solutions where indicated.

10 X Proteinase K buffer — For 10 ml

500 mM NaCl — 0.2922g or 5 ml of 5 M NaCl
50 mM EDTA — 0.1861g or 0.5 ml of 0.5 M EDTA, pH 8
100 mM Tris-HCl — 0.1576g or 1 ml of 1 M Tris, pH 8
3.5 ml sterile dH_2O
-pH to 8.0

20 mM HEPES Use 0.4766g/100 ml, pH to 7.0, autoclave.

1 M HEPES Use 23.83 g/100ml, pH to 7.9, autoclave. Store at RT.

NTPs	MW(g/mol)	For 50 mM (stocks)
CTP	483.2	24.16 mg/ml
GTP	523.2	26.16 mg/ml
UTP	484.1	24.21 mg/ml
ATP	551.1	27.56 mg/ml

Note: These NTPs should be made up in 20 mM HEPES. Make up 1 ml of each as stock. Filter each sterile (using sterile acrodisk).

10 mM NTPs	For 500 µl
10 mM GTP	100 µl of 50 mM GTP stock
10 mM CTP	100 µl of 50 mM CTP stock
10 mM UTP	100 µl of 50 mM UTP stock
20 mM HEPES (pH 7.0)	200 µl of 20 mM HEPES(pH 7.0)

- store in 50 µl aliquots at -20 °C

10 mM ATP	For 500 µl
10 mM ATP	100 µl of 50 mM ATP
20 mM HEPES (pH 7.0)	400 µl of 20 mM HEPES (pH 7.0)

- store in 50 µl aliquots at -20 °C

7-MGG (Pharmacia 27-4635-02)
1 mM stock is made from Pharmacia pellet. 25U is ordered; added to this is 1208 µl of 20 mM HEPES (pH 7.0), yielding a 1 mM stock. Aliquot into 300 µl, store at -20 °C.

Mix 1	For 1200 µl
0.167 M HEPES (pH 7.9)	200 µl of 1 M HEPES (pH 7.9)
0.083 M $MgAc_2$	100 µl of 1 M $MgAc_2$
1.667 M Kac	500 µl of 4 M KAc
1.667 mM spermidine	100 µl of 20 mM spermidine
0.042 M DTT	100 µl of 0.5 M DTT
	200 µl of dH_2O

- store in 100 µl aliquots at -20 °C

RNA guard -- Pharmacia #27-0815-01
Lysate -- Fisher (Promega) L4960
^{35}**S-met** -- Amersham SJ-1515
T7 RNA Polymerase -- Boehringer 881767 (20 U/ µl)
SP6 RNA Polymerase -- Boehringer 1487671 (20 U/ µl)

Solutions for Import

PMSF
Prepare stock of 130mM in DMSO (i.e. 22.65 mg PMSF / ml DMSO). Store at -20 °C.

Breaking Buffer (can leave up to 1 month)	for 100ml
0.6 M Sorbitol	25 ml of 2.4 M Sorbitol -store at 4 °C
20 mM HEPES	2 ml of 1 M Hepes (pH 7.4)
	72 ml dH_20

2.4 M Sorbitol Use 43.73 g / 100 ml. Store at 4 °C.
2.5 M KCl Use 18.64 g / 100 ml. Store at 4 °C.
1 M $MgCl_2$ Use 2.033 g / 10 ml. Store at 4 °C.
1 M HEPES (pH 7.4) Use 238.3 mg/ml, pH to 7.4. Store at 4 °C.

Sucrose cushion (make fresh per experiment) for 25 ml

0.6 M Sucrose	5 g
0.1 M KCl	1 ml of 2.5 M KCl
2 mM $MgCl_2$	50 µl of 1 M $MgCl_2$
20 mM HEPES	0.5 ml of 1 M HEPES (pH 7.4)

Solutions for Fluorography

5% TCA Use 200g / 4 L
10 mM Tris-base Use 4.846 g / 4 L
1 M Salicylic acid Use 640.4 g / 4 L

WESTERN BLOTTING

Reagents:

1. Acrylamide/Bis-Acrylamide, 30% Solution 37.5:1 (BioShop 10.502)
    a. Store at 4°C
2. Under Tris Buffer
    a. 1M Tris-HCl, pH 8.8 (60.5g/500ml)
    b. Store at 4°C
3. Over Tris Buffer
    a. 1M Tris-HCl, pH 6.8 (12.1g/100ml)
    b. Bromophenol Blue (for colour)
    c. Store at 4°C
4. Ammonium Persulfate (APS)
    a. 10% (w/v) APS in ddH_20 (1g/10ml)
    b. Stored at 4°C
5. Sodium Dodecyl Sulfate (SDS)
    a. 10% (w/v) in ddH_20 (1g/10ml)
    b. Store at room temperature
6. TEMED (Sigma T-9281)
7. Electrophoresis Buffer, pH 8.3 (10L)
    a. 25mM Tris 30.34g, 192mM Glycine 144g, 0.1% SDS 10g
    b. Volume to 10L with ddH_20
    c. Store at room temperature
8. 6X SDS
    a. Warm 100% glycerol in water bath at 65°C for 30 minutes
    b. Combine 1.2g SDS, 0.06g Bromophenol Blue, 3mls of 1M Tris, pH 6.8 and 1ml of ddH_20 and stir at 4°C for 5 minutes
    c. Add 3mls of 100% glycerol, stir and aliquot mixture.
    d. Store at -20°C
    e. Add 5% (v/v) ß-mercaptoethanol (Sigma M6250) to 6X SDS <u>just prior</u> to use
9. *tetra*-Amyl alcohol ReagentPlus, 99% (Sigma 152463)

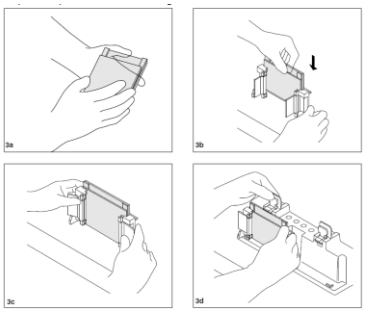

Procedure:

1. **Prepare electrophoresis rack:**
    a. Clean glass plates thoroughly with soap followed by 95% ethanol then ddH_20.
    b. Dry carefully with a kimwipe.
    c. Assemble glass plates as shown below:
    d. Check the seal by adding a small volume of ddH_20 then pour off and let dry.

2. **Prepare separating gels:**
    a. Mini Protean 3 Bio-Rad System volumes:

	8%	**10%**	**12%**	**15%**	**18%**
Acrylamide	2.7 ml	3.3 ml	4.0 ml	5.0 ml	6.0 ml
ddH_20	4.1 ml	3.5 ml	2.8 ml	1.8 ml	0.8 ml
Under Tris	3.0 ml	3.0 ml	3.0 ml	3.0 ml	3.0 ml
SDS	100µl	100µl	100µl	100µl	100µl
APS	100µl	100µl	100µl	100µl	100µl
TEMED	10µl	10µl	10µl	10µl	10µl

    b. Mix the contents of the separating gel without adding APS or TEMED. Stir.
    c. Add APS and TEMED. Stir.
    d. Slowly pour the entire volume of the solution into the space between the two plates while keeping plates tilted to prevent bubble formation.
    e. Add *tert*-Amyl alcohol to coat top surface of gel solution.
    f. Allow 30 minutes for gel polymerization.
    g. Remove *tert*-Amyl alcohol by pouring it off and remove any remainder with a kimwipe. Rinse with ddH_20.

3. **Prepare stacking gel:**
    a. For a single mini gel use the following volumes:

Acrylamide	500 µl
Over Tris	625 µl
ddH_20	3.75 ml
SDS	50 µl
APS	50 µl
TEMED	7.5 µl

    b. Mix the contents of the stacking gel without adding APS or TEMED. Stir.
    c. Add APS and TEMED. Stir.
    d. Using a Pasteur pipette slowly add the entire volume from the beaker in between the plates.
    e. Add comb for desired number of wells.
    f. Allow 30 minutes for gel polymerization.

4. **Prepare samples:**
    a. Turn on the block heater to 95ºC.
    b. Pipette required volume of sample into new eppendorf with same amount of lysis buffer and 5 µl of sample dye. Keep samples on ice until all samples are prepared (use pipette plan).
    c. Briefly spin each sample to bring volume to the bottom of the eppendorf.
    d. Incubate each sample at 95 ºC for 5 minutes in the heating block to denature the proteins.

e. Briefly spin again to return volume to the bottom of the eppendorf.

5. **Assemble Mini-PROTEAN gel caster system:**
    a. See images below
    b. If you are only running one gel a plastic rectangular pseudo plate must be clamped on the other side of the caster.
    c. Fill with electrophoresis buffer between the plates and outside of the plates in the chamber.
    d. Slowly remove the comb using both hands (one on each side) by pulling the comb straight upwards.
    e. Fix any wells that are deformed using a small spatula.
    f. Clean out the wells using a syringe filled with electrophoresis buffer.
    g. Withdraw the entire volume of the sample using a Hamilton syringe. Inject volume slowly into the bottom of the well.

6. **Gel electrophoresis**
    a. Immediately after all samples are loaded place the lid on the gel chamber.
    b. Place positive and negative plugs into the power supply and turn on power supply.
    c. Set power supply to 120V. Gel will run for ~2 hours depending on percent gel made.
    d. When the bromophenol blue has run off the bottom of the gel (or when gel has separated the desire amount) turn off the power supply. Remove plugs from power supply and remove lid.
    e. Prepare for electrotransfer of proteins from the gel to nitrocellulose membrane.

Western Blotting-Transfer and Immunodetection:

Reagents:

1. Transfer Buffer
    a. 0.025M Tris-HCl pH 8.3 12.14g
    b. 0.15M Glycine 45.05g
    c. 20% Methanol 800ml
    d. make up to 4L with ddH_20
    e. store at 4°C
2. Ponceau S stain
    a. 0.1% (w/v) Ponceau S
    b. 0.5% (v/v) Acetic Acid
    c. Store at room temperature
3. Wash Buffer
    a. Tris-HCl pH 7.5 12g
    b. NaCl 58.5g
    c. 0.1% Tween 10ml
    d. Store at room temperature
4. Blocking Solution
    a. 5% (w/v) skim milk power in wash buffer OR
    b. 5% (w/v) BSA in wash buffer

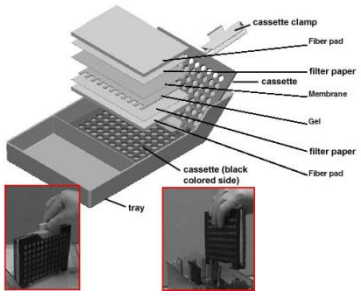

5. Enhanced Chemiluminescence Fluid (ECL; Santa Cruz sc-2048)
6. Film/Developer/Fixer

Procedure:

1. Transfer Procedure

a. Remove electrophoresis plates from chamber and separate the plates.
b. Cut away unnecessary parts of the gel using a spatula and measure remaining gel size.
c. Using a paper cutter cut 6 pieces of Whatman paper per gel to the same size as the gel. Wearing gloves cut nitrocellulose membrane (GE Healthcare RPN303D) to the dimensions of the gel.
d. Assemble Whatman paper, nitrocellulose memebrane and gel as shown above:
e. Close the cassette and place in the transfer chamber with the black side of the cassette facing the back side of the chamber.
f. Place ice pack in the chamber.
g. Place lid on the chamber and connect the leads to the power supply.
h. Turn on the power supply and run at 120V for 2 hours. This can vary depending on the size of the protein of interest.

2. Removal of transfer membrane:

a. Turn off the power supply and disconnect leads from the power supply then remove the lid from the chamber.
b. Remove the cassette from the chamber.
c. With gloves on, remove the Whatman paper and gel and place the nitrocellulose membrane in a plastic dish.
d. Add Ponceau S stain on the membrane and gently swirl.
e. Drain off the remaining Ponceau S and save for reuse.
f. Rinse the membrane with ddH_20 to reduce the red background. Wrap membrane in saran wrap and scan image.
g. Cut the membrane while protein bands are still visible at the desired molecular weight.
h. Rotate membrane at room temperature in wash buffer until remaining Ponceau S has been removed.
i. Incubate membrane for 1 hour with rotation in blocking solution.
j. Incubate membrane with desired antibody diluted in blocking solution overnight at 4ºC. Membrane is placed face up into the solution on a glass plate covered in parafilm. To maintain a moist environment overnight, wet a small kimwipe and form it into a ball and place in each corner of the dish. Cover the dish with saran wrap.

3. Immunodetection

a. Wash the blots in wash buffer with gentle rotation for 5 minutes 3X.
b. Incubate the blots for 1 hour in room temperature with the appropriate secondary antibody diluted in blocking solution.

c. Membrane is placed face up in solution on a glass plate covered with parafilm. Place moist kimwipes in each corner of the dish and cover the dish with saran wrap.
d. Following the incubation, wash the membrane 3X for 5 minutes with wash buffer.

4. Enhanced Chemiluminescence Detection

a. Mix ECL fluids "A" and "B" in a 1:1 ratio in a disposable Rohr tube.
b. Place blots on saran wrap face up and apply ECL solution for 2 minutes.
c. Dab off excess ECL on a kimwipe and place blots face down on a fresh piece of saran wrap and wrap tightly.
d. Expose blot to film (time will vary depending on protein and antibody).
e. Place film into developer (time will vary).
f. Once image appears place film into fixer for 2 minutes. Wash with fresh water when complete.

RNA ISOLATION, REVERSE TRANSCRIPTION AND QPCR

RNA Isolation

Procedure:

1) Homogenize (approximately 30 sec. @ 30-40% power) tissues (200 mg) at 30% in 2 ml Tri-reagent in a 13 ml Sarstedt tube;

OR

Homogenize (approximately 30 sec. @ 30-40% power) tissues (200 mg) at 30% in 1.25 ml solution D + 1.25 ml phenol + 0.125 ml 2M sodium acetate (pH 4.0) in a 13 ml Sarstedt tube

**Note: The homogenizer must be sterilized in 0.1M NaOH and rinsed in sterile water prior to use. Rinse in sterile water between samples.

2) Let stand for 5 min at room temperature;
3) Add 0.4 ml chloroform and shake vigorously for 15 sec, let stand for 2-3 min at room temperature;
4) Spin at 12,000 *g* for 15 min at 4°C;
5) Transfer aqueous phase to 13 ml Sarstedt tube;
6) Add 1 ml isopropanol, gently shake, and allow precipitation of RNA for 5-10 min at room temperature;
7) Spin at 12,000 *g* for 10 min at 4°C;
8) Remove supernatant and add 0.7 ml 75% ethanol;

9) Transfer RNA to eppendorf tube;
10) Rinse 13 ml Sarstedt tube with 0.3 ml 70% ethanol, add to eppendorf tube and mix by vortexing;
11) Spin 5 min in eppendorf centrifuge at 4°C;
12) Discard supernatant;
13) Dry pellet under a vacuum in dessicator (DO NOT DRY PELLET WITH CENTRIFUGATION UNDER A VACUUM);

14) Dissolve pellet in 50-200 µl sterile distilled DEPC water and measure absorbance at 260 nm and 280 nm.

Reagents:

1. *Solution D (Denaturing solution)*

4 M Guanidinium Thiocyanate	125 g
25 mM of 1 M stock NaCitrate (pH 7.0)	6.6 ml
N-Lauroyl Sarcosine;Sigma L-5125 (0.5% Sarcosyl)	1.32 g
ddH_2O	160 ml

**Note: make up solution D and store at RT for up to 3 months. On the day of the experiment, mix 50 ml of Solution D with 0.36 ml of beta-Mercaptoethanol (0.1 M b-MEtOH)

2. *Phenol (Nucleic acid grade)*
   a) Melt solid phenol at 68 °C (cap loose) in H_2O;
   b) Add 0.25 g 8-hydroxyquinoline to 250 ml of phenol, mix;
   c) Add 250 ml 1.0 M Tris HCl (pH 8.0) and stir overnight at 4 °C covered in foil
   d) Remove supernatant;
   e) Add 250 ml 0.1 M Tris-HCl containing 0.2 % b-MEtOH (0.178 ml/100 ml for S.G. = 1.12) and mix thoroughly;
   f) Allow solution to settle and remove supernatant;
   g) Repeat 2 more times as above or until pH of phenol is > 7.6 (test with pH paper).
   h) Store in 25-50 ml aliquots at -20 °C.
3. *2.0 M Na Acetate* (pH 4.0)
   10.88 g/100 ml sterile H_2O
4. *75% ethanol in sterile H_2O*
   (75 ml ethanol + 25 ml dH_2O)

Reverse Transcription, First Strand cDNA Synthesis

First-strand cDNA synthesis is performed following the manufacturer's recommendations that are outlined below:

Reagents:

1. total RNA (isolated as described)
2. Oligo$(dT)_{12-18}$
3. 10 mM dNTPs (dATP, dTTP, dCTP, dGTP; 10 mM each)
4. Sterile dd$H_2$0
5. RNAse OUT (40 units/ µl)
6. 0.1 M DTT
7. 5X First-strand Buffer
8. SuperScript II RT

*Note: All reagents except RNA are supplied with the SSII kit from Invitrogen.

Procedure:

1. Add following components to a nuclease/ RNA-free 500 µl eppendorf:

Oligo$(dT)_{12-18}$	1µl

1 µg of RNA	x µl
dNTP mix	1 µl
Sterile ddH_20	to 20 µl

2. Heat mixture to 65°C for 5 minutes and quick chill on ice. Collect the contents with a quick spin in a tabletop microcentrifuge and then add:

5X First-strand buffer	4 µl
0.1 M DTT	2 µl
RNAse OUT	1 µl

3. Mix contents of tube gently and incubate at 42°C for 2 minutes.
4. Add 1 µl (200 units) of Superscript II RT and mix by pipetting gently up and down.
5. Incubate at 42°C for 50 minutes.
6. Inactivate the reaction by heating at 70°C for 15 minutes.
7. cDNA is ready for use in PCR amplification.

Polymerase Chain Reaction (PCR)

1) 2 ug of RNA is converted to 2 ug of cDNA (STOCK cDNA)
2) We dilute STOCK cDNA to 1:30 (2 uL STOCK cDNA added to 58 uL nuclease-free ddH_2O)
3) We add 4 µL of diluted cDNA, thus loading 10 µg cDNA per well
4) For SYBR Green analyses, primers were optimized, diluted and mixed with PerfeCTa SYBR® Green SuperMix, ROX Master Mix and nuclease-free ddH_2O
5) Total reaction volumes were always 25 µL
6) Samples must be duplicated to ensure accuracy.
7) Use negative wells to monitor contamination, using nuclease-free ddH_2O in place of cDNA.
8) Check for nonspecific amplification and primer dimers by analyzing melt curves

PROTEIN RELEASE AND PEPTIDE ISOLATION

Background*:** Mitochondria are a primary source of reactive oxygen species (ROS) which have been shown to have both direct and indirect effects on apoptosis. ROS cause damage by binding to molecules and changing their conformation and function. Specifically, ROS have been shown to facilitate the opening of the mtPTP, and induce the release of pro-apoptotic products from the mitochondria. Release of either pro-apoptotic proteins cytochrome c and/or apoptosis-inducing factor (AIF) from the mitochondria triggers apoptotic cellular death (albeit acting through different pathways). These proteins are released from the mitochondrion through a specialized pore in the mitochondrial membrane termed the mitochondrial permeability transition pore (mtPTP). Using isolated mitochondria, release of these pro-apoptotic molecules can be induced by exogenous treatment with reactive oxygen species (ROS)-agents, such as H_2O_2. In addition, it has been shown that H_20_2 treatment, in conjunction with a ferrous ion donor, catalyzes a reaction that results in the production of a second more damaging ROS, the hydroxyl radical OH^- (this is due to the ***Fenton reaction-$\mathbf{H_2O_2 + Fe^{2+} = OH^- + OH\bullet + Fe^{3+}}$). Thus, the combination of H_2O_2 and $FeSO_4$ (dissociating in solution to form ferrous ions) causes pro-apoptotic release from

the mitochondrion. Experimentally, release of these pro-apoptotic products can be assessed by treating isolated mitochondria with a combination of $H_2O_2/FeSO_4$ for a set duration of time (60min), followed by centrifugation of the reaction mixture to fractionate mitochondria (pellet) from the supernate. The supernate fraction is then used for Western blot analysis of cytochrome c and AIF.

Resuspension Medium (pH-7.4):
10 mM HEPES
0.25 mM Sucrose
10 mM Sodium Succinate
2.5 mM K_2HPO_4
1 mM DTT
Reagents:
Stock Concentrations
100 uM H_2O_2
100mM $FeSO_4$ (278mg/10mls)
10mM Cyclosporin A in DMSO

Procedure

1. SS and IMF mitochondria are isolated and resuspended as described in the mitochondrial isolation protocol. Determine the concentration of samples using Bradford method.
2. Prepare 6 eppendorf tubes per sample. Follow the pipette plan for the various conditions, adding the mitochondria first, resuspension buffer, H_2O_2, $FeSO_4$, then Cyclosporin A.

Lanes	1	2	3	4	5	6
Sample Name	AO74	AO74	AO74	AO74	AO74	AO74
Sample Description	IMF	IMF	IMF	IMF	IMF	IMF
Protein for 5 ul	58.15	58.15	58.15	58.15	58.15	58.15
Protein ug/ul	11.63	11.63	11.63	11.63	11.63	11.63
Total Protein (ug) 125	10.75	10.75	10.75	10.75	10.75	10.75
H2O2	0.00	2.50	2.50	0.00	2.50	2.50
FeSO4	0.00	0.00	1.00	0.00	0.00	1.00
Cyclosporin A	0.00	0.00	0.00	1.00	1.00	1.00
Resusp. Buffer	39.25	36.75	35.75	38.25	35.75	34.75
Total	50.0	50.0	50.0	50.0	50.0	50.0

3. Incubate reaction mixtures for 60min at 30˚C.
4. Centrifuge eppendorfs for 5min at 14,000g (4˚C) to pellet the mitochondria.
5. Following centrifugation, carefully extract the entire supernate fraction from the mitochondrial pellet (**NOTE:do not disrupt mitochondrial pellet**) and transfer to another set of pre-labelled eppendorf tubes.

6. The entire supernatant volume is transferred to a Spin-X Concentrator (Corning) and centrifuged for 15 mins at 15,000g at room temperature. This separates released fraction by size, allowing the collection of all released products under 3 kDa. Transfer the separated fraction into pre-labelled eppendorfs, keep on ice.
7. Measure the concentration of protein using a spectrophotometer (NanoDrop 2000, Thermo Fisher) at 280nm
8. Store in -80ºC.

APPENDIX D: OTHER CONTRIBUTIONS TO LITERATURE

PEER-REVIEWED PUBLICATIONS

1. Erlich AT, Tryon LD, Crilly MJ, Memme JM, Moosavi ZM, **Oliveira AN**, Beyfuss K, Hood DA. (2016). Function of specialized regulatory proteins and signaling pathways in exercise-induced muscle mitochondrial biogenesis. *Integrative Medicine Research,* 5(3), 187-197.
2. Memme JM, **Oliveira AN**, Hood DA. (2016). The chronology of UPR activation in skeletal muscle adaptation to chronic contractile activity. *American Journal of Physiology- Cell Physiology*, 1(11), C1024-1036.

PUBLISHED ABSTRACTS AND CONFERENCE PROCEEDINGS

1. **Oliveira AN**, Hood DA. Perturbing mitochondrial protein import *in vivo* results in activation of the UPR^{mt}. *Proceedings of the 7th Annual Muscle Health Awareness Day*. Toronto, ON. May 2017 – Poster Presentation.
2. **Oliveira AN**, Hood DA. Knockdown of Tim23 *in vivo* results in the activation of the mitochondrial unfolded protein response. *Experimental Biology 2017*. Chicago, IL. April 2017 – Poster Presentation.
3. **Oliveira AN**, Hood DA. Activation of the mitochondrial unfolded protein response during Tim23 knockdown *in vivo*. *Ontario Exercise Physiology Conference 2017*. Barrie, ON. January 2017 – Poster Presentation.
4. **Oliveira AN**, Hood DA. Possible role of mitochondrially-derived peptides in mediating retrograde signaling in mammalian muscle. *American Physiological Society Intersociety Meeting-Integrative Biology of Exercise VII*. Pheonix, AZ. November 2016 – Poster Presentation.
5. **Oliveira AN**, Memme JM, Hood DA. CHOP signaling is not required for mitochondrial adaptations to chronic contractile activity. *Proceedings of the 6th Annual Muscle Health Awareness Day*. Toronto, ON. May 2016 – Poster Presentation.
6. **Oliveira AN**, Memme JM, Hood DA. Inhibition of the UPR^{ER} does not impair signaling to mitochondrial biogenesis during chronic contractile. *Experimental Biology 2016*. San Diego, CA. April 2016 – Poster Presentation.

ORAL PRESENTATION

1. **Oliveira AN**, Hood DA. Activation of the mitochondrial unfolded protein response during the disruption of protein import. *KAHS Graduate Seminar 2017*. York University, Toronto, ON. February 2017 – Oral Presentation.

JUNIOR REVIEWER

1. Kravic B, et al. In mammalian skeletal muscle phosphorylation of Tom22 by protein kinase CK2 controls mitophagy. *Autophagy*. [In Progress].